MAGNETOM Flash

Issue Number 83 · 1/2023
SCMR Edition

siemens-healthineers.com/magnetom-world

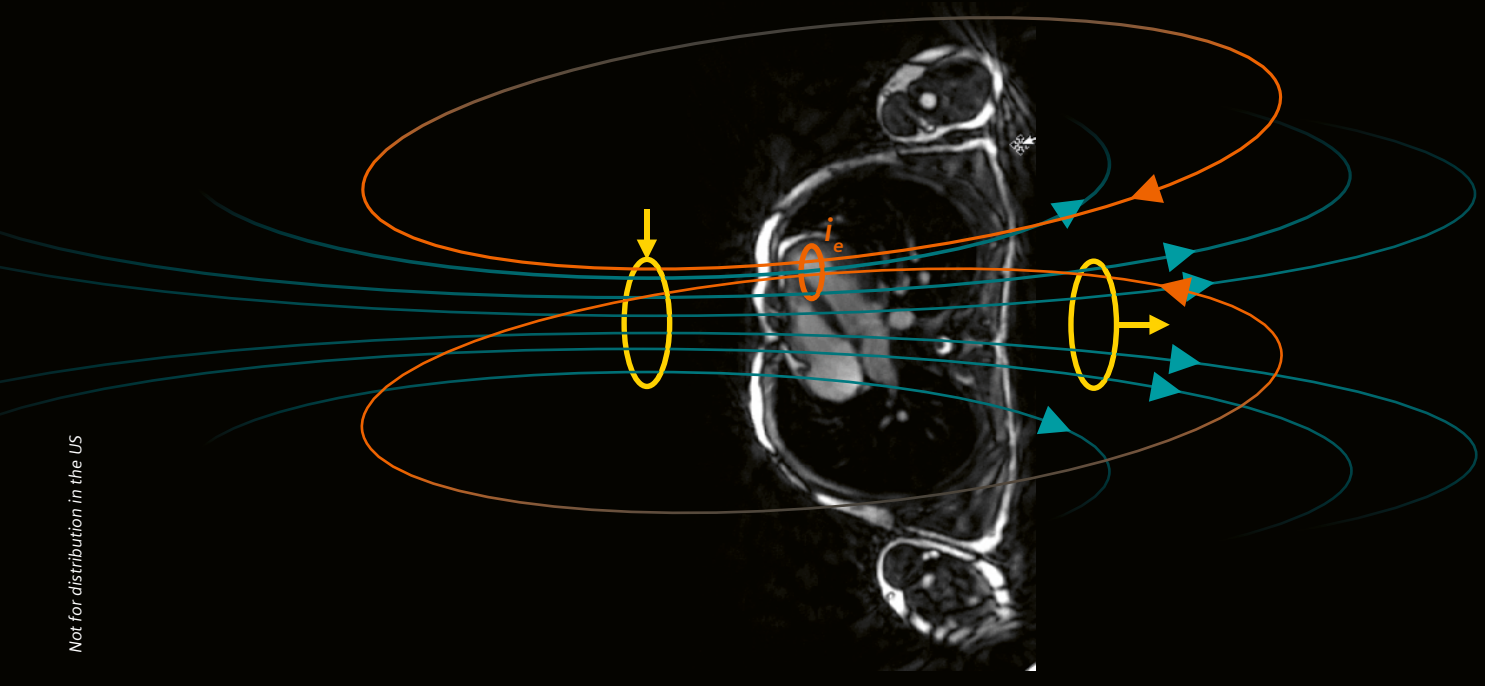

SIEMENS Healthineers

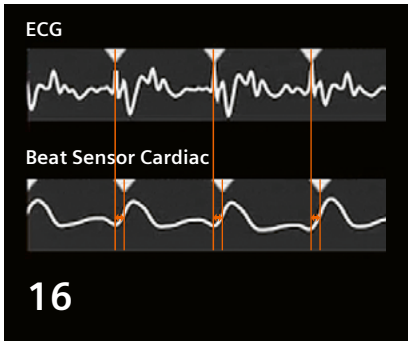

BioMatrix Beat Sensor

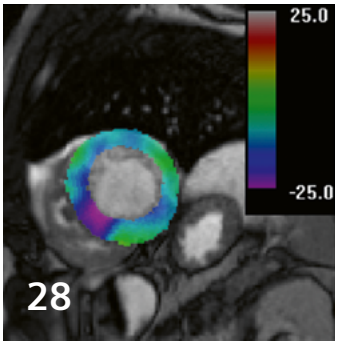

AI-based fully automated GCS measurement

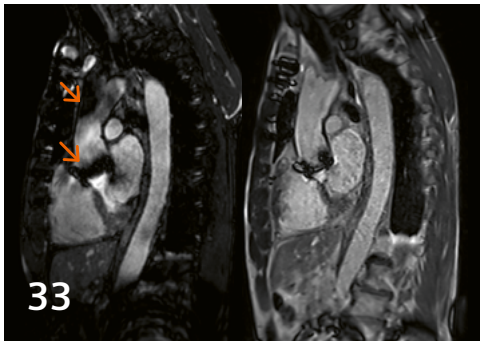

Cardiac MRI at lower-field

Editorial Comment

BioMatrix Beat Sensor

Artificial Intelligence

Access to CMRI

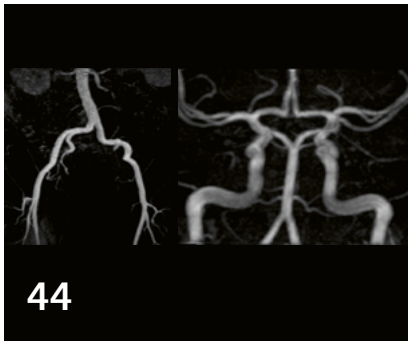

MRA using MAGNETOM Free.Max

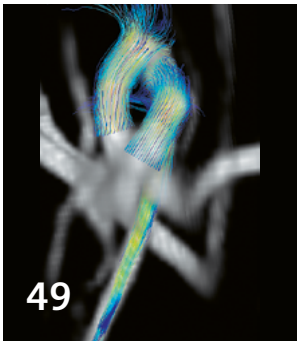

How to do fetal cardiac MRI at 3T

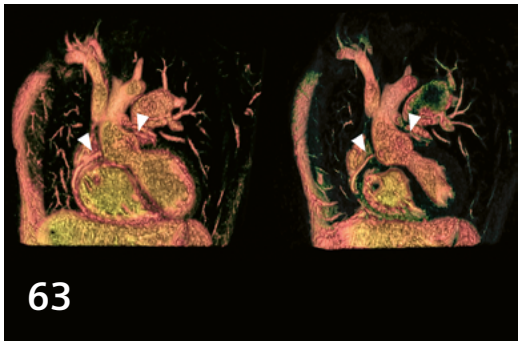

Ferrumoxytol-enhanced free-running 5D whole-heart MRI

Pediatric / Fetal CMR

Meet Siemens Healthineers

[1]Work in progress. The application is currently under development and is not for sale in the U.S. and in other countries. Its future availability cannot be ensured.
[2]MR scanning has not been established as safe for imaging fetuses and infants less than two years of age. The responsible physician must evaluate the benefits of the MR examination compared to those of other imaging procedures.

Matthias Stuber, Ph.D., is the Head of the CIBM MRI CHUV-UNIL Section and is a Full Professor at the University of Lausanne, Switzerland, Visiting Professor at the Johns Hopkins University, Baltimore, MD, USA , and an Invited Chair at Liryc, Bordeaux, France. He studied electrical engineering at the ETH in Zurich, Switzerland, where he also obtained his Ph.D. on cardiac MRI in 1997. From 1997 to 2002, he worked at the Beth Israel Deaconess Medical Center in Boston, MA, USA, both as a clinical scientist for industry and a faculty at Harvard Medical School. From 2002 to 2009, he directed a research team as an NIH-funded principal investigator at the Johns Hopkins University School of Medicine, where he advanced to Full Professor and was awarded tenure.

In summer 2009, Matthias Stuber returned to his native Switzerland. He has authored more than 220 peer-reviewed original articles, holds 11 patents, and has been awarded 40 research grants so far. He served as an elected board member of the International Society for Magnetic Resonance in Medicine (ISMRM) from 2013 to 2016, and is a Past President of both the Society for Magnetic Resonance Angiography (SMRA) and the Society for Cardiovascular Magnetic Resonance (SCMR). He has been distinguished as both a Fellow (FSCMR) and a Master (MSCMR) of SCMR in 2018 and 2020, respectively. Since 2021, he is a member of the research council of the Swiss National Science Foundation (SNSF). Professor Stuber has received many awards for his research, including a "Fellow Award" of the ISMRM at the 2010 annual meeting of the society in Stockholm, Sweden. In 2021, he became a recipient of the prestigious Gold Medal Award, the highest distinction bestowed by SCMR, for his research and his contributions to the field.

Dear readers and colleagues,

Welcome to San Diego, the "Birthplace of California", and to this exciting new edition of MAGNETOM Flash, which is dedicated to the 26th annual scientific sessions of the SCMR, the leading global event that brings together a highly diverse and dedicated group of CMR professionals from all four corners of the world. The theme of the 2023 SCMR is dedicated to "Changing Global Clinical Practice", a most fitting theme as you can see below.

When holding this most recent issue of MAGNETOM Flash in our hands, we cannot but reminisce about the reasons for MRI being such a powerful modality for the management of cardiovascular disease. A relatively sober explanation might include:

> *"MRI is powerful because it provides detailed images of the heart and blood vessels without the use of ionizing radiation. It can be used to evaluate the structure and function of the heart and its major blood vessels and to detect a wide range of cardiovascular conditions, including coronary artery disease, heart failure, and abnormalities of the heart valves. MRI is also useful for guiding interventional procedures, such as stenting or catheter-based treatments for heart disease. Additionally, MRI can be used to monitor the effectiveness of treatment for cardiovascular disease over time."*

Except – this explanation was neither provided by the undersigned nor as a consensus by a group of experts, but it was rather given by *ChatGPT*, an artificial intelligence chatbot that many of you may have gotten to know by now. This unequivocally documents the staggering progress of technology and opportunity that is happening all around us – as much as it should give us reason to pause and reflect on how to best harness this enormous potential for CMR.

At this juncture, major improvements will undoubtedly come from optimized workflow, ease of use, and scan efficiency. Related advancements will critically improve the utilization of CMR. Paired with emerging concepts in telemedicine and low-field MRI, more global dissemination

to geographical regions and settings that have not traditionally had access to CMR is imminent.

In this issue of MAGNETOM Flash dedicated to CMR, we find very exciting content that precisely touches upon these above-mentioned challenges and opportunities.

As for harnessing the seemingly endless power of AI, this is intriguingly exemplified in the article by Théo Pezel and coworkers from Massy, France, in which they convincingly demonstrate that we are at a crossroads of harnessing the potential of CMR in a way that was neither previously possible nor practical. In a large cohort of patients referred for Stress CMR, inducible ischemia was assessed using fully automated, AI-powered global circumferential strain (GCS) measurements[1] during vasodilator stress. The AI algorithm was trained using 3,000 patients from the UK Biobank. Simultaneously, a sophisticated and highly optimized workflow on two parallel scanners that run 55 hours per week is reported and an exam duration of well below 30 minutes has been achieved. Stress GCS was found to be independently associated with cardiovascular events during a five-year follow-up. Taken together, this is a testimony to what AI integration, workflow improvements, and scan efficiency – with a big scoop of dedication mixed in – can accomplish.

At a juncture where the link between COVID-19, mRNA vaccines, and myocarditis remains to be further elucidated, it is critically important to have time-efficient MRI tests at our fingertips for optimized patient management. Therefore, Erin Robins and Claire Harris from Perth, Australia, share their extensive experience on how common inefficiencies in CMR patient setup can be avoided and how the positioning of electrodes even at higher field strengths is no longer "magic" but can be broken down to a mechanistic, well-thought-out, and repeatable procedure that helps improve throughput through a sub-30-minute exam. While such insight comes from very experienced hands, this simultaneously triggers (no pun intended) the question:

> *"What might be a good alternative to ECG triggering in CMR?"*

When the *ChatGPT* oracle in its endless wisdom is queried again for finding an answer, it states with impressive assertiveness:

> *"One alternative to ECG triggering in CMR is breath-holding."*

Of course, we all know this is wrong, and a student would fail if they gave that answer during an exam. Therefore, my take-home message was that this marvel of technology is always certain but not always right – and that knowledge, insight, ingenuity, creativity, and perhaps a smattering of intuition and perseverance may still go a long way in helping move CMR forward.

This is very nicely exemplified by the two articles that grant the reader some precious insight into the inner workings of Siemens Healthineers and the thoughts of some of their very well-known innovators in the field. Peter Speier and Mario Bacher from Erlangen, Germany, and Annemie Steegmans from Brussels, Belgium, take us on a journey that tells a tale of innovation and dedication that led to the development productization, and commercialization of the BioMatrix Beat Sensor on an impressive timescale. The Beat Sensor technology obviates the need for ECG triggering, breath-holding, and navigators, and therefore challenges a decades-old convention in CMR and will undoubtedly help make a decisive step forward in terms of the above-mentioned and much-needed workflow, ease of use, and scan efficiency. Albert Szent-Georgi, a Hungarian biochemist who won no less than the Nobel Prize in Medicine in 1937 and who was the first isolating vitamin C, once quipped:

> *"Discovery consists of seeing what everybody has seen and thinking what nobody has thought."*

And this precisely applies to the invention of the Beat Sensor: It exploits existing hardware and the physical boundary conditions that reign in an MRI scanner, and it draws from knowledge about physiology, electrodynamics, and signal processing, and perhaps from intuition to equal degrees, to come up with a new solution. Peter Speier and Annemie Steegmans are probably right in that we have only begun to scratch the surface of the endless possibilities this provides us with. For starters, and as demonstrated in the article by Christina Karamarkou and coworkers from Essen, Germany, there is tremendous opportunity in using the Beat Sensor clinically for triggering. In patients with a propensity for frequent arrhythmias – a long-standing conundrum for CMR – the Beat Sensor performed extremely well and total scan times were decisively abbreviated when compared to conventional ECG triggering. This is corroborated in the article by Bianca Samsula, from Bremen, Germany, who has successfully used the Beat Sensor clinically in close to 100 patients at both 1.5T and 3T. As this new technology will decisively abbreviate setup time, minimize operator dependency, and maximize ease of use, it will also cater to improved throughput – all of which will be critical in the dissemination of CMR that is depends neither on highly trained personnel nor their

[1] *Work in progress. The application is currently under development and is not for sale in the U.S. and in other countries. Its future availability cannot be ensured.*

ZIP code, as aptly put by Jan Borggrefe, from Minden, Germany. He has ramped up an impressive CMR effort in a rural region of Germany that has not had easy access to CMR before, where AI, ease of use, and telemedicine are critically needed, and where helium-, energy-, and cost-saving low-field units will make a decisive difference.

Finally, Salim Si-Mohamed and co-workers from Lausanne, Switzerland, and Lyon, France, report on Ferumoxytol-enhanced 5D free-running MRI[1] in patients with congenital heart disease. This technology shifts the paradigm from prospective planning and sequence-parameter adjustment to a fully retrospective query of the beating 3D heart with millimetric isotropic resolution, where, owing to total self-navigation, ECG triggering, navigators, or breath-holds are no longer needed. Workflow, ease of use, and scan efficiency are optimized, the five-minute scan is initiated by a single mouse click, and preliminary results show exquisite agreement with the gold standard for the measurement of cardiac function.

Most importantly, at CHUV in Lausanne, this now obviates the need for general anesthesia and intubation during CMR in selected age brackets of congenital heart disease patients[2].

Taken together, the above examples provide abundant reasons for optimism and show that modern CMR is at the dawn of a more widespread global dissemination in the interest of "Changing Global Clinical Practice", the precise theme of the 2023 SCMR Scientific Sessions!

Looking forward to seeing many of you in San Diego and learning about the latest progress in the field of CMR!

Matthias Stuber

[1] Work in progress. The application is currently under development and is not for sale in the U.S. and in other countries. Its future availability cannot be ensured.
[2] MR scanning has not been established as safe for imaging fetuses and infants less than two years of age. The responsible physician must evaluate the benefits of the MR examination compared to those of other imaging procedures.

We appreciate your comments.
Please contact us at magnetomworld.team@siemens-healthineers.com

Editorial Board

Review Board

Clinical Approach of BioMatrix Beat Sensor Cardiac Triggering

Christina Karamarkou, M.D.; Catharina Thielmann, M.D.

Department of Cardiology and Angiology, Contilia Heart and Vascular Centre, Elisabeth-Krankenhaus Essen, Germany

Introduction

The BioMatrix Beat Sensor cardiac triggering technology from Siemens Healthineers is based on constant RF signals which are modulated by the physiological motion of the heart and respiratory system. The modulated signal is received by a standard local body array (BioMatrix Body 12 and BioMatrix Body 18). The Beat Sensor is directly embedded in the coil. The resulting information about the cardiac motion is encoded and used to trigger the MR acquisitions. Because ECG-trigger distortion is always a challenge in cardiac MR (CMR), this technology, in contrast to the usual gold-standard ECG triggering, enables us to increase image quality and scan consistency, which limits costly and time-consuming rescans.

In our current clinical routine, we mainly use the new technology for cardiac patients with conditions that present challenges for scanning, such as pronounced cardiac arrhythmia (atrial fibrillation, ventricular ectopic beats). In this way we can personalize the examination and optimize the results for patients who do not fit the standard application. The successful sampling of high-quality image data remains the basis of diagnostic interpretation, diagnosis, and further therapeutic management.

However, there are also a few pitfalls in data acquisition, so the processor must be well trained, and a few additional steps are necessary. Our clinical experience shows that, with proper handling of the existing tools and modified sequences, the short acquisition time and high image quality are indisputable.

1 Positioning the BioMatrix Body 18 coil.

Clinical examples

1. Heart failure

Patient history: A 54-year-old woman with undefined shortness of breath and palpitations. Medication with prednisolone for 12 months. Pacemaker implantation in 2022 due to sick sinus syndrome and third-degree AV block with total loss of consciousness.

Previously performed diagnostics: PET-CT with suspected cardiac sarcoidosis without extracardiac manifestation. Myocardial biopsy with no indication of cardiac sarcoidosis by sampling error. ECG showed pronounced ventricular extrasystoles, ventricular runs, and ventricular pacemaker rhythm. Echocardiography showed an ejection fraction of 40% with undefined hypokinesia.

Clinical diagnosis: Heart failure of unknown cause

MRI indication: Confirmation of expected cardiac sarcoidosis

Materials and methods:
1.5T CMR system (MAGNETOM Sola, Siemens Healthcare, Erlangen, Germany)

Protocol included electrocardiography-gated and Beat Sensor cardiac-triggered steady state free precession (bSSFP) images of long-axis (LA) 2-, 3-, and 4-chamber views, and short-axis (SA) stacks. For T1 mapping, conventional 5(3)3 modified Look-Locker inversion recovery (MOLLI) sequences were performed before administration of a gadolinium contrast. Phase-sensitive inversion recovery gradient echo sequences were acquired 15–20 minutes after the gadolinium bolus injection for late gadolinium enhancement (LGE) assessment.

The initial electrocardiography-gated (bSSFP) sequences produced a lower image quality due to arrhythmias.

A challenging case executed with high performance thanks to Beat Sensor cardiac triggering.

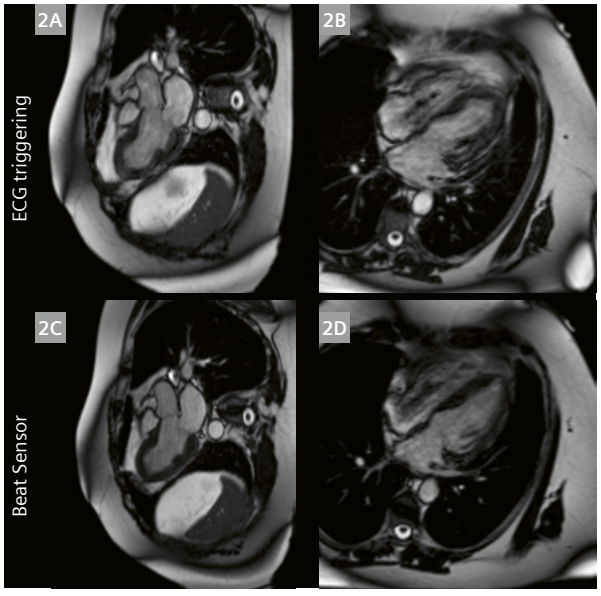

2 **(2A)** Cine 3-chamber view with ECG triggering; **(2B)** Cine 4-chamber view with ECG triggering. After changing to the Beat Sensor cardiac triggering, a higher image quality was achieved. **(2C)** Cine 3-chamber view with Beat Sensor cardiac triggering; **(2D)** Cine 4-chamber view with Beat Sensor cardiac triggering.

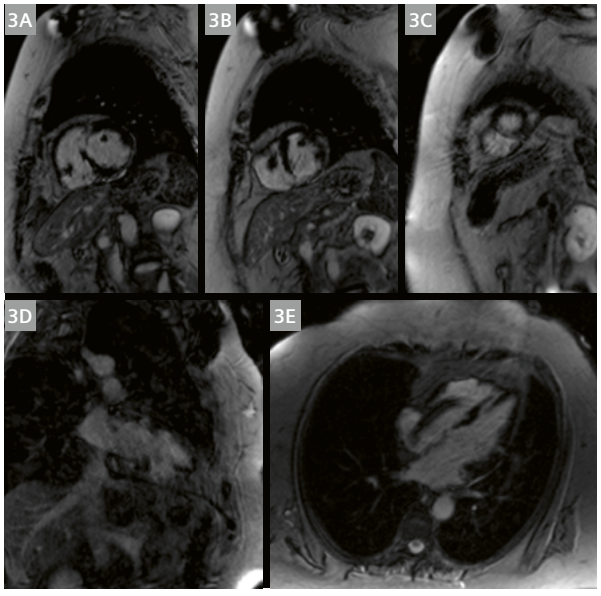

3 **(3A)** LGE in basal SA, **(3B)** midventricular SA, and **(3C)** apical SA; **(3D)** 2-chamber LA; **(3E)** 4-chamber LA with Beat Sensor cardiac triggering.

2. Ischemia

Patient history: A 59-year-old female patient with palpitations, coronary anomalies, progressed peripheral artery disease (PAD), and cerebral circulatory disorders with continued nicotine abuse.

Previously performed diagnostics: 24-hour ECG with pronounced ventricular extrasystoles. Echocardiography showed an ejection fraction of 55%.

MRI indication: Verification of ischemia

Materials and methods:
1.5T CMR system (MAGNETOM Sola, Siemens Healthcare, Erlangen, Germany)

Protocol included electrocardiography-gated and Beat Sensor cardiac-triggered steady state free precession (bSSFP) images of long-axis (LA) 2-, 3-, and 4-chamber views, and short-axis (SA) stacks. For T1 mapping, conventional 5(3)3 modified Look-Locker inversion recovery (MOLLI) sequences were performed before administration of a gadolinium contrast. Phase-sensitive inversion recovery gradient echo sequences were acquired 15–20 minutes after the gadolinium bolus injection for late gadolinium enhancement (LGE) assessment.

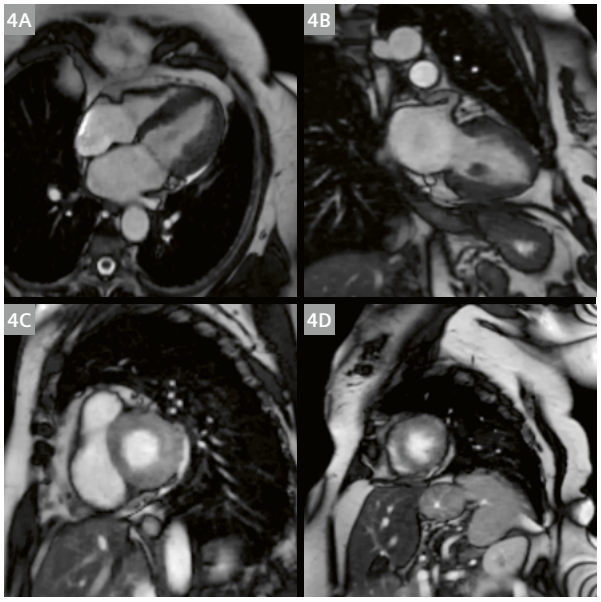

4 **(4A)** Cine 4-chamber view; **(4B)** Cine 2-chamber view; **(4C)** Cine in basal SA; **(4D)** Cine in mid-ventricular SA with Beat Sensor cardiac triggering.

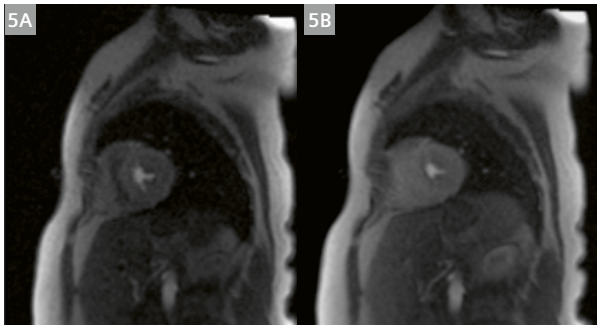

5 Dynamic perfusion in **(5A)** mid-ventricular SA and in **(5B)** apical SA with Beat Sensor cardiac triggering.

The learning phase

In the current implementation, the Beat Sensor requires some additional steps to
1) collect and train the signal for the coil elements;
2) calibrate the signal with respect to RF interference.

Therefore, we position the body array on the thorax, taking care to ensure the coil is fixed securely to the table. The Beat Sensor is positioned right on top of the heart. The center of the coil should be over the heart in the head-feet direction. The BioMatrix Body 18 coil cable should leave the coil in the feet direction. When using the BioMatrix Body 12 coil, the cable should leave the coil in the head direction. After finalizing the table position, the localizer-heart protocol is performed. The software acts like a coil memory for subsequent Beat Sensor cardiac-triggered acquisition, and the learning phase starts. The calibration protocol starts immediately after the learning phase with a series of RF pulses which are then used to calibrate the sensor signal. After these essential sequences, further diagnostic scans can be performed.

Gold-standard ECG triggering vs. Beat Sensor cardiac triggering in cardiac imaging

Overall we scanned approximately 50% of our patients in particular with an adenosine stress protocol using the Beat Sensor with a BioMatrix Body 18 array coil on a 1.5T MAGNETOM Sola system (Siemens Healthcare, Erlangen, Germany).

Especially in patients with cardiac arrhythmia, we find this to be a time-saving alternative to the gold-standard ECG triggering, which is susceptible to artifacts. The Beat Sensor triggering avoids potential problems such as low-voltage ECG due to poor skin contact, suboptimal electrode placement, anatomical/disease-related conditions (COPD, respiratory problems), and magnetohydrodynamic signal distortion, especially at high field strengths. It also removes the need for time-consuming procedures like chest-shaving for optimal electrode contact and monitoring the ECG signal to ensure sufficient quality.

Using the Beat Sensor means we can achieve high-quality results and, thanks to shorter scan times, we save time in our clinical routine and give patients a more comfortable examination experience.

A typical ECG-triggered CMR examination is timed so that the static acquisitions are performed in the late diastolic phase by placing the acquisition as late as possible in the cardiac cycle. The trigger time of the Beat Sensor is 200 milliseconds later than the R-wave, in response to the systolic contraction. This time shift is automatically generated based on the collected data from the learning phase. No ECG triggering is required.

For static acquisitions in the end-diastolic resting phase of the heart cycle, the sequences have been modified so that it is possible to adjust the acquisition window to the end-diastolic resting phase of the heart cycle. When using this feature, recognizing when the processor is exchanged between scans is crucial. Otherwise, there is a risk of missing triggers and unstable signal in the switching phase, which will make further manual modifications necessary. Alternatively, you can set a fixed interval for the entire examination.

Challenges

There are some clinical constellations in which the Beat Sensor technology does not lead to satisfactory image data acquisition. In these cases, it may be necessary to rescan the image record, or it might not even be possible to create acceptable results. We have found that obese female patients with very large chest areas are a particularly vulnerable group in this regard. The presence of more tissue can make it challenging or even impossible to achieve proper signal acquisition from the Beat Sensor.

Conclusion

We started the Beat Sensor cardiac triggering as part of a clinical study of specific patient groups, such as patients with pronounced arrhythmia and expected poor image quality. The time savings achieved by the reduction in rescans and by shorter acquisition times were significant.

Having compared Beat Sensor triggering with gold-standard ECG triggering across multiple CMR applications, we found the image quality to be subjectively equivalent. The function, LGE, and perfusion maps showed no significant difference in all measurements we have performed so far. The high-quality results with arrhythmia patients and the need for only a few/short examination requirements were convincing. We also see great potential and further scope for validation in a more diverse patient cohort, such as patients with abnormal anatomy and body habitus. By incorporating respiratory gating and prospective slice correction, we are continuing our development efforts to improve accuracy and precision.

Contact

Christina Karamarkou, M.D.
Specialist in Internal Medicine, Cardiology, and Emergency Medicine
Department of Cardiology and Angiology
Contilia Heart and Vascular Centre
Elisabeth Hospital Essen
Klara-Kopp-Weg 1
45138 Essen
Germany
Tel: +49 (0)201-897 86278
c.karamarkou@contilia.de

Christina Karamarkou, M.D.

Catharina Thielmann, M.D.

BioMatrix Beat Sensor – the Technologist's Perspective

Bianca Samsula

ZEMODI, Zentrum für moderne Diagnostik, Bremen, Germany

Introduction

We frequently perform cardiac MRI at our facility in Bremen – a private MRI, PET-MRI, and CT imaging center which has been an international reference site for Siemens Healthineers for many years.

We run the cardiac MRI examinations on all of our five MRI scanners: We have a 3T MAGNETOM Lumina, a 3T MAGNETOM Skyra, a 1.5T MAGNETOM Altea, a 1.5T MAGNETOM Avanto^{fit}, and a Biograph mMR PET-MR system.

Time is often a challenge, as the exams require us to perform multiple preparatory tasks. These include establishing venous access; preparing the patient's skin with an abrasive gel; shaving men's chest hair; and applying four ECG electrodes to ensure a stable trigger signal, which also needs some waiting/learning time before the patient goes into the magnet.

In light of this, we were very curious when our MAGNETOM Altea received a test version of the new *syngo* XA51 software. This allowed us to try the BioMatrix Beat Sensor, which is integrated into the BioMatrix Body 12 coil.

The technology removes the need for ECG electrodes, which means we technologists have a much easier and faster workflow when it comes to patient preparation.

BioMatrix Beat Sensor workflow

Make sure the coil is positioned correctly with the Beat Sensor over the heart (Fig. 1). That's it!

Right from the beginning, we used only the Beat Sensor for triggering. The protocol requires an additional

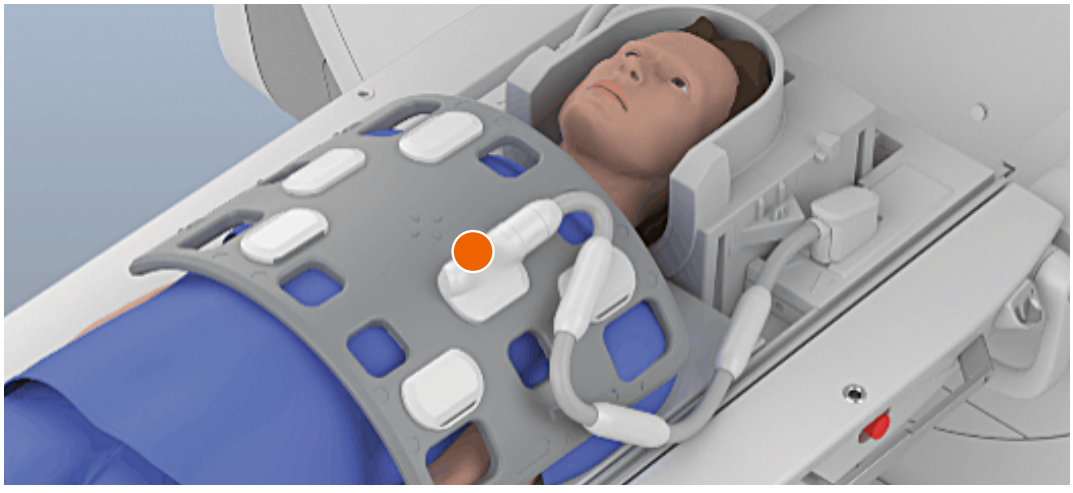

1 Positioning of the Beat Sensor which is integrated into the BioMatrix Body 12 coil.

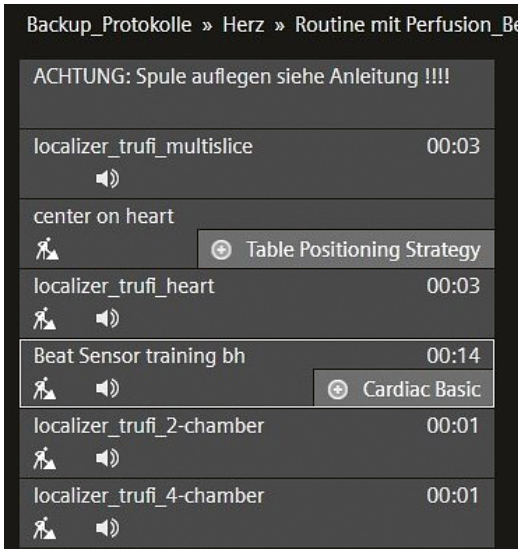

2 Beat Sensor training.

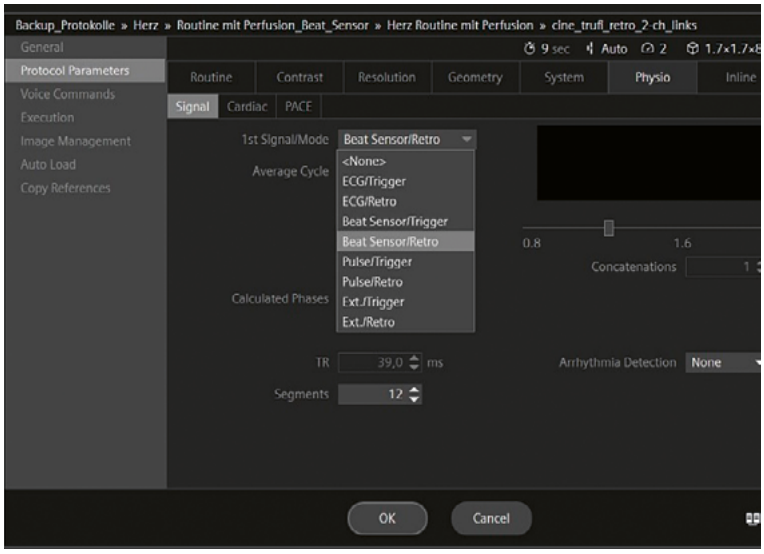

3 Selecting the trigger source.

training step (Fig. 2), which we set manually after the heart localizer.

This training step can be done during breath-hold or in free breathing. After the training, the Beat Sensor signal appears and can be used for physiological triggering.

You need to select the desired trigger source in the cardiac protocols (Fig. 3).

We use the myExam Cardiac Assist workflow, which means we just have to choose the correct trigger source at the beginning, and all subsequent protocols are adapted accordingly. If you don't have the myExam Cardiac Assist workflow, I recommend saving special Beat Sensor protocols, in which the trigger source is already correctly selected. This will minimize the need for manual changes during the scanning process.

So for our team, we can easily select the right program – including Flow, T1/T2 mapping, thalassemia, and LGE – without needing to select the Beat Sensor as the trigger every time (Fig. 4).

Challenges

Of course, we compared the standard ECG trigger with the Beat Sensor trigger in a few cases with additional measurements. There was almost no difference in image quality and robustness of triggering, except with T1-weighted TSE, where the ECG-triggered sequences showed a slightly better dark-blood suppression. For all other sequences, the two methods appeared to be identical.

So far, we have examined between 50 and 80 cardiac MRI patients with the Beat Sensor. The exams have addressed a variety of different clinical questions and different types of patients, aged between 11 and 83 years. Another area in which we found no difference was between obese or thin patients – the signal remained stable in both cases.

Just once, at the very beginning of our test period, we were running in a signal change during the cardiac examination. In that case, we repeated the Beat Sensor training step, after which the signal was stable again.

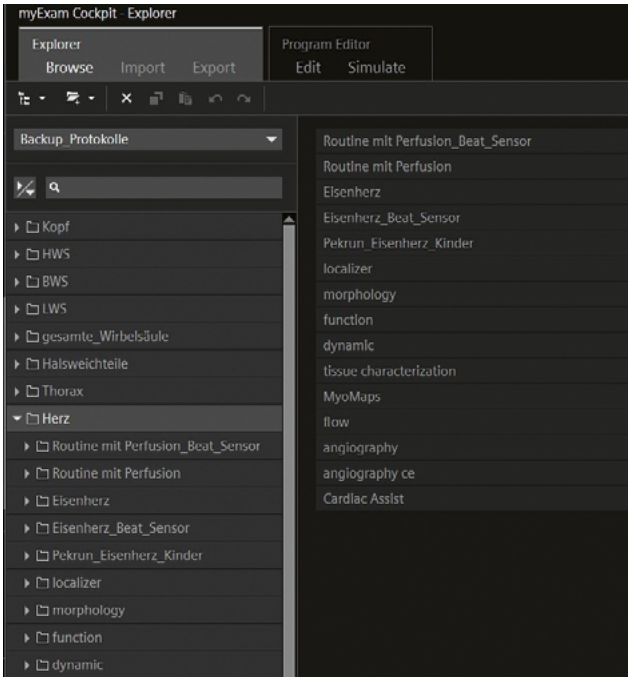

4 Pre-set protocols for various clinical questions.

Case examples

Case 1

57-year-old male patient with hypertrophic cardiomyopathy; mid-myocardial fibrosis.
(1A) Cine 4-chamber view;
(1B) Cine short axis view;
(1C–E) T1-maps

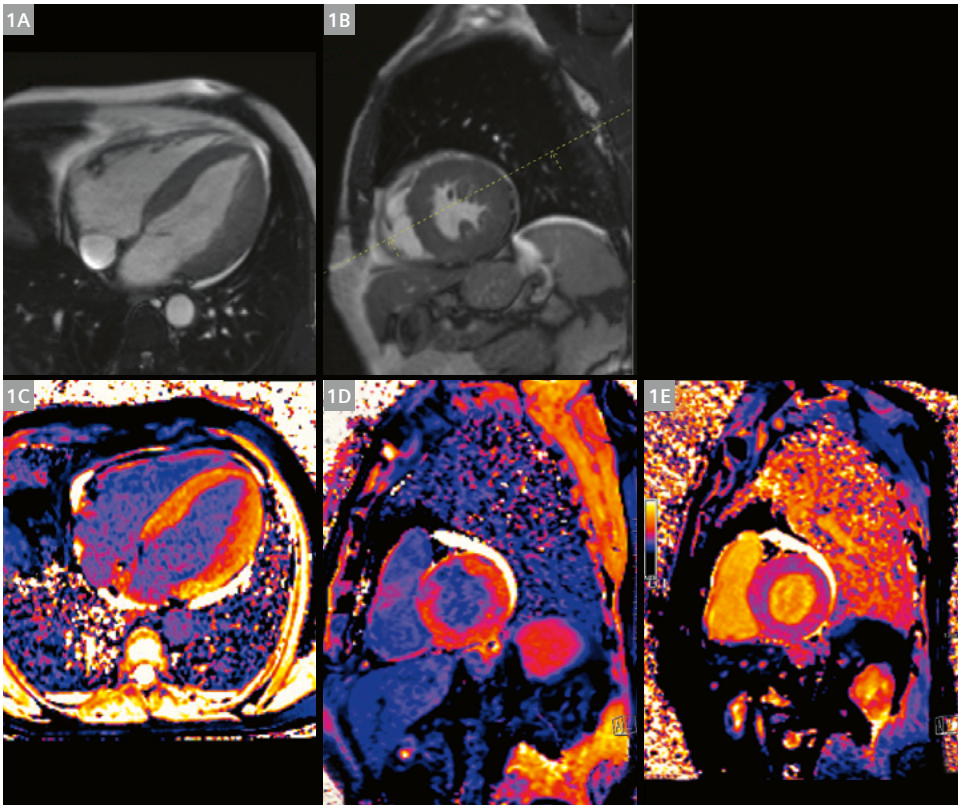

Case 2

11-year-old female patient with homozygous thalassemia and high ferritin. Pathological iron accumulation in the liver; no cardiac involvement.
(2A, B) T2* source images;
(2C, D) Color maps

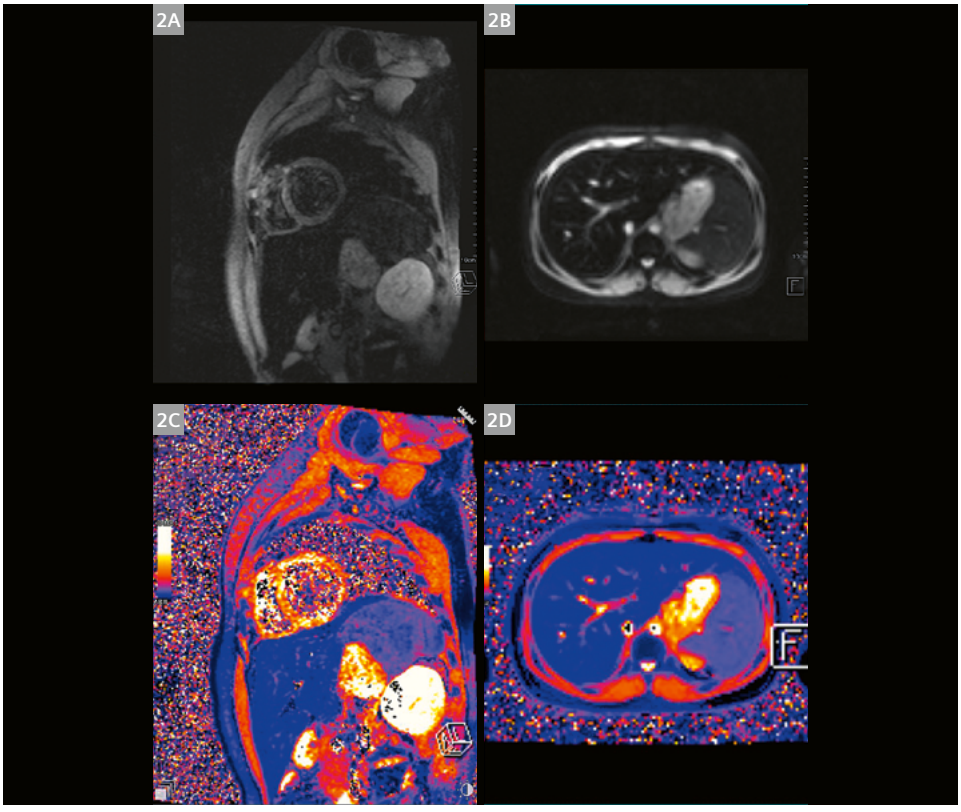

Case 3

30-year-old female patient with mixed aortic valve disease with valvular stenosis.
(3A) Through-plane phase contrast image, Venc 350 ml/s;
(3B) Magnitude image;
(3C) Flow curve;
(3D) Planning Cine

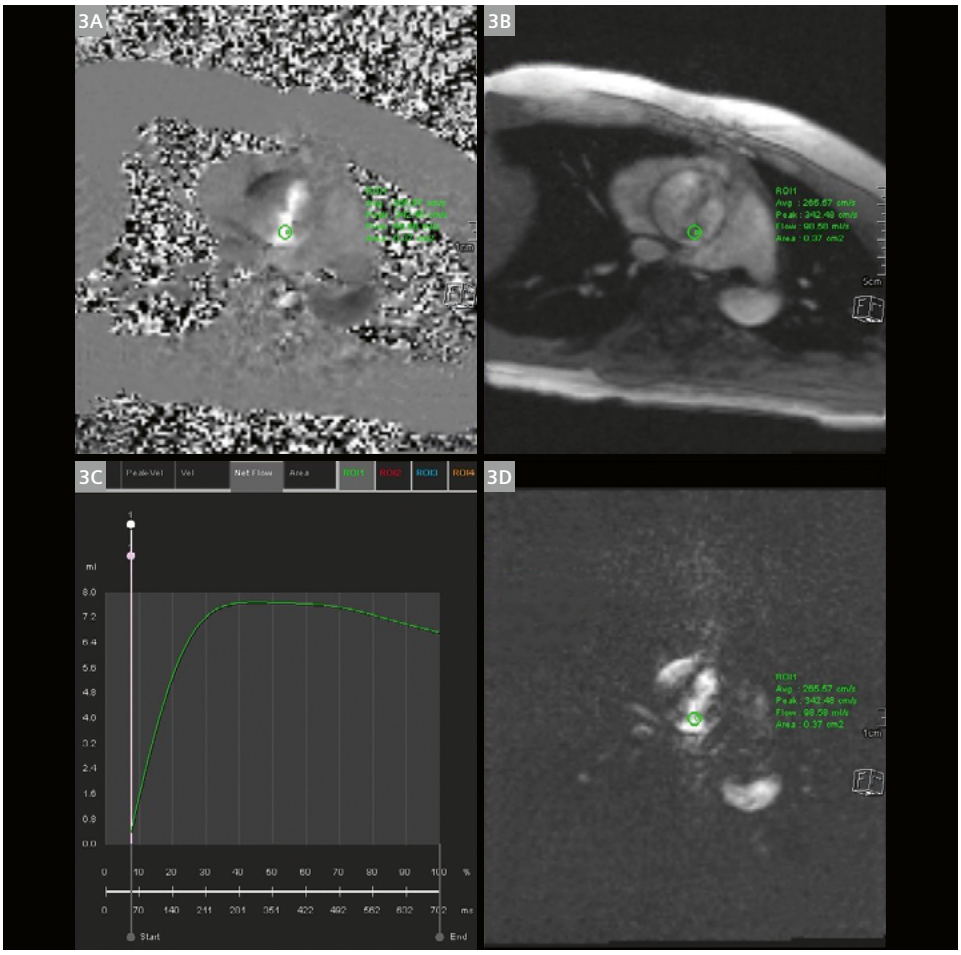

Case 4

75-year-old female patient with myocardial fibrosis, and with tricuspid, mitral, and aortic insufficiency.
(4A) STIR short-axis view;
(4B) Cine 3-chamber view;
(4C) LGE 4-chamber view

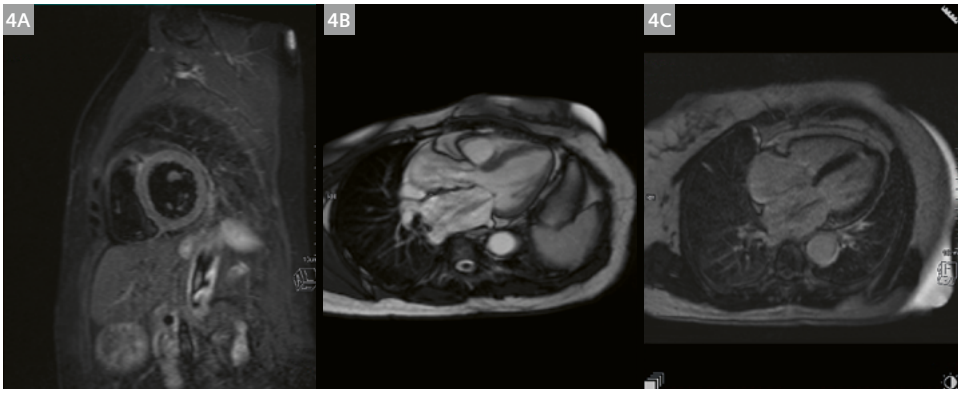

Contact

Bianca Samsula
ZEMODI – Zentrum für moderne Diagnostik
Schwachhauser Heerstraße 63a
28211 Bremen
Germany
bianca.samsula@zemodi.de

Try them on your system

Trial licenses for many of the applications featured in this issue of MAGNETOM Flash are available as a trial license free of charge for a period of 90 days.

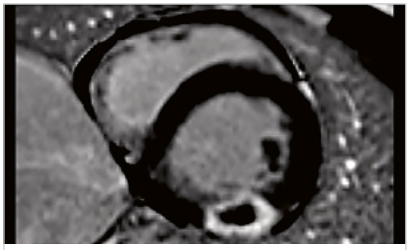

PSIR HeartFreeze

Late Gadolinium Enhancement (LGE) imaging in free-breathing.

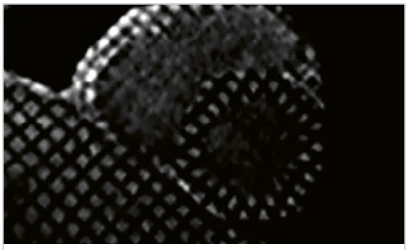

Advanced Cardiac

Special sequences and protocols for advanced cardiac imaging.

MyoMaps

The next step in quantitative cardiac assessment.

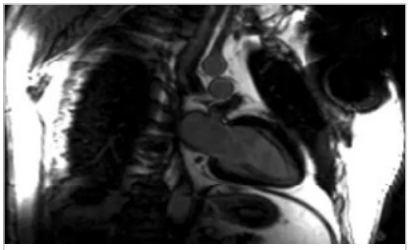

High Bandwidth Inversion Recovery

Cardiac inversion recovery for patients prone to susceptibility artefacts.

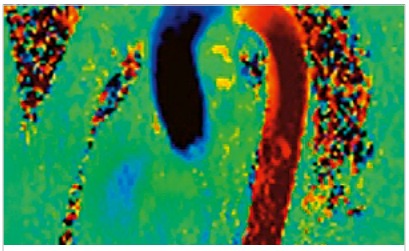

Flow Quantification

Special sequences (only AWP) for quantitative flow determination studies, measuring blood/CSF flow non-invasively.

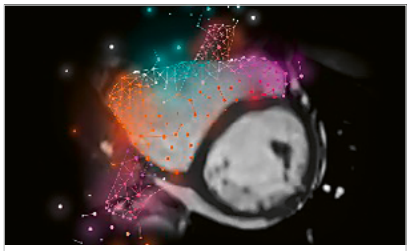

Compressed Sensing Cardiac Cine

Beyond speed.
Beyond breathholds.

Additional technical prerequisites may apply. Upon receiving your request, your local Siemens Healthineers representative will clarify whether your system meets the requirements.

For further details, product overviews, image galleries and general requirements please visit us at:

www.siemens-healthineers.com/magnetic-resonance-imaging/options-and-upgrades

Skip the Electrodes, But Not A Beat: The Engineering Behind the Beat Sensor

Peter Speier, Ph.D. (manuscript) and Mario Bacher (box texts)

Siemens Healthineers, Erlangen, Germany

Introduction

Early in the development of cardiac MR, even long before bSSFP/TrueFISP made it clinically useful [1], the ECG was established as the standard trigger source [2] despite its well-known drawbacks of complex patient preparation and MR-related artifacts caused by the magnetohydrodynamic (MHD) effect and the radio frequency (RF) pulses of the MR measurement [3, 4]. Its main advantage is the early and well defined trigger time point based on the R-wave that precedes the ventricular contraction.

The only other clinically adopted cardiac trigger method is the finger-tip pulse sensor peripheral plethysmogram (PPG) [5], but its late and patient-state-dependent trigger position in the cardiac cycle reduces both its versatility and stability. Therefore, PPG is used only as a back-up.

Over the years, the reliability and ease of use of the ECG have been improved dramatically by the introduction of the vector ECG [6], wireless connections, and standardized handling procedures [3, 4]. Still, over the last 12 years, quite a few alternative methods of cardiac triggering have been proposed [7–12], indicating that there is still a need for more reliable and easier-to-use cardiac trigger methods. Some of these methods are based on optical or mechanical measurements. However, the MRI scanner is already a very sophisticated electromagnetic signal generation and sensing device. Therefore, trigger methods like the BioMatrix Beat Sensor (Glossary), which are based on electromagnetic effects are a good match as they can re-use already existing facilities of the MRI machine.

BioMatrix Beat Sensor – the Pilot Tone

The development of the BioMatrix Beat Sensor started with a power pitch presentation that I attended at the ISMRM 2014 in Milan, Italy. It was about respiratory noise navigation and was given by Anna Andreychenko [13]. It is well known that respiration modulates the electric load of the MR receiver coils. If the receivers are matched to maintain constant signal under load variations, this results in a modulation of the thermal noise power. Andreychenko demonstrated that respiratory navigation can be derived from measurements of the noise power. I was intrigued by this method and tried it out upon my return from the conference. I quickly realized that the number of noise data points required to characterize respiration is quite high and difficult to achieve during fast measurements like bSSFP. Luckily, I remembered a presentation that Lars Hanson had given at the IDEA developer conference in Freiburg, Germany, back in 2007 [14]. There, he described a system for "burning" electroencephalography (EEG) information into MR images by modulating the information onto a weak RF carrier close to Larmor frequency. The modulation is extracted by the MR receiver together with the MR data, and the EEG data appears as a stripe artifact in the image, or, if the carrier frequency is placed just outside of the frequency band of the image, i.e., in the oversampling region, the MR data remains uncontaminated by the additional signal. I postulated that any body-motion would modulate a constant coherent RF signal and that the achievable SNR per unit time would be higher than for noise navigation. I discussed the idea with a few experts in the factory in Erlangen who agreed that it should be feasible to use the signal for respiratory navigation. Markus Vester suggested the term "Pilot Tone" (PT) for the new motion-sensing method. In communication engineering, a Pilot Tone refers to a reference signal that is transmitted together with the payload signal to characterize the transmission path.

We presented our case and received approval from MR management for an initial cross-departmental investigation. We started the first volunteer tests with an off-the-shelf signal generator in the control room connected through the wave-guide hole to an untuned pickup loop taped to the funnel of a 1.5T MAGNETOM Espree. For the setup, see Figure 1A. The first experiment featured a series of breath-holds alternating between inspiration and expiration. We looked at the data in the command line tool *measdataviewer* directly on the scanner and could immediately see a strong and clean modulation with respiratory position. Over the year, we continued experiments and built an inline-processing module in our image reconstruction environment ICE that would generate live respiratory information and clean up the MR data. I presented the initial results at the ESMRMB 2015 in Edinburgh, UK [15].

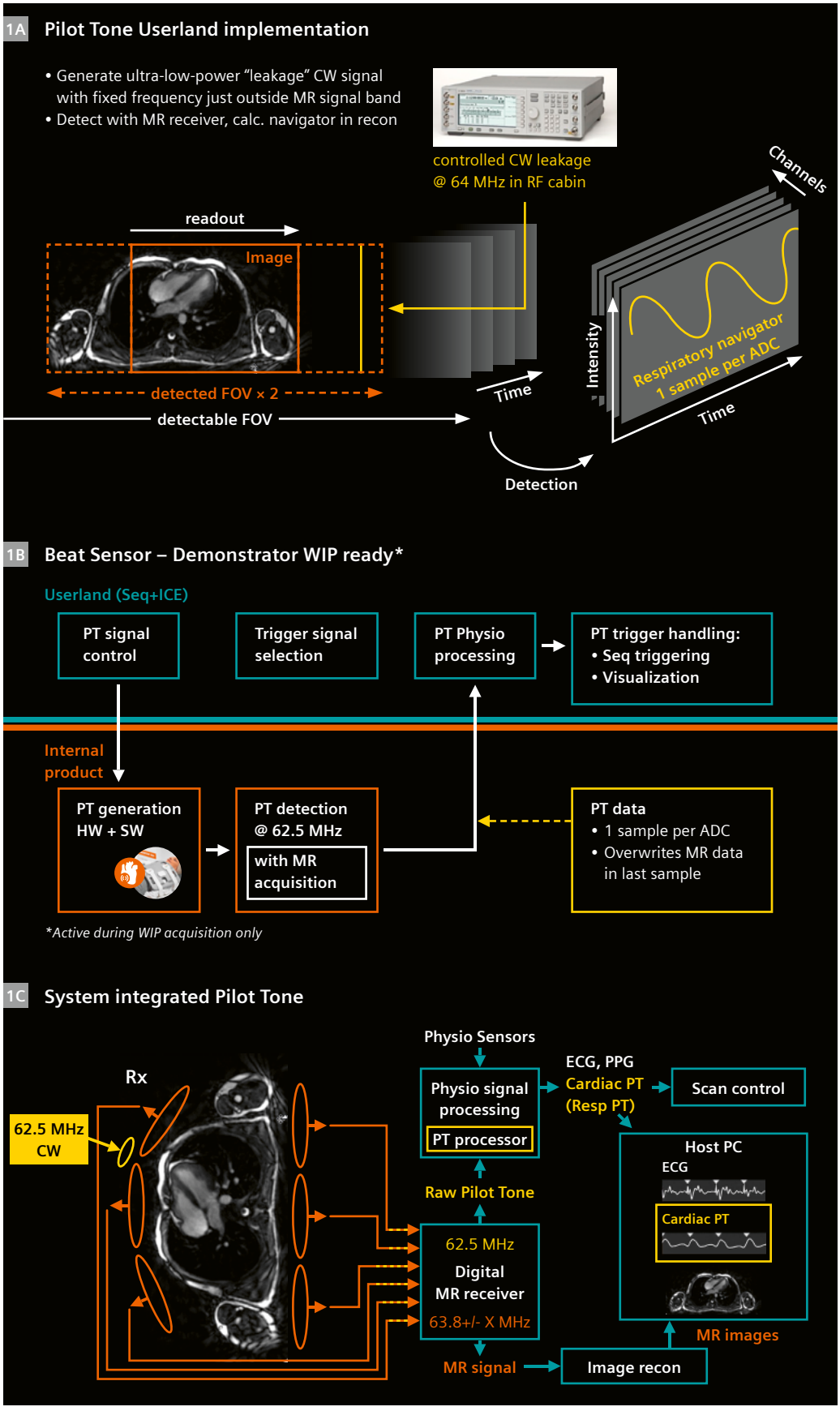

1 Three integration levels of the Pilot Tone subsystem: **(1A)** Vendor-independent "userland" implementation; **(1B)** Integrated PT generation and detection for increased signal stability for experimental use by collaboration partners; **(1C)** Fully integrated PT subsystem to continuously provide physiological information.

Since this abstract is difficult to obtain, it is reprinted with kind permission of ESMRMB in the Appendix.

In summer 2015, we started a collaboration with Fernando Boada's group at CAI2R at NYU. They set up their own version of the experiment on their Biograph mMR and published their first results at the ISMRM 2016 in Singapore [16]. They have continued to develop respiratory PT applications for MR-PET [41, 17] and they even offer their own version of a battery-powered PT generator[1]. Other sites also built their own PT setups for respiratory work and investigated its application to free-breathing MR Fingerprinting (MRF) [18] and prospective slice tracking in free-breathing cardiac MRI [19, 20].

This "userland"[2] approach to PT applications is vendor agnostic, but has three main drawbacks which introduce complications that can reduce their stability:

1. The PT data is acquired only when the sequence plays out an ADC. So, if the measurement is not continuous (e.g., a cine), but contains recovery periods or other pauses (e.g., TSE), no PT data is available in the pauses unless the sequence is modified to fill the gaps with ADCs. However, additional ADCs increase the raw data size significantly. Also, there is no PT data in pauses between measurements.
2. The frequency of the PT must be adapted to the frequency band used by the current protocol: It must fall into the oversampling region that is outside the reconstructed frequency band but inside the oversampled band. The width of the frequency band depends on the protocol (the receiver bandwidth). In addition, the band shifts with in-plane slice shifts in readout direction. The frequency selection becomes easier to fulfill if the oversampling factor (standard is factor 2) is increased, but this also increases the raw data size by the same factor and might not be possible for protocols that utilize high receiver bandwidth.

[1] *https://cai2r.net/resources/3t-pilot-tone*

[2] *The term "userland" is used here in analogy to the usage in the Linux community to denote functionality programmed only using the vendor-provided programming toolset, for MRI typically limited to sequence and image reconstruction.*

Box 1: A history of electromagnetic monitoring and MR

In 1958, YE Moskalenko, who worked on electroplethysmography in the context of the Russian space program, demonstrated that a radar transmission setup operating at 1 GHz (much higher than the operating frequency of a clinical MRI scanner) could be used to observe respiration and cardiac activity [33].

The first report on an electromagnetic navigation (EMN) signal at low frequency observed in humans was published ten years later by Tarjan and McFee [34]. Their goal was a contactless measurement of blood volume. They adapted a method known in geophysics as an "induction measurement": They projected a magnetic field with a frequency of only 100 kHz into the chest of a volunteer and observed the resulting field with a set of two coaxially aligned receive coils while suppressing direct coil-to-coil coupling. A change in body conductivity would result in a modulation of the received field. They observed a modulation of a few percent due to respiration and a smaller modulation due to cardiac motion of about one percent. They also noted that the signal seems to represent cardiac volume change.

While it has been known in NMR and MRI that an electrically conductive sample loads the coil, and that for optimal efficiency and SNR, the coil must be tuned and matched to the sample, the effect was not exploited for physiologic monitoring until 1988, when Buikman et al. proposed to measure the modulation of the reflection of an RF pulse in the body coil to record respiratory and cardiac information [35].

However, the idea was not picked up widely until quite recently, when new developments enabled robust separation of the different modulation sources: the availability of near-infinite computing power, the availability of massively parallel receive systems on virtually all clinical MRI scanners, and the availability of highly parallel transmit systems on high-field MRI scanners. Where highly parallel transmit systems are available, the reflection of all their elements can be monitored during RF pulses [36]. When measuring the coupling between all elements, high-quality rich data is obtained that allows separation of multiple motion contributions [37], but only while transmitting RF pulses.

The noise navigator [13] and the Pilot Tone [15] require multi-channel capability on the receive side only. Therefore, they can be implemented on all modern MRI systems and while the MR receiver operates, navigation data can be obtained.

The most recent development in EMN for MRI is the "Beat Pilot Tone" [38]: The method removes the requirement that the PT frequency be near the Larmor frequency by generating the signal close to the Larmor frequency only in the MR receive chain as an intermodulation product of two electromagnetic signals with higher frequencies, where these two frequencies are separated by approximately the Larmor frequency. This approach allows low-cost integration of EMN at radar frequencies into the MR scanner by using the MR receive system as a continuous wave (CW) radar detector.

3. The PT appears as a peak in the Fourier-transformed ADC. The peak position is a function of the PT frequency and the scanner's detection frequency; thus, it depends on the slice geometry, i.e., on the off-center shift in readout direction. This correction is deterministic and can be calculated exactly from protocol parameters and raw data headers. However, the eddy current compensation contains a B_0 correction, which is realized by varying the receive frequency. The correction thus generates additional, small transient shifts in the PT peak position when gradients are applied. These will become noticeable when the eddy current steady state changes markedly, e.g., when toggling between slice orientations. To avoid this problem, the PT peak position must be redetermined with every substantial change in the gradients, e.g., when switching slice orientations or when playing out large phase encoding jumps. In addition, the PT frequency from a generator that is not synchronized to the MR scanner will drift with time, and the detection frequency must be adapted if the drift is too large.

To eliminate these problems, we integrated the Pilot Tone generation into the MAGNETOM architecture as a prototype. The solution was to generate the PT at a fixed frequency and detect it directly after digitization before the "userland" signal with all corrections is derived. This made it necessary to implement the PT detection in firmware. To save field-programmable-gate-array (FPGA) resources we picked as frequency Nyquist/2 in the digitized frequency band, where the detection algorithm would not require multiplications but only additions. This led to the currently used PT frequency 62.5MHz @ 1.5T. To avoid drifts of the PT signal in frequency and phase, and thus enable complex valued processing, the PT signal is generated by the scanner itself using a "spare" frequency generator.

In parallel, we continued to explore the possibilities of the new method in a master's thesis in the cardiac predevelopment team, together with the local university [21]. Our department head, Lars Lauer, challenged us to extend the scope of the thesis beyond respiratory navigation and aim for cardiac triggering. At that time, we had no indication that this would be feasible, as we had never seen a cardiac signal with our remote generator set-up. If we had studied the scientific literature better (Box 1), we might have been more hopeful, but this only happened in the following master's thesis [22]. Halfway into Lea Schröder's thesis, Jan Bollenbeck built a battery-powered PT generator that could withstand the RF pulses of the MR experiment. The aim was to place the generator closer to the patient's chest to reduce sensitivity to non-respiratory motion, e.g., head or foot movement. We first attached the generator to the scanner's inner bore cover over the chest and didn't see anything new. However, when we placed it directly on the chest of the volunteer, we could see the cardiac signature directly in the raw data. These results were presented at ISMRM 2016 in Singapore [23] (Fig. 2). Internally, they also raised a lot of interest because of the potential for developing the new method into an alternative to ECG.

These initial results were seen promising enough to start the product integration. The first goal was to enable collaboration sites to start their own PT experiments with an integrated, stable, and easy-to-use system that featured local PT generation. I was able to convince Peter Gall, the product manager of the new system platform that was in the planning stage at that time, to include the necessary hardware (HW) and software (SW) in the system project.

Early in 2016, we started a second master's thesis on PT, this time with the Graz University of Technology in Austria, to further develop the cardiac application of the PT [22]. Using a second generation of the battery-powered PT generator, Mario Bacher ran a volunteer cohort study and developed signal processing SW for retrospective and

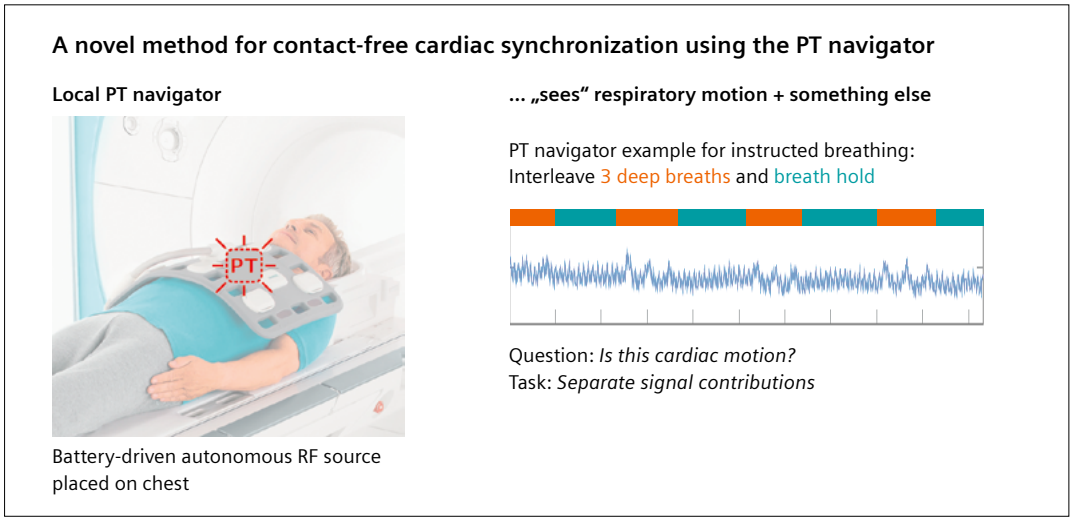

2 The key slide from [23] demonstrates that cardiac motion can be detected using a locally generated Pilot Tone.

Box 2: PT physics: The transformer model

The PT signal, like all electromagnetic applications, is a result of the Maxwell equations ;-) To understand real-world scenarios, especially complex ones like humans, numerical simulations are required. However, insight into the basic principles can be obtained with idealized, simple models: the main mechanism of the PT modulation by cardiac motion can be understood by comparing the setup to an electric transformer. The pre-condition is that the PT-generating loop is much smaller than the electromagnetic wavelength and thus mainly generates a magnetic field and only a negligibly small electric field. Thus, the PT is a purely magnetic signal which exists only as a near field; contrary to radar, which is a self-propagating electromagnetic wave, used in its far field.

A transformer consists of two coils: The primary driving coil (yellow, left side) produces an oscillating magnetic field. The resulting flux through the second coil (yellow, right side) induces a voltage. The flux between the coils is maximized by connecting the two coils with a magnetic, but non-conductive medium. Luckily for us MRI people, the human body is only weakly magnetic and it conducts electricity quite well. Therefore, the body can be seen as a magnetically transparent but lossy transformer core. The primary magnetic field (blue) will generate eddy currents in the tissues (orange), depending on the local conductivity. These eddy currents in turn generate secondary magnetic fields (orange). The secondary field opposes the primary field at the point of origin. In this example we observe the superposition of both fields in the receive coil on the right where both field lines point in different directions. Thus, depending on the geometry the secondary field can cause decreasing or increasing amplitude and/or phase shifts.

The body consists of tissues that have different electrical conductivity and change their position during motion. When conductive tissues move, the eddy current distribution changes and the net secondary field with it. The resulting modulation of the received fields is observed as the Pilot Tone signal. Even though the heart is relatively small, its motion is clearly observable because during cardiac contraction, highly conductive heart muscle and blood are replaced by weakly conductive fat and lung tissue.

As mentioned earlier, the Pilot Tone frequency needs to be chosen fairly close to the Larmor frequency: 62.5 MHz for 1.5T systems. Again, we were lucky: These frequencies hit a sweet spot where on the one hand wavelengths are long enough (2.4 m to 4.8 m in a vacuum, a few dezimeters in tissues) so that the signal penetrates the body quite freely and can therefore be described by this simple model, and where, on the other hand the frequency is high enough that the induced eddy currents and consequently the secondary magnetic fields are strong enough to be easily detected.

All these factors together enable reliable detection of cardiac, respiratory, and even head motion at standard clinical field strengths. However, as Anand et al. [38] have shown, exciting opportunities also await at very high frequencies! When venturing into the GHz range, the transformer model is no longer applicable, as we are entering the domain of radar. Here, higher order interactions start to dominate the signal and limit its penetration into the body, which is expected to optimize the detection of rigid motion.

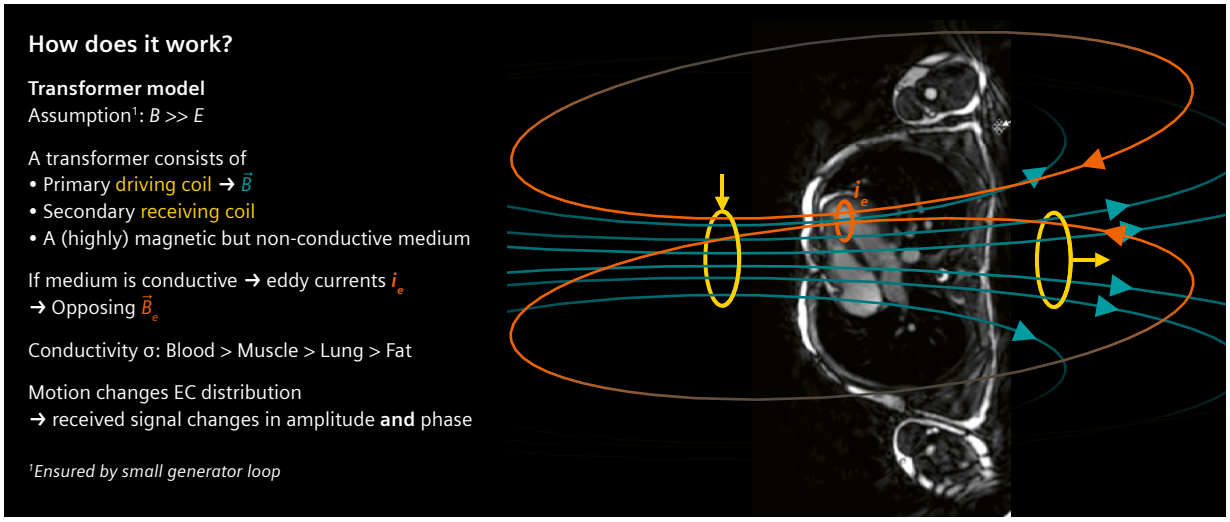

finally also for prospective cardiac triggering (Box 3). He obtained his first prospectively triggered cardiac cine still with a battery-powered generator and a pure "userland" implementation. He went on to work on a PhD thesis on the topic at Lausanne University Hospital (CHUV) in Switzerland. In his work, he also unearthed the early history of electromagnetic navigation and its use in MRI (Box 1), and the physics of signal generation (Box 2).

For the first version of the integrated PT-generation and detection system, (Fig. 1B) the PT was generated inside the new BioMatrix 12 coil. The PT was still detected only during ADCs and evaluated in ICE, but it was already much more stable. In this context, the term "Beat Sensor" was introduced to describe the cardiac application of the Pilot Tone (Glossary). This system was subsequently used at the Royal Brompton Hospital (RBH) in London, UK, to acquire the first cardiac PT patient data [24], and at CHUV and Ohio State University (OSU), Columbus, OH, USA, to develop and evaluate respiratory and retrospective cardiac applications (see e.g., Falcão [25] and Chen [26]).

Developing a robust and complete cardiac PT application takes time, and we went through several releases that gradually moved us closer to the current product. First, we implemented a general PT framework (see Fig. 1C) with the following main features:

- An acquisition-independent and continuously acquired PT data stream, with samples being flagged as invalid during RF pulses
- Pairing each PT sample with information about the preceding RF pulse to enable spike subtraction
- A PT-processing framework that can be exchanged and reconfigured for individual measurements to enable rapid prototyping and work-in-progress packages.

The first point amounts to quite a substantial paradigm shift: Before, the MR receiver had to be configured and active only during measurements. Now, the receiver had to be always configured and active to receive PT data during and between measurements. To achieve this, a dedicated team spent much of the development time

Box 3: Signal processing basics

A key advantage of the PT method is the use of all connected coil elements for receiving the PT signal. Each receive coil "sees" a different combination of cardiac, respiratory and other motion, depending on its location. Since we are interested in observing cardiac and respiratory motion by themselves, these components must be separated first.

This can be accomplished by a class of algorithms known as "Blind Source Separation". The problem statement is simple: Given a multitude N of sensors measuring signals x which are a combination A of M < N independent signals, separate the underlying signals s.

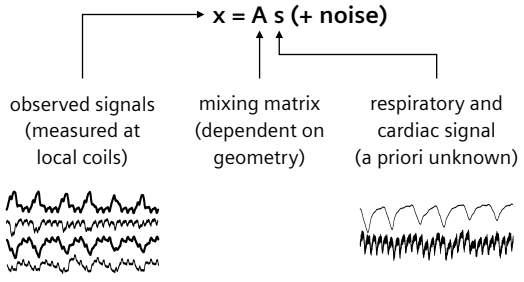

In other words: the equation needs to be solved for A, the so-called mixing matrix. Initially we used FastICA (Independent Component Analysis, [39]), in which the non-Gaussianity is optimized as a proxy for statistical independence [22]. While this algorithm worked well for Cine sequences, which are not affected by RF interference, a new PCA-based algorithm was developed in collaboration with the Shenzhen team, based on [27], in which the RF contamination of the PT signals is minimized by mixing vectors that are orthogonal to the main principal components of the eigenspace of interference signals.

To enable robust cardiac triggering, the cardiac motion signal needs to be de-noised in real-time. Classical digital filters, however, would introduce an unacceptably large time delay for the cardiac application (e.g., > 600 ms for an 80 dB stopband FIR lowpass at 6 Hz).

In [12, 22], we proposed to use a Kalman filter to denoise the signal. A Kalman filter, named after Rudolf E. Kalman, is an algorithm that uses a series of measurements, including noise and other inaccuracies, and attempts to fit these measurements in a least-squares sense to a predefined signal model. In our case, the signal is modeled using a constant velocity motion model similar to Spincemaille et al. [40], in which the signal evolution is modeled as the 1D motion of a particle with constant velocity. This approach has two additional advantages: First, it does not only provide a de-noised signal, but also an estimation of the signals first derivative, i.e., velocity, which is subsequently used for trigger detection (see Box 4). And second, it can interpolate over short gaps in the data that occur while sending RF pulses.

on writing and debugging the HW–SW interconnectivity. The flexible processing framework drastically sped up the subsequent development by enabling us to test new code on previous stable baselines and SW versions. To minimize porting efforts, we kept interfaces constant and minimized dependencies on other modules.

In 2021, we released the first clinical application: Beat Sensor triggering for Cines only. The limitation to Cine was necessary because we had not yet implemented a general RF-artifact compensation, and for Cine a simple signal average is sufficient. Most of the development time was spent on optimizing signal processing and workflow. For about one year we had regular volunteer shifts to test stability and usability of the latest developments. A lot of time was spent on the special coil handling required for Beat Sensor-triggered measurements: The PT signal is acquired using the coil elements currently selected for imaging, and signal-processing training is valid for one coil select only. Therefore, Beat Sensor-triggered protocols must automatically select the coils used in training.

While the team in Erlangen, Germany, had been working towards productization of the cardiac application of PT, the Siemens Healthineers development team in Shenzhen, China, had been developing the respiratory application of PT. After an initial ramp-up phase, the team in Shenzhen independently developed and released a first product for respiratory triggering on MAGNETOM Amira – A BioMatrix System. After this release, the two groups intensified their collaboration: Yan Tu Huang in Shenzhen integrated his respiratory processing into the PT framework, and several algorithms were exchanged between the sites and applications. The cardiac application benefited most by rebasing on the robust method for RF-artifact suppression [27] that Shenzhen had developed for the respiratory application. We jointly extended this algorithm for the cardiac application. Based on this algorithm we were able to stabilize

Box 4: PT signal characteristics and trigger time point

The cardiac component of the Pilot Tone closely follows the cardiac volume curve without a delay: At the time of the R-wave, in end-diastole, when the heart is fully expanded, it assumes its maximum value. During end-systole, when the heart is fully contracted, it assumes its minimum value, and during the static mid-diastolic period it plateaus at an intermediate value. The Beat Sensor signal, shown on the right, is the inverted time derivative of this cardiac component. It has the advantage that it features a rather narrow positive peak at the beginning of the cardiac cycle and provides additional suppression of respiratory contamination.

The Beat Sensor triggers when the systolic contraction starts (specifically, when the derivative reaches 40% of its maximum value). This trigger point was chosen for its stability and occurs approximately 100 ms after the R-wave. This wave delay is learned during the Beat Sensor training phase using only the waveform of the cardiac component as the distance between trigger point and the preceding maximum. Low-pass filters in the signal processing add roughly 100 ms to this, resulting in a total delay of about 200 ms. If a finger pulse sensor (PPG) is present as well, its delay with respect to the R-wave is also determined.

One crucial functionality for cardiac exams is "Capture Cycle": based on the current heart rate, an algorithm places the acquisition in the end-diastolic cardiac phase where motion is minimal. For the ECG, that triggers on the R-wave, this placing is achieved by maximizing the trigger delay. For Beat Sensor and PPG triggering, the algorithm has been modified to account for the trigger delays learned during Beat Sensor training. Thus, after the training "Capture RR" can be used for all three trigger sources.

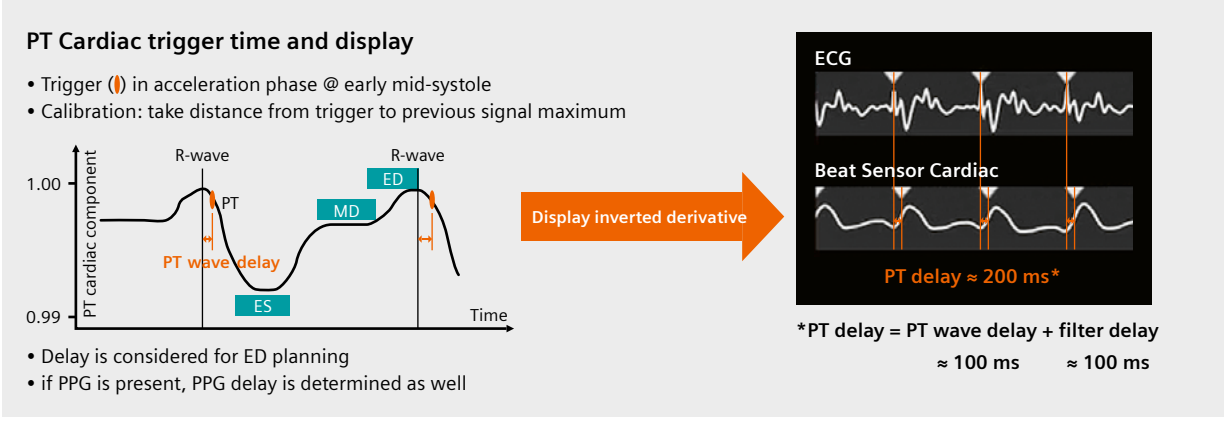

cardiac triggering for all cardiac protocols. The signal characteristics of the current implementation are described in Box 4.

To collect customer feedback early, we developed a work-in-progress package (WIP) of Beat Sensor triggering for the whole cardiac exam. The WIP was initially installed at four different sites (Jan Yperman Hospital, Ieper, Belgium; Royal Brompton Hospital, London, UK; Ohio State University, Columbus, OH, USA; and Northwestern University (NWU), Evanston, IL, USA). While the feedback on clinical performance was positive [28–30], the calibration workflow proved to be too complex and error-prone. Thus, we reworked and hardened the calibration workflow just before the development deadline and could release Beat Sensor triggering for the whole cardiac exam for the current SW version *syngo* MR XA51A for the 1.5T BioMatrix Systems MAGNETOM Sola, MAGNETOM Altea, and MAGNETOM Sola Fit. The next SW version for 3T systems will bring this functionality to MAGNETOM Vida and MAGNETOM Lumina.

The development of PT-based methods is ongoing. The clinical use of the first complete release of the Beat Sensor will certainly reveal limitations, but it will also show distinct advantages when compared with the ECG. We are committed to removing limitations and turning the advantages into clinically useful features. So please try out the Beat Sensor in your clinical routine and let us know about your experiences.

Looking beyond cardiac to general motion management, the use of Pilot Tone is still in its infancy and we have only scratched the surface of many aspects and applications. Two examples are two-dimensional characterization of respiration [31] and characterization of head motion [32]. The scanner-integrated PT with its continuous data stream and its flexible processing framework is a powerful tool to enable these upcoming investigations and developments.

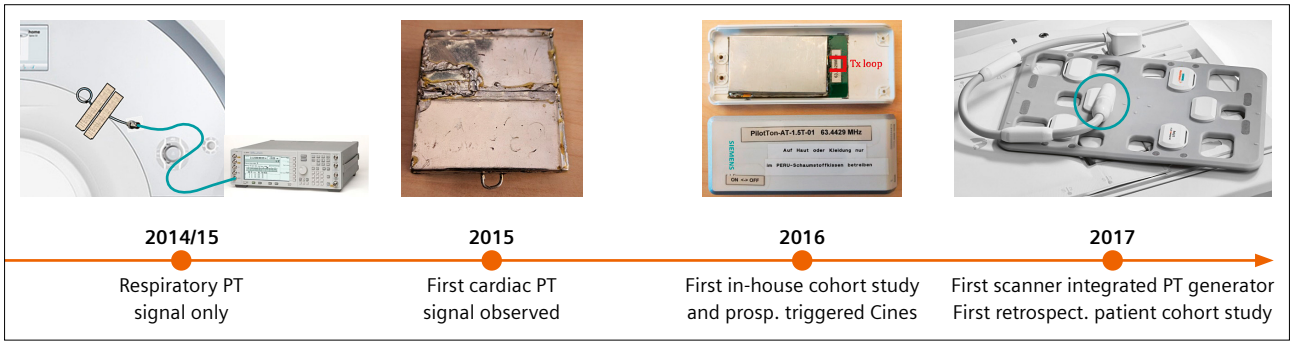

3 Four generations of Pilot Tone generators: From initial respiratory experiments to a scanner-integrated solution.

Acknowledgment

A big Thank you to all contributors. Especially:

- **Generator hardware:** Jan Bollenbeck
- **Physio-SW:** Michael Schwertfeger
- **PT processing:** Mario Bacher, Yan Tu Huang
- **Sequences, exam prototypes and data analysis:** Carmel Hayes, Randall Kroeker
- **Volunteer data:** Manuela Rick
- **Early patient data:** Peter Gatehouse (RBH)

Appendix: Reprint of Ref. 15

PT-Nav: a novel respiratory navigation method for continuous acquisitions based on modulation of a pilot tone in the MR-receiver

P. Speier[1], M. Fenchel[1], R. Rehner[2]

[1]MR PI, Siemens Healthcare, Erlangen, Germany
[2]MR R&D, Siemens Healthcare, Erlangen, Germany

Purpose/Introduction

High-resolution 3D abdominal or cardiac MR imaging requires synchronization to respiratory motion. The motion can be tracked by dedicated respiratory sensors, MR navigators, selfgating algorithms, or, as recently proposed, by analyzing the received noise [1] or measuring load changes of the transmit coil [2]. These methods increase setup complexity, require interruption of steady state, special k-space trajectories and high SNR per scan, long averaging times, or additional scanner-integrated hardware. We hypothesize that a coherent signal from an independent source, received in parallel with the MR signal, can be used as a high-quality navigator that does not suffer from the drawbacks of the previous methods.

Subjects and methods

Continuous series of sagittal bSSFP or GRE images (500...1000 images, 3...5 images/s, (1.5...2 mm)^2 × 10 mm) of the right liver dome were acquired with anterior and posterior multi-channel receive coils. Meanwhile, a continuous-wave (CW) RF signal, generated by a commercial signal generator, was transmitted as a pilot tone into the magnet bore by a non-resonant pickup coil, placed on the table or outer magnet cover, with a frequency outside of the frequency band of the MR signal and the FOV, but inside the received frequency band, and an amplitude adjusted to be detectable in the linear operating regime of the receiver.

Image reconstruction was modified in-house for pilot tone detection: During a learning phase, the pilot tone frequency f in the received data was determined. Then, for each k-space line and channel, the pilot tone was fit to the model $A \times \exp(i2\pi ft)$, the complex amplitude A logged as PT-navigator, and the model subtracted from the data (Fig. 1). Offline processing was performed in MATLAB (Math-Works). The positions of the liver dome (HF direction) or abdominal wall (AP direction) were tracked in the images, and their correlations to low-pass (1 Hz-Hann-window)-filtered PT-navigators were calculated for all channels.

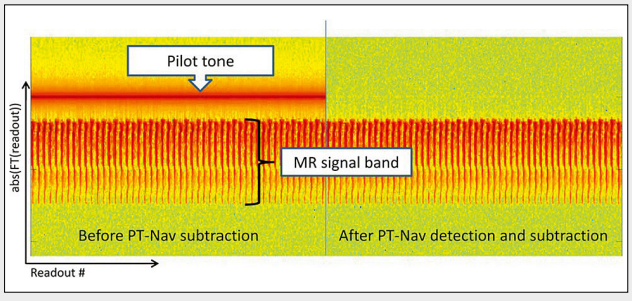

1 Exemplary Fourier-transformed raw data (one channel), demonstrating successful detection and elimination of a pilot tone placed next to the MR-signal band

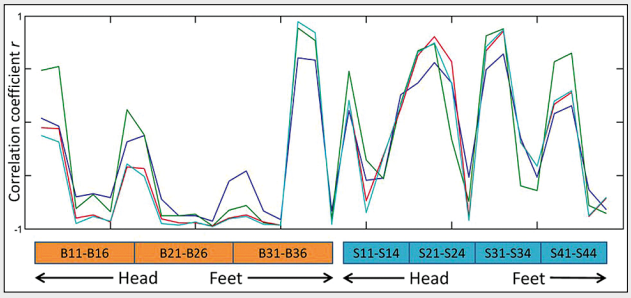

2 Exemplary correlation coefficients of anterior (orange) and posterior (blue) coil elements for 4 measurements of volunteer B

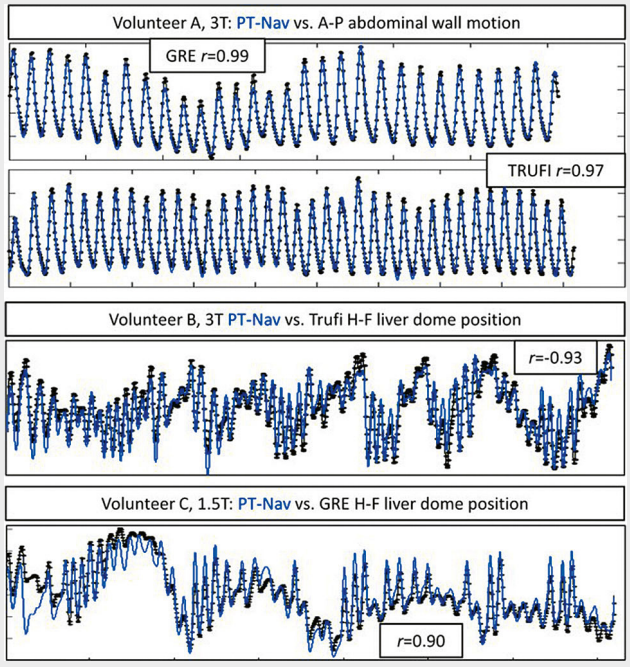

3 Exemplary correlations between best PT-Nav channel and image-based navigators (curves shown after mean subtraction and amplitude normalization)

Results

Measurements of 5 volunteers were performed on three systems (MAGNETOM Espree, Aera, and Skyra, Siemens Healthcare). Correlation factors varied in sign and amplitude between channels (Fig. 2). For all volunteers, receive channels with high correlation coefficients $r \geq 0.9$ were found while volunteers laid still, allowing precise characterization of even quite irregular respiratory patterns (Fig. 3). Correlations could be slightly improved by combining channels.

Discussion/Conclusion

Our early results suggest that the proposed PT-Nav method can provide, with minimal hardware requirements, respiratory information for continuous sequences that is comparable to that of "gold-standard" MR navigators.

References

1 A. Andreychenko, ISMRM 2014, #92.
2 I. Graesslin, ISMRM 2010, #3045.

Glossary

Electromagnetic navigation (EMN)
Characterizing motion by its influence on low-frequency electro-magnetic fields inside the body, used here with a focus on scanner-integrated methods

Pilot Tone (PT)
MR-integrated EMN, the only hardware part is the field generator

BioMatrix Beat Sensor
1. Cardiac application of Pilot Tone
2. Hardware integrated Pilot Tone generator (BioMatrix 12, BioMatrix 18 coils)

BioMatrix Respiratory Sensor
1. Respiratory Sensor hardware in BioMatrix Spine coils on 1.5T MAGNETOM Sola, and MAGNETOM Altea, as well as on 3T MAGNETOM Vida, and MAGNETOM Lumina (this is EMN, but not PT based)
2. Respiratory PT application on 1.5T MAGNETOM Amira - A BioMatrix System (uses a PT generator in the BioMatrix 13 coil)

Why is "Beat Sensor" an appropriate term for the Pilot Tone generator?
Like the finger pulse sensor, the Beat Sensor is an active sensing method: It emits a signal into the body and receives the motion-induced modulation of this signal. The Beat Sensor hardware, that is built into the BioMatrix 12 and BioMatrix 18 coils, fulfils the function of a signal generator but does not receive the signal. It can be likened to the light emitter in the finger pulse sensor. The role of the light receiver is implemented by modifying the SW of the already existing MR receive system.

HW	Pulse Sensor	Beat Sensor
Generator	Light emitter	PT generator: dedicated hardware in BioMatrix 12 and BioMatrix 18 coils
Receiver	Light detector	PT receiver (reuse MR receive system)

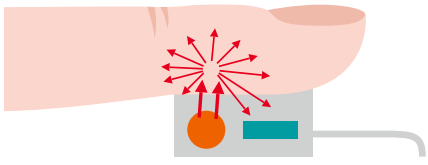

References

1 Carr JC, Simonetti O, Bundy J, Li D, Pereles S, Finn JP. Cine MR angiography of the heart with segmented true fast imaging with steady-state precession. Radiology. 2001;219(3):828-834.
2 Lanzer P, Botvinick EH, Schiller NB, Crooks LE, Arakawa M, Kaufman L, et al. Cardiac imaging using gated magnetic resonance. Radiology. 1984;150(1):121-7.
3 Niendorf T, Winter L, Frauenrath T. Electrocardiogram in an MRI Environment: Clinical Needs, Practical Considerations, Safety Implications, Technical Solutions and Future Directions. In: Millis RM (Editor). Advances in Electrocardiograms. IntechOpen.2012. doi:10.5772/24340.
4 MRI Questions: EKG Detection [Internet]. Elster LLC; 2021 [cited November 29, 2022]. Available from: https://mriquestions.com/ekg-problems.html
5 Denslow S, Buckles DS. Pulse oximetry-gated acquisition of cardiac MR images in patients with congenital cardiac abnormalities. AJR Am J Roentgenol. 1993;160(4):831-3.
6 Chia JM, Fischer SE, Wickline SA, Lorenz CH. Performance of QRS detection for cardiac magnetic resonance imaging with a novel vectorcardiographic triggering method. J Magn Reson Imaging. 2000;12(5):678-88.
7 Frauenrath T, Hezel F, Renz W, d'Orth Tde G, Dieringer M, von Knobelsdorff-Brenkenhoff F, Prothmann M, Schulz Menger J, Niendorf T. Acoustic cardiac triggering: a practical solution for synchronization and gating of cardiovascular magnetic resonance at 7 Tesla. J Cardiovasc Magn Reson. 2010 Nov 16;12(1):67. doi: 10.1186/1532-429X-12-67. PMID: 21080933; PMCID: PMC2998500.
8 Nedoma J, Fajkus M, Martinek R, Nazeran H. Vital Sign Monitoring and Cardiac Triggering at 1.5 Tesla: A Practical Solution by an MR-Ballistocardiography Fiber-Optic Sensor. Sensors (Basel). 2019;19(3):470.
9 Spicher N, Kukuk M, Maderwald S, Ladd ME. Initial evaluation of prospective cardiac triggering using photoplethysmography signals recorded with a video camera compared to pulse oximetry and electrocardiography at 7T MRI. Biomed Eng Online. 2016;15(1):126.
10 Kosch O, Thiel F, Seifert F, Sachs J, Hein MA. Motion detection In-Vivo by multi-channel ultrawideband radar. IEEE International Conference on Ultra-Wideband. 2012:392-396. doi: 10.1109/ICUWB.2012.6340451.
11 Kording F, Schoennagel B, Lund G, Ueberle F, Jung C, Adam G, et al. Doppler ultrasound compared with electrocardiogram and pulse oximetry cardiac triggering: A pilot study. Magn Reson Med. 2015;74(5):1257-65.
12 Bacher M, Speier P, Bollenbeck J, Fenchel M, Stuber M. ISMRM 2018 Paris, Abstract #2960, Pilot Tone Navigation Enables Contactless Prospective Cardiac Triggering: Initial Volunteer Results for Prospective Cine.
13 Andreychenko A, Crijns S, Raaijmakers A, Stemkens B, Luijten P, Lagendijk J, et al. ISMRM 2014 Milan, Abstract #0092, Noise variance of an RF receive array reflects respiratory motion: a novel respiratory motion predictor.
14 Hanson LG, Lund TE, Hanson CG. Encoding of electrophysiology and other signals in MR images. J Magn Reson Imaging 2007, 25(5), 1059-1066.
15 Speier P, Fenchel M, Rehner R. PT-Nav: a novel respiratory navigation method for continuous acquisitions based on modulation of a pilot tone in the MR-receiver. ESMRMB 2015, 32nd Annual Scientific Meeting, Edinburgh, UK, 1-3 October: Abstracts, Thursday, Magnetic Resonance Materials in Physics, Biology and Medicine. 2015; 28:1–135.
16 Koesters T, Brown R, Zhao T, Fenchel M, Speier P, Feng L, et al. ISMRM 2016 Singapore, Abstract #4250, Motion Correcting Complete MR-PET Exams Via Plot Tone Navigators.
17 Solomon E, Rigie DS, Vahle T, Paška J, Bollenbeck J, Sodickson DK, et al. Free-breathing radial imaging using a pilot-tone radiofrequency transmitter for detection of respiratory motion. Magn Reson Med. 2021;85(5):2672-2685.
18 Huang SS, Boyacioglu R, Bolding R, MacAskill C, Chen Y, Griswold MA. Free-Breathing Abdominal Magnetic Resonance Fingerprinting Using a Pilot Tone Navigator. J Magn Reson Imaging. 2021;54(4):1138-1151.
19 Ludwig J, Speier P, Seifert F, Schaeffter T, Kolbitsch C. Pilot tone-based motion correction for prospective respiratory compensated cardiac cine MRI. Magn Reson Med. 2021;85(5):2403-2416.
20 Ludwig J, Kerkering KM, Speier P, Schaeffter T, Kolbitsch C. Pilot tone-based prospective correction of respiratory motion for free-breathing myocardial T1 mapping. MAGMA. 2022 Aug 3. doi: 10.1007/s10334-022-01032-4. Online ahead of print. PMID: 35921020.
21 Schröder, L. Information content of a novel MR navigator relating to physiological activities. Advisors: Haderlein T, Maier A, Wetzl J, Speier P. Siemens Healthcare GmbH. Started June 2015. [Not accessible online].
22 Bacher M. Cardiac Triggering Based on Locally Generated Pilot-Tones in a Commercial MRI Scanner: A Feasibility Study [master's thesis. Graz: Graz University of Technology; 2017. 103 p.] https://diglib.tugraz.at, linked via https://graz.pure.elsevier.com/de/publications/cardiac-triggering-based-on-locally-generated-pilot-tones-in-a-co
23 Schroeder L, Wetzl J, Maier A, Lauer L, Bollenbeck J, Fenchel M, et al. ISMRM 2016 Singapore, Abstract #410: A Novel Method for Contact-Free Cardiac Synchronization Using the Pilot Tone Navigator.
24 Bacher, M. SCMR 2020 Orlando, FL, USA, co-workshop. [Not accessible online].
25 Falcão MBL, Di Sopra L, Ma L, Bacher M, Yerly J, Speier P, et al. Pilot tone navigation for respiratory and cardiac motion-resolved free-running 5D flow MRI. Magn Reson Med. 2022;87(2):718-732.
26 Chen C, Liu Y, Simonetti OP, Tong M, Jin N, Bacher M, et al. Cardiac and respiratory motion extraction for MRI using Pilot Tone-a patient study. arXiv:2202.00055 [eess.SP].
27 Inventors: Huang YT, Zhang QY, Li ZB. Using eigenvector algorithm to reduce RF interference in respiration or heartbeat detection. CN112415453-A. Publication: 2021-02-26.
28 Pan Y, Varghese J, Jin N, Hayes C, Speier P, Ahmad R, et al. ISMRM 2022 London, UK, Abstract #4770: Validation of Beat Sensor Cardiac Triggering against ECG Cardiac Triggering in both Volunteer and Patient Cohorts.
29 Hayes C, Huang YT, Rick M, Kroeker R, Bacher M, Pan Y, et al. ISMRM 2022 London, UK, Abstract #4786: Multi-center evaluation of the novel Beat Sensor Cardiac triggering technology,
30 Lin K, Sarnari R, Speier P, Hayes C, Davids R, Carr JC, et al. Pilot Tone-Triggered MRI for Quantitative Assessment of Cardiac Function, Motion, and Structure. Invest Radiol. 2022. doi: 10.1097/RLI.0000000000000922. Online ahead of print. PMID: 36070525.
31 Schroeder L, Wetzl J, Maier A, Rehner R, Fenchel M, Speier P. ISMRM 2016 Singapore, Abstract #3103: Two-Dimensional Respiratory-Motion Characterization for Continuous MR Measurements Using Pilot Tone Navigation.
32 Speier P, Bacher M, Bollenbeck J, Fenchel M, Kober T. ISMRM 2018 Paris, Abstract #4101: Separation And Quantification Of Head Motion Modes By Pilot Tone Measurements.

33 Moskalenko YE. Utilization of superhigh frequencies in biological investigations. Biophysics (USSR) (English translation).1958;3:619–26. [Only second hand knowledge! We have not been able to get a copy of the original article yet.]
34 Tarjan PP, McFee R. Electrodeless measurements of the effective resistivity of the human torso and head by magnetic induction. IEEE Trans Biomed Eng. 1968;15(4):266-78.
35 Buikman D, Helzel T, Röschmann P. The rf coil as a sensitive motion detector for magnetic resonance imaging. Magn Reson Imaging. 1988;6(3):281-9.
36 Graesslin I, Stahl H, Nehrke K, Harvey P, Smink J, Mens G, et al. An alternative concept for non-sequence interfering, contact-free respiration monitoring. In: Proceedings of the 17th Annual Meeting of ISMRM, Honolulu, HI, USA. 2009:753.
37 Jaeschke S, Robson MD, Hess AT. Cardiac gating using scattering of an 8-channel parallel transmit coil at 7T. Magn Reson Med. 2018;80(2):633–640.
38 Anand S, Lustig M. ISMRM 2021 online, Abstract #0568: Beat Pilot Tone: Exploiting Preamplifier Intermodulation of UHF/SHF RF for Improved Motion Sensitivity over Pilot Tone Navigators.
39 Hyvärinen A. Fast and Robust Fixed-Point Algorithms for Independent Component Analysis. IEEE Trans Neural Netw. 1999;10(3):626-634.
40 Spincemaille P, Nguyen TD, Prince MR, Wang Y. Kalman filtering for real-time navigator processing. Magn Reson Med. 2008;60(1):158-168.
41 Vahle T, Bacher M, Rigie D, Fenchel M, Speier P, Bollenbeck J, et al. Respiratory Motion Detection and Correction for MR Using the Pilot Tone: Applications for MR and Simultaneous PET/MR Examinations. Invest Radiol. 2020;55(3):153-159.

Contact

Peter Speier, Ph.D.
Cardiovascular Application Development
SHS DI MR RCT CLS CARD
Allee am Roethelheimpark 2
91052 Erlangen
Germany
peter.speier@siemens-healthineers.com

Artificial Intelligence-based Fully Automated Global Circumferential Strain in a Large Cohort of Patients Undergoing Stress CMR

Théo Pezel, M.D.[1]; Solenn Toupin, Ph.D.[2]; Teodora Chitiboi, Ph.D.[2]; Puneet Sharma, Ph.D.[2]; Jérôme Garot, M.D, Ph.D.[1]

[1]Institut Cardiovasculaire Paris Sud, Cardiovascular Magnetic Resonance Laboratory, Hôpital Privé Jacques Cartier, Ramsay Santé, Massy, France
[2]Siemens Healthineers

Introduction

Stress cardiovascular magnetic resonance (CMR) imaging has emerged as a very accurate modality for the diagnosis of obstructive coronary artery disease (CAD) without ionizing radiation [1]. Several studies have shown the strong prognostic value of both inducible ischemia and myocardial infarction (MI) above traditional cardiovascular risk factors in patients with suspected or known CAD [1, 2].

Recent studies have also underlined the potential prognostic value of global longitudinal strain (GLS) using feature-tracking imaging (FTI) assessed during vasodilator stress. In particular, perfusion abnormalities on stress CMR are associated with a significant decrease in GLS [3]. Recent data suggest that circumferential strain could be more effective than longitudinal strain in detecting myocardial ischemia [4]. Although recent FTI techniques allow measurement of strain using standard cine CMR images [3], post-processing and inter-observer reproducibility of FTI strain measurements [8], limit their widespread use in clinical routine. Artificial intelligence (AI)-based algorithms can compute left ventricular (LV) strain fully automatically. However, the prognostic value of AI-based fully automated global circumferential strain (GCS) determined during stress CMR is not well established. Therefore, our working group aimed to determine whether AI-based fully automated GCS assessed during vasodilator stress could provide additional prognostic value beyond traditional cardiovascular risk factors to predict cardiovascular events. The aim of this article is to review our experience of more than 15 years with stress CMR in patients using a dedicated workflow, and to present the main findings of a recent work supported by a collaboration with Siemens Healthineers to assess the clinical interest of a new, full-AI automated algorithm[1] for assessing LV strain during a stress CMR exam.

[1] *Work in progress. The application is currently under development and is not for sale in the U.S. and in other countries. Its future availability cannot be ensured.*

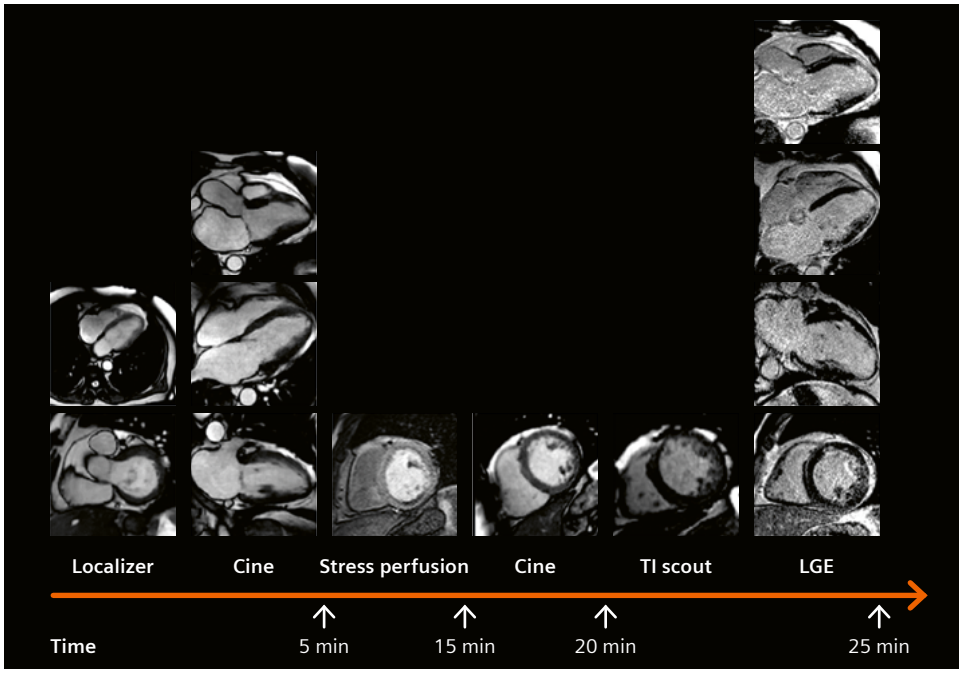

1 Perfusion stress CMR imaging protocol [9] After individual patient planning, short- and long-axis cine images were acquired; then, intravenous dipyridamole was given at 0.84 mg/kg or 0.56 mg/kg over 3 or 4 minutes, and first-pass stress myocardial perfusion imaging was acquired in the short- and long-axis views (typically four short-axis and two long-axis views every other heart beat after 0.1 mmol/kg gadolinium contrast agent bolus through the myocardium at 5 mL/s). Ten minutes after injection, a modified Look-Locker inversion time scout was performed before late gadolinium enhancement (LGE) imaging in short- and long-axis views.

Description of our CMR workflow

In our CMR laboratory, which is accredited by the European Association of Cardiovascular Imaging (EACVI) for stress CMR, we perform stress CMR at 1.5 Tesla using dipyridamole as vasodilator agent following a stress CMR protocol depicted in Figure 1. Following a very standardized, published workflow [9], our CMR laboratory is dedicated to cardiovascular imaging, with designated and experienced staff (eight CMR technologists, one technologist assistant) working on two MR scanners for 55 hours per week per scanner, specifically for CMR (Fig. 2). The medical team

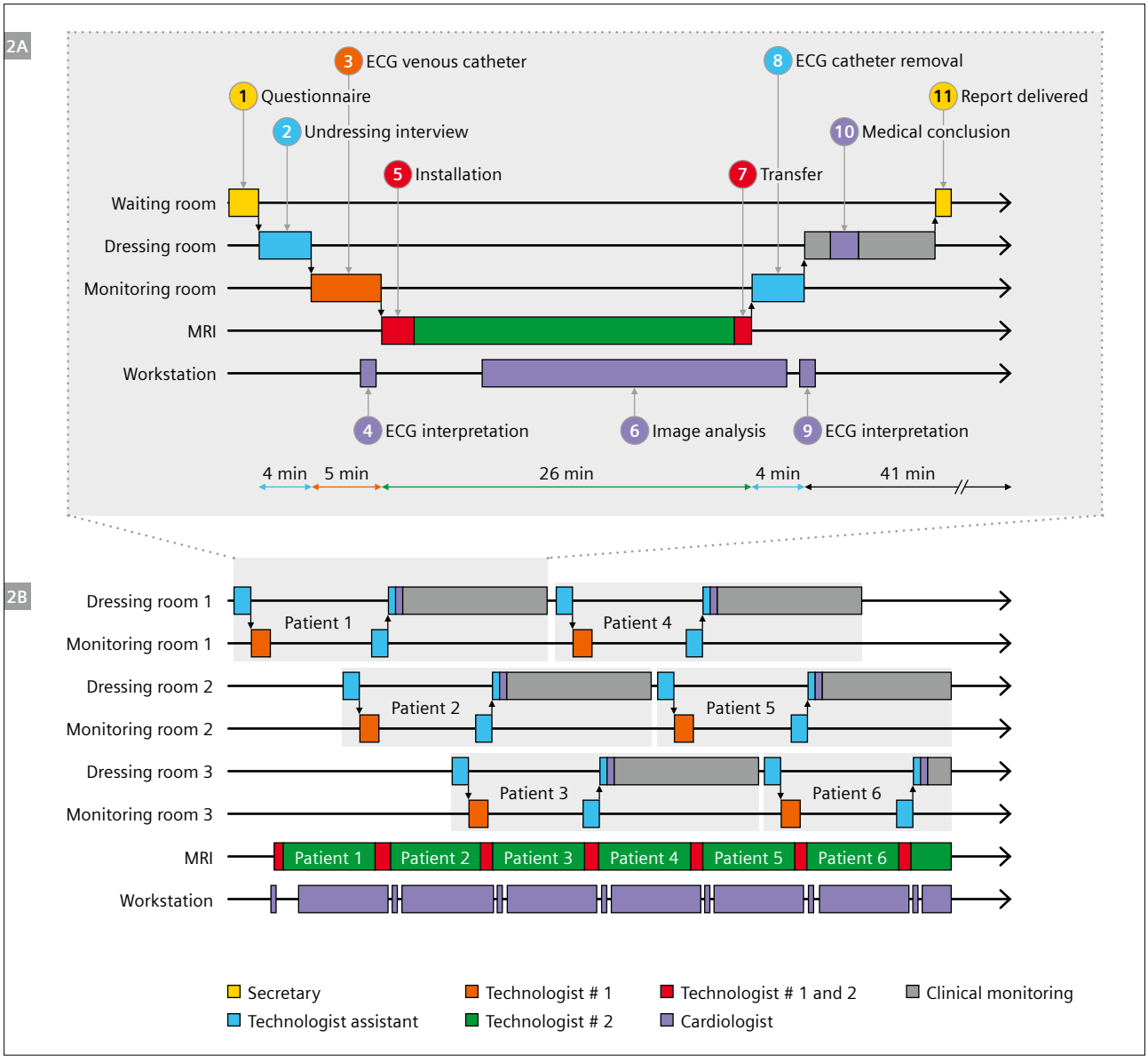

2 **Optimized stress CMR workflow**
The different steps of the final workflow were described at the patient scale **(2A)** and the CMR laboratory scale **(2B)**. On arrival in the waiting room, the patient fills in a questionnaire with the help of the administrative assistant ①. Then the patient undresses in a changing room. The technologist assistant checks the questionnaire and contraindications for CMR and perfusion stress studies, while providing explanations of the CMR study ②. The patient is brought into in a monitoring room on a stretcher, where a 12-lead pretest electrocardiogram (ECG) is performed ③ ④ and a venous catheter is inserted. Both technologists position the patient in the magnetic resonance scanner, with ECG for triggering, appropriate surface coils, and stress-test monitoring ⑤. The cardiologist is present throughout the study, analyses the images and produces a final report shortly after the end of the study ⑥. After performing the stress CMR test, the patient is transferred back to the room on a stretcher ⑦, the venous catheter is removed, and a post-test ECG is performed and interpreted ⑧ ⑨. During a 45-minute clinical monitoring period, the cardiologist provides the final conclusions of the study before discharge ⑩ ⑪.

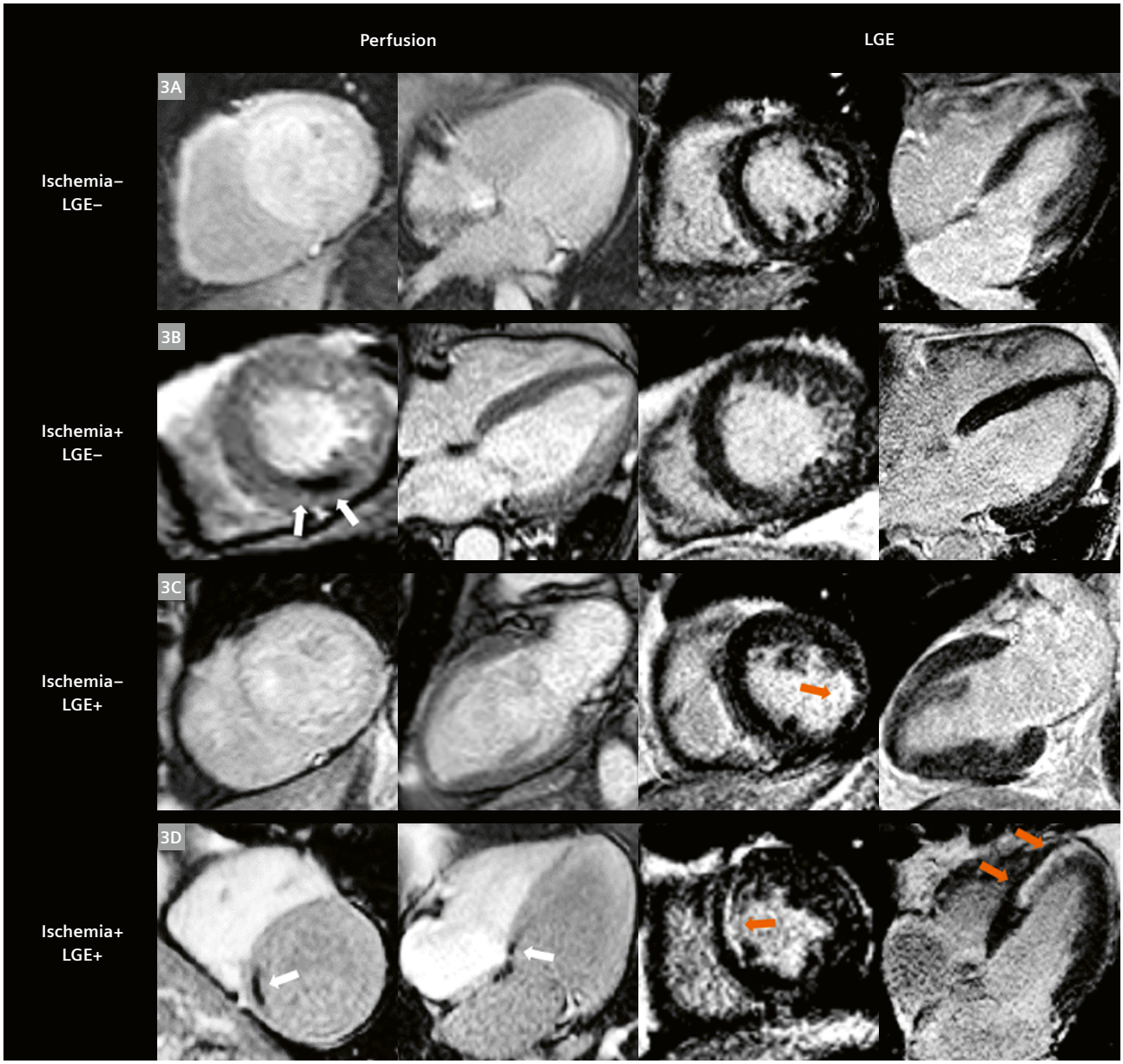

3 **Examples of inducible ischemia on stress CMR in patients suspected of CAD.**
(3A) Normal: 79-year-old female presenting with atypical angina. Stress CMR revealed no perfusion defect and LGE was negative, ruling out the diagnosis of myocardial ischemia.
(3B) Inducible ischemia: 81-year-old male with diabetes and hypertension, presenting with dyspnea on exertion. First-pass myocardial stress perfusion images revealed a reversible perfusion defect of the inferior wall (white arrows) without LGE, indicative of myocardial inducible ischemia suggestive of significant RCA stenosis, confirmed by coronary angiography.
(3C) Myocardial scar without ischemia: 75-year-old female with a history of lateral STEMI treated by PCI of the Cx six years ago and a prior inconclusive stress echocardiography, presenting with atypical angina. Stress CMR showed a subendocardial lateral scar on LGE (orange arrow), without any perfusion defect and, therefore, no inducible ischemia.
(3D) Myocardial scar with additional inducible ischemia: 68-year-old male with a history of anterior STEMI treated by PCI of the LAD, presenting with dyspnea on exertion. Stress CMR showed a subendocardial scar on the antero-septo-apical wall on LGE sequences (orange arrows), and a perfusion defect of the inferior and infero-septal wall (white arrows) on first-pass perfusion images, indicative of inducible myocardial ischemia. Coronary angiography revealed high-grade stenoses of the RCA.

Abbreviations: CAD: coronary artery disease; Cx: circumflex coronary artery; ECG: electrocardiogram; LAD: left anterior descending; MI: myocardial infarction; PCI: percutaneous coronary intervention; RCA: right coronary artery; STEMI: ST-segment elevation myocardial infarction.

comprises six senior cardiologists who have over 15 years' experience in CMR and are trained in intensive cardiovascular care. Two of them have EACVI level 3 accreditation. Stress CMR sessions require two technologists (one at the CMR workstation, one for patient preparation and discharge), one technologist assistant and one physician for an optimized patient workflow. Notably, the mean duration of a stress CMR study (from the beginning of the first localizer sequence to the exit of the magnet) is 27 ± 5 minutes.

Stress CMR analysis to identify inducible ischemia

According to the current SCMR guidelines, inducible ischemia is defined as a sub-endocardial or transmural perfusion defect that

1) occurred in at least 1 myocardial segment;
2) persisted for at least 3 phases beyond peak contrast enhancement;
3) followed a coronary distribution and
4) occurred in the absence of co-location with LGE (Fig. 3) [10].

AI-based fully automated global circumferential strain (GCS) at stress

With the support of Siemens Healthineers within a strong collaboration for several years, we assessed the prognostic value of a full-AI algorithm for assessing the LV strain. Indeed, a fully automatic machine learning algorithm was developed to segment the myocardium and to assess the stress GCS from a short-axis cine stack of slices (Fig. 4). The AI-algorithm combines a deep learning network for segmentation with an active-contours approach to segment the endocardial and epicardial borders of LV into individual 2D short-axis views images [11]. A dense Unet [12] was trained on 3,000 CMR studies (10% reserved for validation) from the UK Biobank resource [13, 14]. The AI segmentation algorithm was tested on 1,719 unseen CMR studies [13], obtaining a dice score of 96.2% for the LV. The contours were automatically detected at several timepoints in the cine series and were automatically propagated to the rest of the phases, to minimize propagation errors. The strain tensors were projected in cylindrical coordinates centered with respect to the LV axes in radial, circumferential, and longitudinal directions. The global radial, circumferential, and longitudinal strain values were computed, which corresponds to the maximum strain magnitude values from the temporal series [6].

Prognostic impact of AI-based fully automated GCS measured at stress

In this study with a large cohort of consecutive patients referred for stress CMR, AI-based fully automated stress GCS measurement was feasible in 98% of patients referred for stress CMR with a good accuracy. In addition, stress GCS was independently associated with the occurrence of cardiovascular events (cardiovascular death or non-fatal myocardial infarction) during a median follow-up of five years. Our findings are in line with data by Romano et al. using GLS [3], which strongly suggests that a blunted stress GCS could impact clinical decision-making in those patients. Further clinical prospective trials are warranted to assess the clinical yield of strain imaging during stress CMR.

Conclusion

In patients referred for stress CMR, AI-based fully automated GCS assessed during vasodilator stress was a significant independent predictor of cardiovascular events.

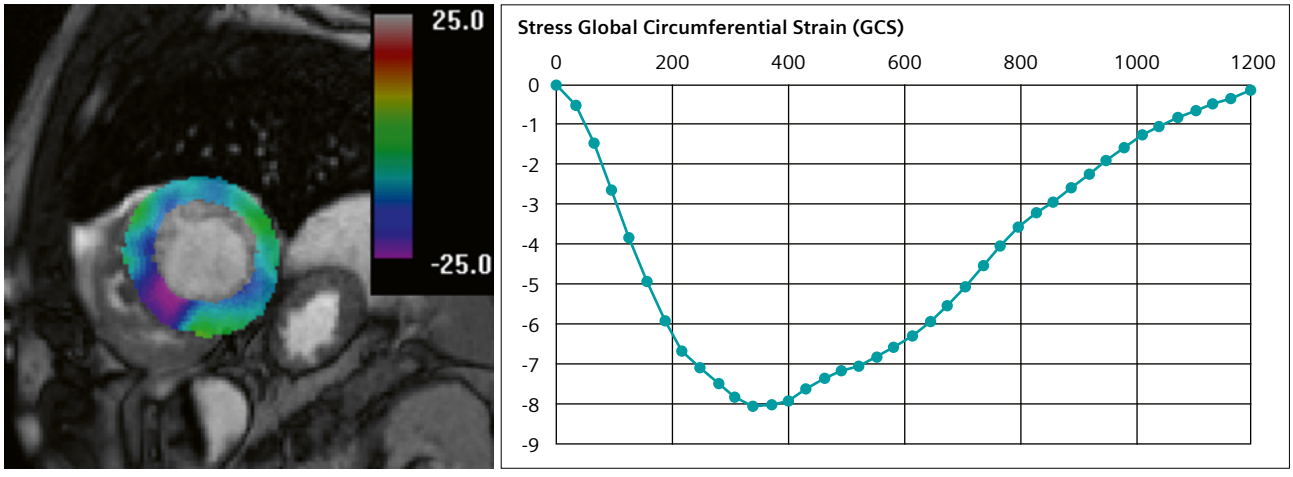

4 Example of AI-based fully automated global circumferential strain (GCS) measurement during a stress CMR exam from cine images performed immediately after stress using vasodilator agent.

References

1 Kwong RY, Ge Y, Steel K, Bingham S, Abdullah S, Fujikura K, et al. Cardiac Magnetic Resonance Stress Perfusion Imaging for Evaluation of Patients With Chest Pain. J Am Coll Cardiol. 2019;74(14):1741-55.
2 Pezel T, Garot P, Kinnel M, Hovasse T, Champagne S, Sanguineti F, et al. Long-term prognostic value of ischaemia and cardiovascular magnetic resonance-related revascularization for stable coronary disease, irrespective of patient's sex: a large retrospective study. Eur Heart J - Cardiovasc Imaging. 2021;22(11):1321-31.
3 Romano S, Romer B, Evans K, Trybula M, Shenoy C, Kwong RY, et al. Prognostic Implications of Blunted Feature-Tracking Global Longitudinal Strain During Vasodilator Cardiovascular Magnetic Resonance Stress Imaging. JACC Cardiovasc Imaging. 2020;13(1):58-65.
4 Steen H, Montenbruck M, Kelle S, Esch S, Schwarz AK, Giusca S, et al. Fast-Strain Encoded Cardiac Magnetic Resonance During Vasodilator Perfusion Stress Testing. Front Cardiovasc Med. 2021;8:765961.

Contact

Professor Jérôme Garot, M.D., Ph.D.
IRM cardiovasculaire – ICPS
Hôpital Privé Jacques Cartier
Ramsay Santé
6 Av du Noyer Lambert
91300, Massy
France
jgarot@angio-icps.com

Théo Pezel, M.D.
IRM cardiovasculaire – ICPS
Hôpital Privé Jacques Cartier
Ramsay Santé
6 Av du Noyer Lambert
91300, Massy
France
tpezel@angio-icps.com

5 Choi EY, Rosen BD, Fernandes VRS, Yan RT, Yoneyama K, Donekal S, et al. Prognostic value of myocardial circumferential strain for incident heart failure and cardiovascular events in asymptomatic individuals: the Multi-Ethnic Study of Atherosclerosis. Eur Heart J. 2013;34(30):2354-61.
6 Amzulescu MS, De Craene M, Langet H, Pasquet A, Vancraeynest D, Pouleur AC, et al. Myocardial strain imaging: review of general principles, validation, and sources of discrepancies. Eur Heart J - Cardiovasc Imaging. 2019;20(6):605-19.
7 Almutairi HM, Boubertakh R, Miquel ME, Petersen SE. Myocardial deformation assessment using cardiovascular magnetic resonance-feature tracking technique. Br J Radiol. 2017;90(1080):20170072.
8 Feisst A, Kuetting DLR, Dabir D, Luetkens J, Homsi R, Schild HH, et al. Influence of observer experience on cardiac magnetic resonance strain measurements using feature tracking and conventional tagging. Int J Cardiol Heart Vasc. 2018;18:46-51.
9 Pezel T, Garot P, Hovasse T, Unterseeh T, Champagne S, Kinnel M, et al. Vasodilatation stress cardiovascular magnetic resonance imaging: Feasibility, workflow and safety in a large prospective registry of more than 35,000 patients. Arch Cardiovasc Dis. 2021;114(6–7):490-503.
10 Pezel T, Lacotte J, Toupin S, Salerno F, Said MA, Manenti V, et al. Diagnostic Accuracy of Stress Perfusion CMR for Risk Stratification in Patients With MR-Conditional Pacemakers. JACC Cardiovasc Imaging. 2021;14(10):2053-4.
11 Chitiboi T, Georgescu B, Wetzl J, Borgohain I, Geppert C, Piechnik SK, Neubauer S, Petersen S, Sharma P. Deep learning-based strain quantification from CINE cardiac MRI. InISMRM Annual Meeting 2020.
12 Huang G, Liu Z, Van Der Maaten L, Weinberger KQ. Densely connected convolutional networks. In: IEEE Conference on Computer Vision and Pattern Recognition (CVPR). 2017:2261-69. doi: 10.1109/CVPR.2017.243.
13 Sudlow C, Gallacher J, Allen N, Beral V, Burton P, Danesh J, et al. UK biobank: an open access resource for identifying the causes of a wide range of complex diseases of middle and old age. PLoS Med. 2015;12(3):e1001779.
14 Second Annual Data Science Bowl – Transforming How We Diagnose Heart Disease. The National Heart, Lung, and Blood Institute (NHLBI). s.l. : Booz Allen Hamilton, 2016. Available from https://www.kaggle.com/c/second-annual-data-science-bowl.

Cardiac MRI on the MAGNETOM Free.Max: The Ohio State Experience

Orlando P. Simonetti[1], Juliet Varghese[1], Ning Jin[2], Daniel Giese[3], Yingmin Liu[1], Chong Chen[1], Rizwan Ahmad[1], Yuchi Han[1]

[1]The Ohio State University, Columbus, OH, USA
[2]Siemens Healthineers, Malvern, PA, USA
[3]Siemens Healthineers, Erlangen, Germany

Background

As the cardiovascular magnetic resonance (CMR) program at The Ohio State University has expanded, we added both a higher (3T, MAGNETOM Vida) and a lower (0.55T, MAGNETOM Free.Max) field system to our existing 1.5T MAGNETOM Sola. Having access to scanners with three different field strengths has enabled us to investigate the pros and cons of each across different CMR applications, with the aim to match the right field strength for the right patient and pathology. The first step in this process was to develop and implement cardiac imaging techniques for the MAGNETOM Free.Max, which was delivered without CMR product pulse sequences. We have worked closely with our colleagues at Siemens Healthineers to put together a comprehensive package of CMR techniques[1], which currently are still in the preliminary stage of development.

While signal-to-noise ratio (SNR) is directly proportional to the main magnetic field (B_0), lower B_0 offers a number of potential advantages for CMR [1, 2]. The higher field homogeneity and lower specific absorption rate (SAR) at lower-field benefits techniques that are dependent on balanced steady-state free precession (bSSFP), potentially increasing safety and reducing artifacts in patients with implanted devices[2]. Lower B_0 means lower Lorentz forces, reducing audible noise and potentially improving the patient experience. Reduced B_0 also offers greater flexibility in magnet design. The Free.Max platform has a unique, 80 cm diameter bore and an optional 705 lb / 320 kg patient table limit, which eliminates barriers to MRI for those with severe obesity. One of our primary motivations to pursue the development of CMR techniques on the MAGNETOM Free.Max is to increase the accessibility to CMR for obese patients, as well as those with severe claustrophobia who may benefit from the larger bore and quieter scans.

The United States Centers for Disease Control and Prevention (CDC) reports that the prevalence of obesity (body mass index (BMI) > 30 kg/m^2) now exceeds 40% and is projected to affect 50% of the U.S. population by 2025 [3]. The obesity epidemic is not unique to the USA, with a prevalence now exceeding 20% in most Western European countries. Obesity increases the risk of cardiovascular disease (CVD) [4] and these risks are even greater in those with severe obesity, i.e., BMI > 40 kg/m^2, which now accounts for more than 9% of the adult USA population. This significant population segment faces serious healthcare challenges, especially in terms of access to non-invasive cardiovascular imaging. Most cardiac imaging equipment is not designed to accommodate the weight and girth of severely obese patients; furthermore, radiation-based modalities such as CT and SPECT require excessive radiation for adequate image quality, while attenuation of ultrasound by adipose tissue limits the utility of echocardiography [5, 6]. If not for the bore diameter (60 cm – 70 cm) and table weight limits (typically < 450 lbs / 200 kg) of standard magnetic resonance imaging (MRI) systems, MRI could provide a safe, comprehensive assessment of CVD in even the most severely obese patients. The 80 cm bore and optional 705 lb / 320 kg table weight limit of MAGNETOM Free.Max offer this possibility.

Several years ago, our group recognized the potential for low-field cardiovascular MRI [1], and demonstrated the feasibility of CMR at 0.35T in comparison with standard field strengths [7]. Our work, together with preliminary results published by others using a prototype scanner

[1]Work in progress: the application is currently under development and is not for sale in the U.S. and in other countries. Its future availability cannot be ensured.
[2]The MRI restrictions (if any) of the metal implant must be considered prior to patient undergoing MRI exam. MR imaging of patients with metallic implants brings specific risks. However, certain implants are approved by the governing regulatory bodies to be MR conditionally safe. For such implants, the previously mentioned warning may not be applicable. Please contact the implant manufacturer for the specific conditional information. The conditions for MR safety are the responsibility of the implant manufacturer, not of Siemens Healthineers.

ramped-down to 0.55T [2, 8], supported the concept that high quality CMR could be feasible at reduced field strength. We hypothesized that the ultra-wide bore MAGNETOM Free.Max system could deliver the proven benefits of CMR to the severely obese patient population, i.e., patients who face significantly limited diagnostic image quality and radiation dosing challenges from other imaging modalities, and set a goal of developing a comprehensive suite of CMR techniques for the MAGNETOM Free.Max. To achieve this goal, however, requires overcoming two primary technical challenges;

1) the deficit in SNR as compared to higher field systems, and
2) the reduced gradient performance (26 mT/m max. amplitude and 45 mT/m/ms max. slew rate) of MAGNETOM Free.Max, resulting in longer echo times (TE) and repetition times (TR).

Taken together, these performance differences can lead to significantly longer scan times, and compromised spatial and temporal resolution. These factors are especially critical in CMR where scan time is often limited to a short breath-hold to avoid respiratory motion, and sufficient temporal resolution is required to avoid cardiac motion artifact, or to accurately resolve cardiac motion and flow. The initial steps we have taken to address these limitations include the implementation of dedicated pulse sequences, optimization of scan parameters, judicious use of advanced reconstruction strategies, and machine learning driven denoising. Preliminary results are shown in the following sections where we review the various component techniques that comprise the comprehensive cardiac package, and present example results we have obtained to date in animal models, healthy volunteers, and patients with cardiovascular disease, including those with severe obesity.

Our cardiac package

Overview

As the MAGNETOM Free.Max does not include dedicated sequences released for cardiac imaging, all of the following sequences and reconstruction techniques are research packages[1] that were enabled and/or developed by our group in collaboration with Siemens Healthineers. Furthermore, the MAGNETOM Free.Max does not have an integrated ECG triggering system; yet, it is capable of accepting an external triggering signal, and this can be provided by a variety of third-party patient monitoring systems.

At this early stage of the project, we have developed working techniques covering all of the clinical CMR applications shown in Figure 1. Our ultimate goal is to run protocols that obviate the need for patient breath-hold, and can be completed within 30 minutes; however, at this stage of development, some methods still rely on conventional segmented *k*-space, breath-hold acquisition. As we continue to innovate and combine advanced compressed sensing (CS) and deep learning-based reconstruction techniques paired with custom data acquisition strategies, we fully expect to achieve our goal of a rapid, comprehensive free-breathing CMR suite.

Morphology

Dark-blood turbo spin echo (TSE) based techniques are useful to distinguish morphological features and to characterize masses and tumors. The limited SNR and gradient speed available on MAGNETOM Free.Max impact the performance of some CMR techniques more than others. Given that TSE images tend to have relatively high SNR and the sequence is not reliant on fast gradients, the translation from higher field and faster gradient systems was

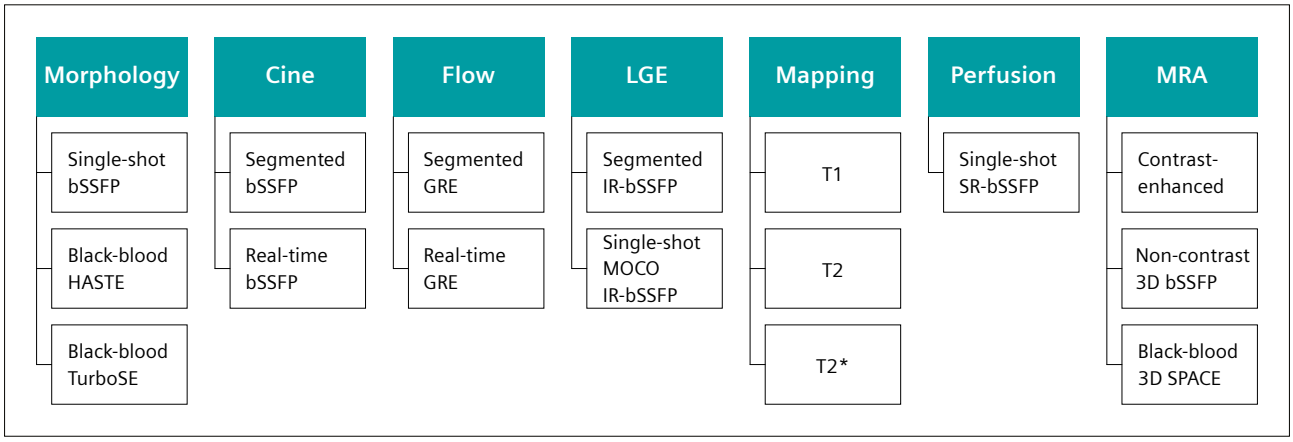

1 Shown are the primary components of the comprehensive cardiac imaging package[1]. All of the basic components are in place, although many of these techniques rely on breath-hold, segmented *k*-space acquisitions. Optimization of techniques and scan parameters is ongoing in our effort to maximize SNR, contrast, and image quality. We also continue working to develop strategies to support free-breathing image acquisition across all categories.

straightforward, and the technique performed well at low field with little modification. Example images in a healthy volunteer are shown in Figure 2, demonstrating the commonly used variants of black-blood T1 and T2-weighted TSE, and STIR. These are standard acquisitions with each 2D slice acquired in a short breath-hold of 10 to 12 heartbeats, and employed the Deep Resolve AI-based image denoising technique provided by Siemens Healthineers. Exemplary scan parameters used at 0.55T and 1.5T are listed in Table 1. Example images (Fig. 3) at both 1.5T and 0.55T in a patient with Harrington rods in their spine illustrate the reduced artifact surrounding metal implants[2] that can be expected at lower B_0 field strength.

Cine

Cine imaging is at the core of every CMR exam, providing information on cardiovascular morphology and function. Measurements can be made on the cine images to quantify global and regional cardiac function. Cine typically relies on balanced steady-state free precession, (bSSFP) and therefore has inherently high SNR relative to other techniques. Thus, the reduced SNR at low field is not a significant obstacle; however, bSSFP cine does require short TR for high temporal resolution, thus presenting a challenge on this scanner where gradient performance is limited. We have addressed this challenge through the utilization of CS reconstruction methods [9]. Table 2 lists the imaging parameters achieved at 0.55T, in comparison to a 1.5T scanner with faster gradients. With highly accelerated CS-based sequences, we have been able to achieve high-quality cine results with segmented breath-hold techniques, as well as real-time, free-breathing imaging. Segmented *k*-space, breath-hold cine images acquired in the same patient at 1.5T and at 0.55T are shown in Figure 4. This patient has an artificial aortic valve with metallic components[2]. The size of the signal void around the valve is less in the 0.55T images, as might be expected due to the reduced susceptibility gradients surrounding the metal. The degree of metal artifact is highly dependent on the specific material used to construct the implant[2].

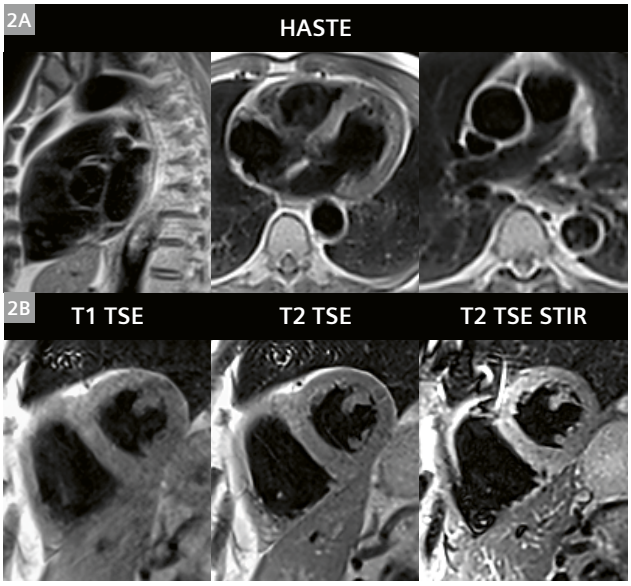

2 Dark-blood images acquired in a volunteer. Single-shot HASTE images in different cardiac views are shown in the top row **(2A)**. The bottom row shows T1 TSE, T2 TSE and T2 TSE STIR images in a mid-short axis view **(2B)**. Each TSE image was acquired in a 12-heartbeat breath-hold.

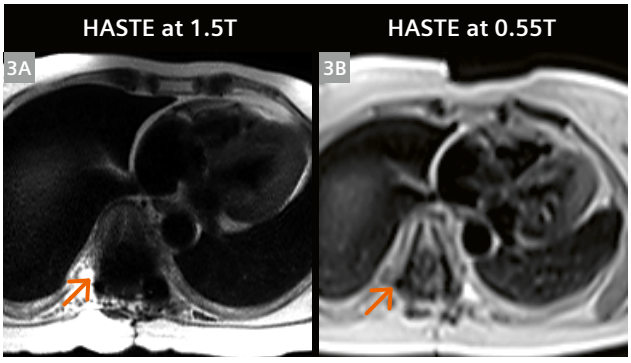

3 Single-shot axial images acquired in a patient with Harrington rods post spinal fusion[2]. HASTE images acquired on a 1.5T MAGNETOM Avanto system **(3A)** from a prior exam demonstrate significant susceptibility artifact (orange arrows) compared to localized artifact on the corresponding HASTE image at 0.55T **(3B)**.

	Scanner	Flip angle (deg)	TE (ms)	Echo spacing (ms)	RBW Hz/pixel	Turbo factor	Temporal resolution (ms)	Slice thickness (mm)	Pixel size (mm)	Acceler-ation	Scan time
T2 TSE	1.5T MAGNETOM Sola	180	60	3.54	849	17	60	5	1.3 × 1.3	G 2	10 HB
	0.55T MAGNETOM Free.Max	180	43	5.36	401	14	75	6	2.0 × 2.0	G 2	12 HB
HASTE	1.5T MAGNETOM Sola	120	35	3.94	501	104	409	6	1.3 × 1.3	none	1 HB
	0.55T MAGNETOM Free.Max	160	16	4.1	1502	72	295	10	3.6 × 3.6	G 2	1 HB

Table 1: Acquisition parameters for breath-hold segmented turbo spin echo (TSE) (top rows) and single-shot HASTE (bottom rows) shown for 1.5T MAGNETOM Sola and 0.55T MAGNETOM Free.Max.

It is also dependent on TE and TR, and therefore will be affected by gradient performance as well as field strength. Figure 5 shows a comparison of breath-held segmented *k*-space cine images and real-time cine images, all acquired at 0.55T using the scan parameters listed in Table 2. Despite the high acceleration rates used to overcome slower gradient performance, SNR and overall image quality are maintained with CS reconstruction.

Flow quantification

Phase contrast (PC) imaging is the standard MRI method used to measure blood flow. While low-field offers advantages of reduced susceptibility and greater field homogeneity, the inherently low SNR of the spoiled gradient echo (GRE) sequences used for PC MRI can be challenging at low-field, and higher acceleration is needed to overcome slower gradients. We have successfully implemented segmented *k*-space, breath-hold flow quantification on the MAGNETOM Free.Max [10] and sample results

	Scanner	Flip angle (deg)	TE (ms)	TR (ms)	RBW Hz/pixel	Segments	Temporal resolution (ms)	Slice thickness (mm)	Pixel size (mm)	Acceleration	Scan time
BH-Cine	1.5T MAGNETOM Sola	75	1.16	2.71	930	12	32.5	6	1.8 × 1.8	CS 4.3	3 HB
	0.55T MAGNETOM Free.Max	110	1.95	4.65	930	6	27.9	8	1.8 × 1.8	CS 4.3	6 HB
RT-Cine	1.5T MAGNETOM Sola	75	1.04	2.43	1184	18	43.7	8	2.0 × 2.0	CS 7.4	1 HB
	0.55T MAGNETOM Free.Max	110	1.84	4.55	1002	10	45.5	8	2.0 × 2.0	CS 9.7	1 HB

Table 2: Acquisition parameters for breath-hold segmented *k*-space cine (top rows) and real-time free-breathing cine (bottom rows) shown for 1.5T MAGNETOM Sola with faster gradients than the 0.55T MAGNETOM Free.Max. Higher acceleration rates are used for real-time cine on the MAGNETOM Free.Max to overcome the slower gradients.

4 End-diastole (ED) and End-systole (ES) cine frames acquired in a three-chamber view (3CH) and left ventricular outflow tract (LVOT) are shown. The 1.5T (MAGNETOM Avanto) **(4A)** images shown were acquired in the same patient in a prior exam using a GRAPPA-based breath-held segmented SSFP method. Images at 0.55T **(4B)** were acquired using a compressed sensing-based breath-held segmented SSFP method. Note that the patient has an artificial valve[2], and the metal artifacts in proximity to the valve are reduced at 0.55T.

in comparison with GRAPPA parallel imaging are shown in Figure 6. In preliminary testing, CS-based reconstruction provides the high acceleration rates needed while maintaining spatial and temporal resolution and SNR. Real-time flow imaging requires significantly higher acceleration rates and is still under development, but free-breathing acquisition can be achieved through the use of signal averaging to suppress respiratory motion artifact, as also shown in Figure 6. Exemplary PC-MRI scan parameters are listed in Table 3. Although initial results demonstrate the feasibility of flow quantification on the MAGNETOM Free.Max, several sources of errors related to low-field and/or lower gradient performance (e.g., Maxwell-Terms and Flow Displacement Artifacts) are still under investigation.

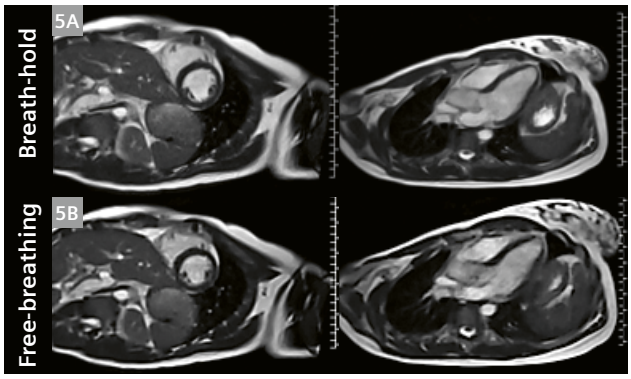

5 Breath-held segmented *k*-space cine frames **(5A)** and real-time free-breathing cine frames **(5B)** acquired in a healthy volunteer. Despite use of a high under-sampling rate of near 10× in real-time cine, CS reconstruction provides sufficient image quality at 0.55T.

	Scanner	Flip angle (deg)	TE (ms)	TR (ms)	RBW Hz/pixel	Segments	Temporal resolution (ms)	Slice thickness (mm)	Pixel size (mm)	Acceleration	Scan time
BH Flow	1.5T MAGNETOM Sola	15	2.26	4.23	501	5	42.3	6	2.0 × 2.0	G 2	10 HB
	0.55T MAGNETOM Free.Max	12	4.49	7.64	427	3	45.8	6	1.8 × 1.8	CS 3	13 HB
FB Flow	1.5T MAGNETOM Sola (RT)	12	2.51	4.41	560	6	52.9	10	2.8 × 2.8	CS 16	1 HB
	0.55T MAGNETOM Free.Max (avg)	12	3.67	6.55	427	3	39.3	8	1.9 × 1.9	G 2	58 HB

Table 3: Acquisition parameters for breath-hold segmented *k*-space flow quantification sequence (top rows) and free-breathing acquisition (bottom rows) shown for 1.5T MAGNETOM Sola and 0.55T MAGNETOM Free.Max. Free-breathing (FB) acquisition is currently achieved by signal averaging to suppress respiratory motion on MAGNETOM Free.Max, while real-time (RT) flow data acquisition is possible at 1.5T using compressed sensing. Real-time flow requires significantly higher acceleration, which is challenging in face of the reduced SNR at 0.55T.

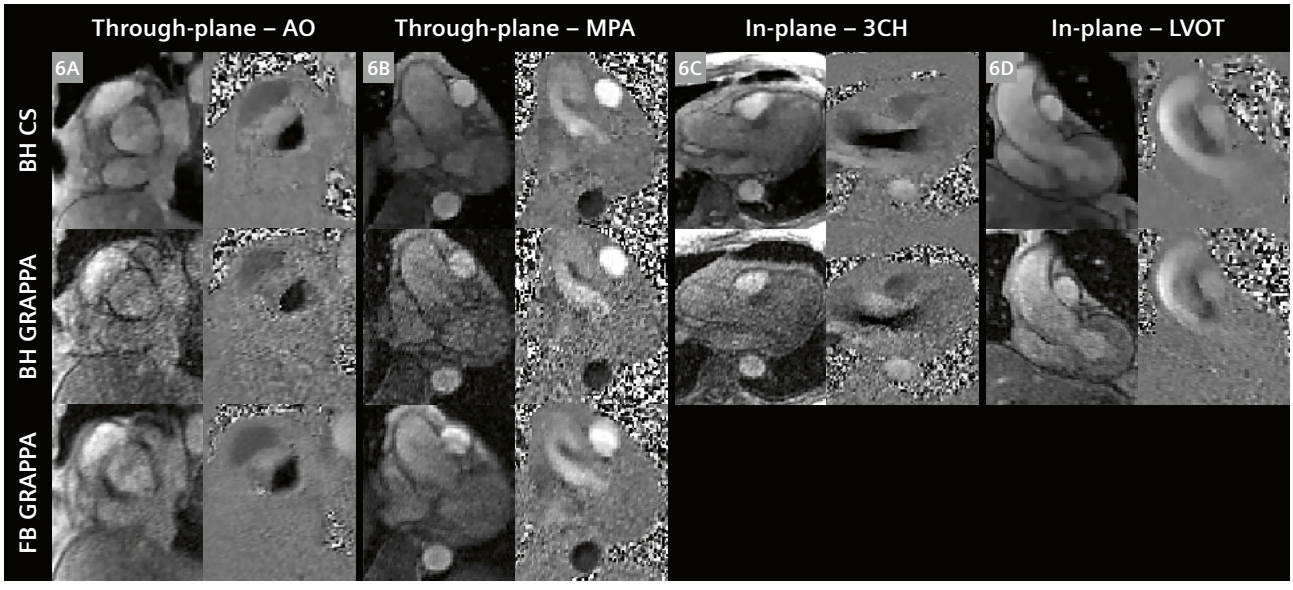

6 Through-plane (**6A** aortic root and **6B** main pulmonary artery) and In-plane (**6C** 3-chamber view and **6D** left ventricular outflow tract) 2D phase contrast flow images acquired in a patient with a bicuspid aortic valve, aortic dilatation and aortic regurgitation. The top row shows magnitude and phase images acquired with a breath-held compressed sensing-based 2D PC MR sequence, while the middle row shows images from a breath-held GRAPPA sequence. Images in the bottom row were acquired free-breathing using a GRAPPA sequence with four averages to boost SNR. AO = aorta, MPA = main pulmonary artery, 3CH = cardiac 3-chamber view, LVOT = left ventricular outflow tract view.

Late Gadolinium Enhancement (LGE)

LGE provides unique information on myocardial tissue changes, including scar, fibrosis, and edema. We are currently optimizing both breath-hold segmented LGE and single-shot free-breathing LGE with motion correction and averaging, all based on bSSFP readout which provides high SNR. Exemplary scan parameters are listed in Table 4, along with 1.5T parameters for reference. Example images from two patients with non-ischemic cardiomyopathies showing segmented breath-hold, single-shot, and free-breathing, motion corrected LGE at 0.55T, along with comparative images acquired at 1.5T and 3T, are shown in Figure 7. Additional improvements in acquisition speed and image quality are anticipated as we incorporate compressed sensing into LGE image acquisition and reconstruction.

Gadolinium contrast agent T1 relaxivity is generally a function of field strength, and as shown by Campbell-Washburn et al., relaxivity at 0.55T may be slightly higher or lower than at 1.5T, depending on the particular agent [2]. All of the contrast-enhanced images shown here used gadobutrol, which may have a slightly lower (worse) relaxivity at 0.55T than at 1.5T. Additionally, because the native T1 times are shorter, the differential contrast enhancement at lower field may be less. Thus far, in our preliminary studies, we have observed the use of gadolinium-based contrast agent to be effective for the visualization of myocardial scar, perfusion defects, and blood pool in MRA, but careful studies are required to evaluate the diagnostic efficacy.

Myocardial relaxation parameter mapping

Myocardial longitudinal (T1) and transverse (T2) relaxation times are elevated with fibrosis, edema, and inflammation. Quantitative myocardial parameter mapping methods are being used clinically at higher field to evaluate these pathological changes in myocardium that can accompany a variety of diseases. We implemented parameter mapping schemes for T1 and T2 taking into consideration the shorter T1 relaxation times and longer T2 relaxation times at 0.55T in comparison to higher field. The T1-mapping scheme was based on that typically used for post-contrast T1 mapping at 1.5T (4(1)3(1)2), with the addition of a fourth inversion pulse and two more images at the shorter

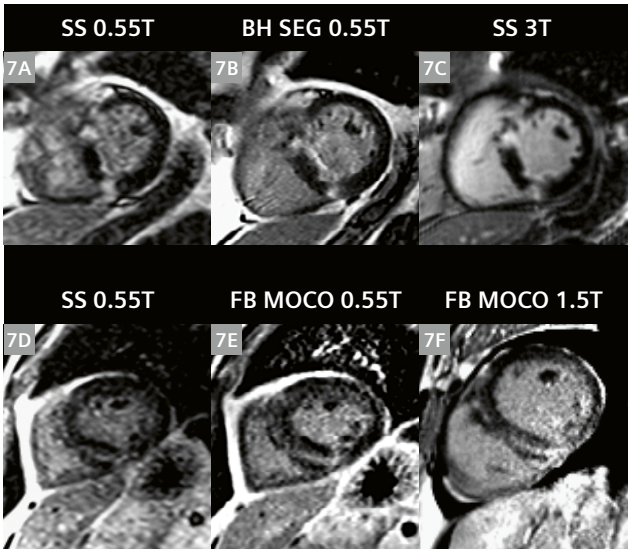

7 Top row **(7A–7C)** shows LGE images acquired in a patient with hypertrophic cardiomyopathy with fibrosis of the left ventricle. **(7A)** Single-shot inversion recovery prepared bSSFP image at 0.55T, **(7B)** breath-held segmented LGE image at 0.55T, and **(7C)** single-shot IR-prepared bSSFP LGE acquired on a 3T MAGNETOM Vida system for comparison.
Bottom row **(7D–7F)** shows LGE images acquired in a different patient with non-ischemic septal mid-wall fibrosis. Single-shot **(7D)** and free-breathing motion-corrected averaged **(7E)** LGE images were acquired on MAGNETOM Free.Max, while the corresponding MOCO LGE image, shown in **(7F)**, was acquired on a 1.5T MAGNETOM Sola system.

	Scanner	Flip angle (deg)	TE (ms)	TR (ms)	RBW Hz/pixel	Segments	Temporal resolution (ms)	Slice thickness (mm)	Pixel size (mm)	Acceleration	Scan time
BH LGE	1.5T MAGNETOM Sola (GRE)	20	1.55	4.06	465	31	142	8	1.4 × 1.4	none	8 HB
	0.55T MAGNETOM Free.Max (bSSFP)	80	2.48	6.66	200	21	140	10	1.6 × 1.6	none	12 HB
MOCO LGE	1.5T MAGNETOM Sola (bSSFP)	50	1.18	2.79	1085	86	240	8	1.4 × 1.4	G 2	16 HB
	0.55T MAGNETOM Free.Max (bSSFP)	50	1.84	4.69	698	63	295	8	1.5 × 1.5	G 2	24 HB

Table 4: Acquisition parameters for breath-hold segmented *k*-space LGE (top rows) and free-breathing LGE based on single-shot acquisition with motion correction (MOCO) and averaging (bottom rows) shown for 1.5T MAGNETOM Sola and 0.55T MAGNETOM Free.Max. Additional averages were used at 0.55T in the MOCO LGE scan to boost SNR. Note also that the standard segmented breath-hold approach at 1.5T and 3T typically utilizes a GRE readout, while bSSFP is employed at 0.55T to boost SNR. The higher B_0 homogeneity allows broader utilization of bSSFP without risk of dark band artifacts that could confound the interpretation of LGE, first pass perfusion, and other techniques where changes in myocardial signal intensity are of interest.

inversion times (4(1)3(1)2(1)2). The T2 mapping scheme was modified to acquire 6 source images at 3 different T2 preparation times (0, 25, and 60 ms). Scan parameters are listed in Table 5, along with typical parameters used at 1.5T for comparison. Results shown in Figure 8 acquired in a porcine infarct model at 0.55T utilized an increased number of source images to boost SNR through the pixel-wise parameter fitting process. We are continuing to work on applying the same CS strategies that have been instrumental in boosting SNR and acceleration rates in cine and flow, and expect that this will improve SNR and sharpness in the resulting parameter maps, while reducing the scan duration. Prospective respiratory motion compensation techniques based on the Pilot Tone technology [11] are under development and will be used to further improve free-breathing methods.

	Scanner	Flip angle (deg)	TE (ms)	TR (ms)	RBW Hz/pixel	Segments	Temporal resolution (ms)	Slice thickness (mm)	Pixel size (mm)	Acceleration	Scan time
T1 mapping	1.5T MAGNETOM Sola	35	1.01	2.42	1085	60	145	8	2.0 × 2.0	G 2	11 HB
	0.55T MAGNETOM Free.Max	50	1.77	4.3	539	60	258	10	2.4 × 2.4	G 2	14 HB
T2 mapping	1.5T MAGNETOM Sola	70	1.04	2.43	1184	55	133	8	2.1 × 2.1	G 2	7 HB
	0.55T MAGNETOM Free.Max	70	1.69	4.18	558	60	250	10	2.4 × 2.4	G 2	16 HB

Table 5: Acquisition parameters for myocardial T1 mapping (top rows) and T2 mapping (bottom rows) listed for both 1.5T MAGNETOM Sola and 0.55T MAGNETOM Free.Max. Additional source images are acquired at 0.55T to boost SNR, leading to slightly longer scan times. Longer TR due to slower gradients also degrades temporal resolution, and this can cause some motion artifact at higher heart rates. Approaches to increase acceleration rate to improve temporal resolution are being developed using Compressed Sensing.

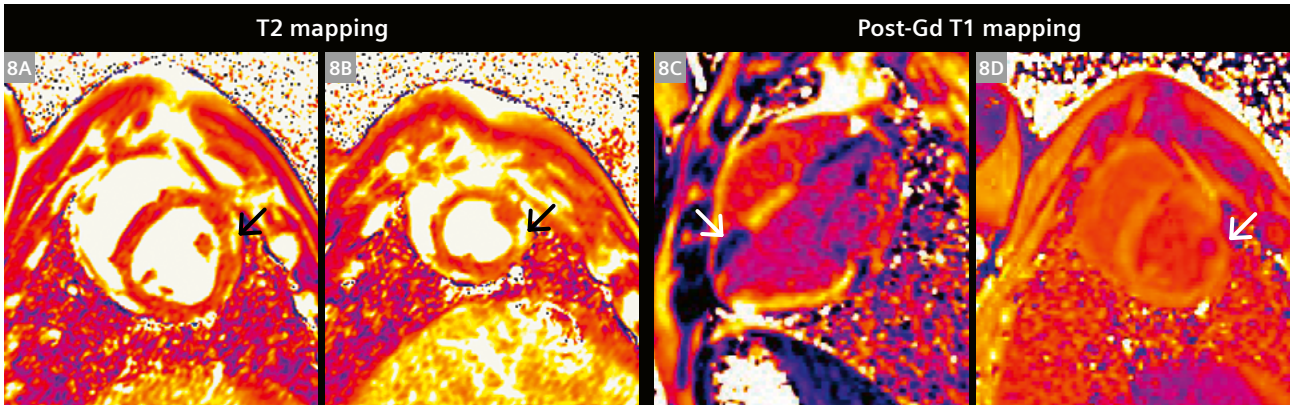

8 Myocardial T2 **(8A, 8B)** and post-Gd T1 **(8C, 8D)** maps acquired in a porcine model of acute myocardial infarction. These images, acquired five days post 90-minute occlusion-reperfusion of the left circumflex coronary artery, illustrate the feasibility of parameter mapping at 0.55T. Antero-lateral infarct is visible as regionally elevated T2 (black arrows in panels 8A and 8B), and shortened post-contrast T1 (white arrows in panels 8C and 8D).

	Scanner	Flip angle (deg)	TE (ms)	TR (ms)	RBW Hz/pixel	Segments	Temporal resolution (ms)	Slice thickness (mm)	Pixel size (mm)	Acceleration	Scan time
First-pass Perfusion SR-bSSFP	1.5T MAGNETOM Sola (bSSFP)	50	1.04	2.5	1085	37	92.5	8	1.9 × 1.9	G 3	50 HB
	0.55T MAGNETOM Free.Max (bSSFP)	90	1.81	4.04	868	25	101	8	3.0 × 3.0	CS 4	50 HB

Table 6: Acquisition parameters for myocardial first-pass perfusion imaging for 1.5T MAGNETOM Sola (top row) and 0.55T MAGNETOM Free.Max (bottom row). Saturation-recovery (SR) bSSFP is used on both scanners. Compressed Sensing is used on MAGNETOM Free.Max to push the acceleration rate to 4× to overcome the longer TR, and to maintain SNR. Even with higher acceleration there is some compromise in spatial and temporal resolution when compared to 1.5T. Further investigation is required to determine the impact of these parameter differences.

First-pass perfusion

Gadolinium-enhanced first-pass perfusion imaging, combined with vasodilator stress, is the most critical component of the CMR evaluation of patients with known or suspected ischemic heart disease. With the requirements of delivering multi-slice coverage within a single heartbeat, and high T1-contrast images with little motion artifact, first-pass perfusion imaging pushes the speed and SNR limits of CMR even at higher field. Whether or not these requirements can be met at lower field with reduced

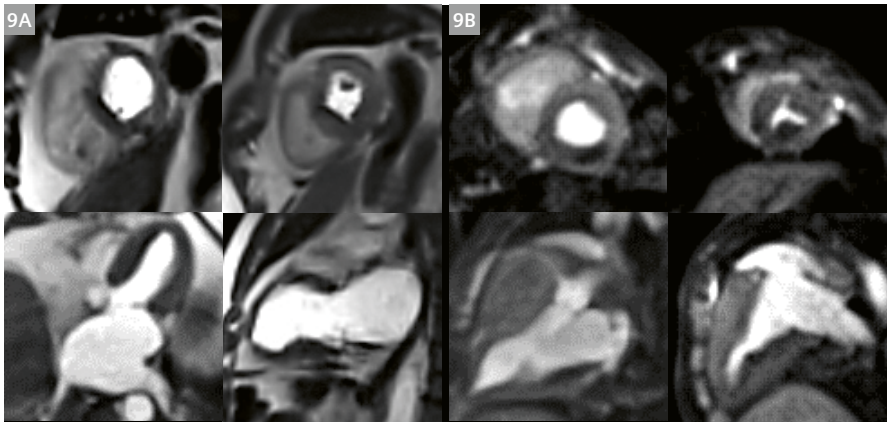

9 Rest perfusion images indicate perfusion defect in a patient with hypertrophic cardiomyopathy **(9A)** and in a porcine model with left circumflex artery infarct **(9B)**.

	Scanner	Flip angle (deg)	TE (ms)	TR (ms)	RBW Hz/pixel	Segments or turbo factor	Temporal resolution (ms)	Slice thickness (mm)	Pixel size (mm)	Accel-eration	Scan time
non-contrast MRA navigator bSSFP	1.5T MAGNETOM Sola	90	1.45	3.38	592	35	118	1.3	1.6 × 1.6	G 2	78 HB
	0.55T MAGNETOM Free.Max	110	1.89	4.61	501	35	161	1.5	1.6 × 1.6	G 2	142 HB
non-contrast MRA navigator SPACE	1.5T MAGNETOM Sola	variable	23	1RR	744	35	130	1.3	1.3 × 1.3	G 2	205 HB
	0.55T MAGNETOM Free.Max	variable	23	1RR	630	25	214	1.3	1.6 × 1.6	G 2	289 HB
Gd ce-MRA ECG gated GRE	1.5T MAGNETOM Sola	30	1.25	2.97	591	100	297	1.4	1.4 × 1.4	CS 9	10 HB
	0.55T MAGNETOM Free.Max	30	1.71	3.68	781	80	294	1.5	1.6 × 1.6	CS 7	13 HB

Table 7: Acquisition parameters for 3D MR angiography (MRA) sequences used on the 1.5T MAGNETOM Sola and 0.55T MAGNETOM Free.Max. Three different techniques are listed: 3D navigator respiratory gated bSSFP (top rows), 3D navigator gated dark-blood SPACE (middle rows), and 3D contrast enhanced ECG-gated MRA. Some compromises are made in spatial resolution on the MAGNETOM Free.Max to offset reduced SNR and gradient speed.

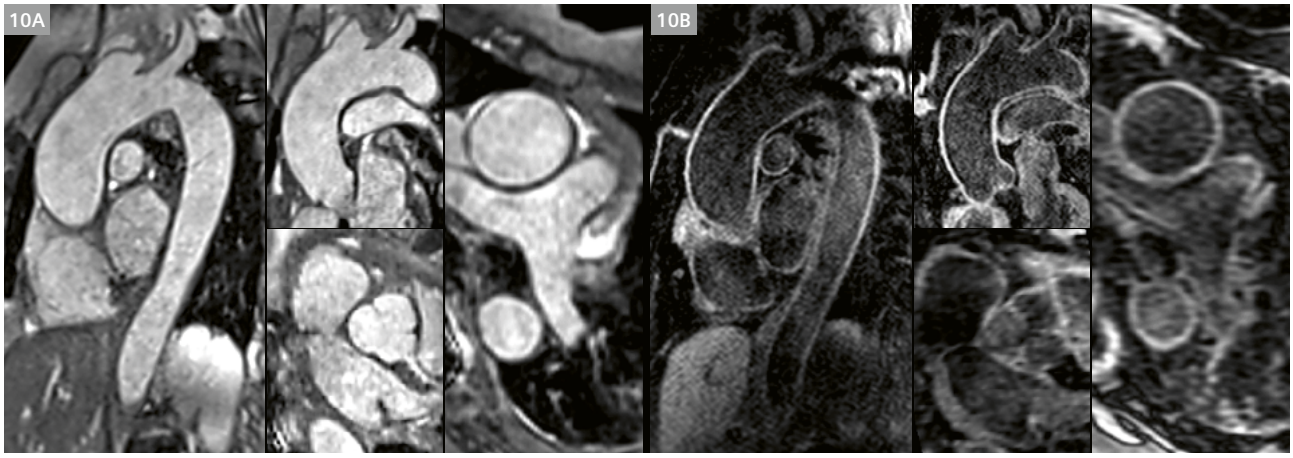

10 2D reformatted images from non-contrast 3D MRAs acquired in a patient with Harrington spinal rods[2] being evaluated for aortic dilatation. Images in **(10A)** show reconstructions from a bright-blood ECG-triggered, navigator gated bSSFP MRA, while **(10B)** shows reconstructions from a dark-blood 3D SPACE sequence used to highlight vessel wall anatomy.

gradient performance is an important question. We have experimented with a bSSFP perfusion sequence (parameters listed in Table 6) that applies the same CS-based approach to data sampling and reconstruction [9] that has been successfully utilized to accelerate real-time cine imaging without sacrificing SNR. While this method has yet to be tested with vasodilator stress, initial results acquired at rest in a porcine model of myocardial infarction, and in volunteers and patients, are promising (Fig. 9).

MR Angiography

Thoracic MR angiograms of the aorta, pulmonary arteries, and pulmonary veins form an important component of the comprehensive cardiovascular imaging exam in many of our patients. While the standard method is contrast-enhanced MR angiography (ce-MRA), non-contrast MRA using a 3D bSSFP sequence with navigator respiratory gating is now being utilized more frequently at our institution. We also frequently employ a 3D dark blood SPACE sequence to visualize vessel wall morphology; SPACE is also less sensitive to metal artifact around implants[2]. Parameters for all three methods are listed in Table 7 for 0.55T and 1.5T. We have implemented and investigated all three of these MRA techniques in volunteers and patients. Contrast-enhanced MRA has been tested both with and without ECG gating, while the non-contrast technique is always ECG-triggered. ECG-gated ce-MRA places high demands on acceleration and we have employed a CS-based technique to maintain high spatial resolution and a reasonable breath-hold duration of 18 heartbeats or less.

Navigator-gated non-contrast MRA data were acquired during free-breathing with scan times of 6 minutes or less, depending on heart rate and the extent of anatomical coverage. 3D SPACE acquisition times are longer as signal averaging is used at both 1.5T and 0.55T. Examples of non-contrast and contrast-enhanced MRA acquired at 0.55T are shown in Figures 10, 11, and 12.

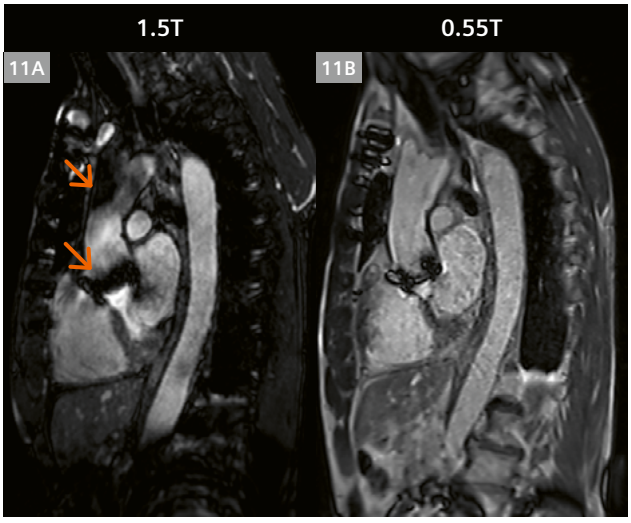

11 2D reformatted images from ECG triggered, navigator gated non-contrast enhanced 3D bSSFP MRA scans acquired in the same patient at 1.5T **(11A)** and at 0.55T **(11B)**. This patient has an artificial aortic valve[2] and sternal wires. The extent of signal dephasing artifacts (orange arrows) seen at 1.5T are reduced at 0.55T. Cine images from this patient are shown in Figure 4.

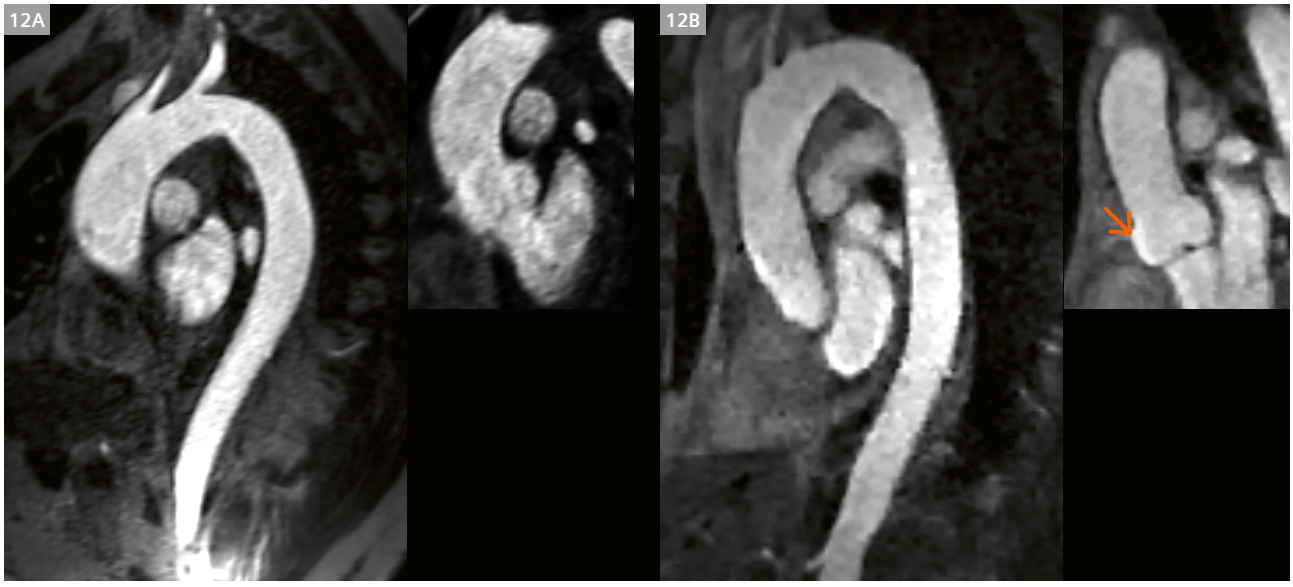

12 2D reformatted images from 3D contrast-enhanced (ce-)MRA scans in two different subjects. On the left **(12A)** a non-gated contrast-enhanced 3D MRA acquired in an obese patient shows a dilated thoracic aorta. The patient was unable to proceed with a cardiac MR exam in a standard 70 cm bore MR system but successfully completed an evaluation on the MAGNETOM Free.Max; additional images from this patient are shown in Figure 13. On the right **(12B)** is an ECG-gated ce-MRA scan from a healthy volunteer. Note the clear delineation of the aortic root and valve leaflets in the gated MRA (orange arrow), as compared to the non-gated MRA.

Putting it all together

After compiling the sequences required to cover all of the basic cardiac imaging applications, we have recently begun to identify and scan severely obese patients who were referred for clinical CMR, but whose body habitus made it impossible, or too uncomfortable, to be scanned on systems with a standard 70 cm bore diameter. In Figure 13, images acquired on the MAGNETOM Free.Max are shown from a patient weighing 350 lbs / 159 kg with BMI > 48 being evaluated for possible cardiomyopathy and dilated

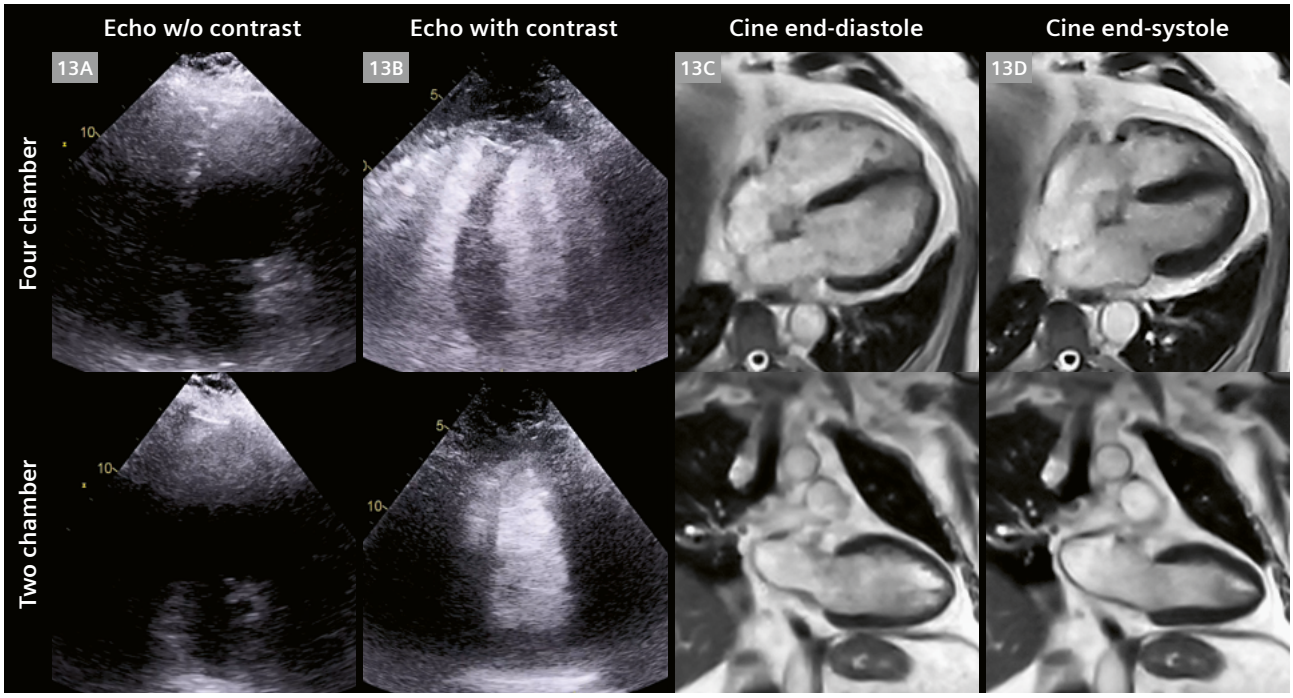

13 4-chamber view (top row) and 2-chamber view (bottom row) echocardiographic (**13A** without contrast, and **13B** with contrast) and CMR images (**13C** end-diastole, and **13D** end-systole) acquired in an obese patient with BMI > 48 kg/m^2. Echo image quality is degraded by large body habitus, and this patient could not fit into a 70 cm magnet bore. The MAGNETOM Free.Max provides access to MRI for severely obese patients for whom no other good options exist for cardiac imaging. MRA for this patient is shown in Figure 12.

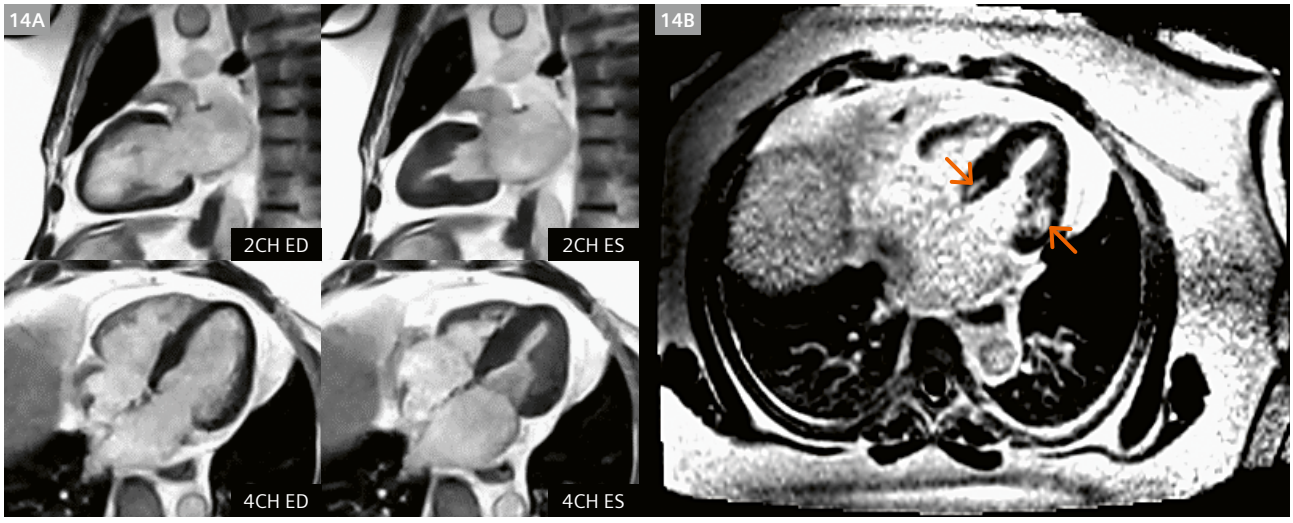

14 Example images from a patient weighing 410 lbs / 186 kg with BMI 57 kg/m^2. This patient being evaluated for cardiomyopathy, was unable to complete the exam on a 70 cm bore system. Compressed Sensing-based breath-held segmented bSSFP cine images acquired on the MAGNETOM Free.Max are shown in panel **(14A)** on the left. End-diastolic and end-systolic cardiac phases are shown. In panel **(14B)** on the right is shown an LGE image acquired during free-breathing using the technique of single-shot motion corrected (MOCO) imaging with averaging. Basal regions of enhancement (orange arrows) indicate areas of fibrosis.

aorta. While the weight of this patient can be accommodated by most scanners, their body habitus prevented them from fitting into a 70 cm bore. They were comfortably scanned on the MAGNETOM Free.Max, and the bSSFP cine images are shown here in comparison to echocardiography images acquired with and without echo contrast. The echo image quality is poor, and MAGNETOM Free.Max offers the potential for high-quality cardiac imaging for these severely obese patients in whom other modalities including echo and CT may be limited. The contrast-enhanced MR angiogram acquired in this patient is shown in Figure 12. MAGNETOM Free.Max images from another patient with a BMI of 57 (weight 410 lbs / 186 kg) diagnosed with heart failure with preserved ejection fraction (HFpEF) being evaluated for cardiomyopathy are shown in Figure 14. This patient was able to initially enter the bore of a 70 cm scanner, but was too uncomfortable to complete the exam. The patient reported being comfortable in the MAGNETOM Free.Max. The exam, including cine and LGE imaging was successfully completed, revealing normal biventricular function, but scarring evident at the base of the left ventricle.

Summary

While this project to develop and optimize cardiac imaging techniques for the 0.55T MAGNETOM Free.Max is still in relatively early stages, the images and results obtained thus far show great promise for the breadth of techniques and image quality that this system will be able to deliver in the future. We will continue to explore the cardiac imaging potential for this ultra-wide bore 0.55T system and anticipate that in the near future it will provide a solution to accurately diagnose and guide clinical cardiovascular care of patients with severe obesity, as well as those with severe claustrophobia.

Acknowledgements

The entire OSU CMR team, and Siemens Healthineers collaborators. Funding support from National Heart Lung and Blood Institute (R01HL161618) and The Robert F. Wolfe and Edgar T. Wolfe Foundation. Columbus, Ohio, USA.

References

1 Simonetti OP, Ahmad R. Low-Field Cardiac Magnetic Resonance Imaging: A Compelling Case for Cardiac Magnetic Resonance's Future. Circ Cardiovasc Imaging. 2017;10(6):e005446.
2 Campbell-Washburn AE, Ramasawmy R, Restivo MC, Bhattacharya I, Basar B, Herzka DA, et al. Opportunities in Interventional and Diagnostic Imaging by Using High-Performance Low-Field-Strength MRI. Radiology. 2019;293(2):384-393.
3 Hales CM, Carroll MD, Fryar CD, Ogden CL. Prevalence of Obesity and Severe Obesity Among Adults: United States, 2017-2018. NCHS Data Brief. 2020;(360):1-8.
4 Virani SS, Alonso A, Aparicio HJ, Benjamin EJ, Bittencourt MS, Callaway CW, et al. Heart Disease and Stroke Statistics-2021 Update: A Report From the American Heart Association. Circulation. 2021;143(8):e254-e743.
5 Fursevich DM, Limarzi GM, O'Dell MC, Hernandez MA, Sensakovic WF. Bariatric CT Imaging: Challenges and Solutions. RadioGraphics. 2016;36(4):1076-1086.
6 Finkelhor RS, Moallem M, Bahler RC. Characteristics and impact of obesity on the outpatient echocardiography laboratory. Am J Cardiol. 2006;97(7):1082-1084.
7 Varghese J, Craft J, Crabtree CD, Liu Y, Jin N, Chow K, Ahmad R, Simonetti OP. Assessment of cardiac function, blood flow and myocardial tissue relaxation parameters at 0.35 T. NMR Biomed. 2020;33(7):e4317.
8 Bandettini WP, Shanbhag SM, Mancini C, McGuirt DR, Kellman P, Xue H, et al. A comparison of cine CMR imaging at 0.55 T and 1.5 T. J Cardiovasc Magn Reson. 2020;22(1):37.
9 Chen C, Liu Y, Schniter P, Jin N, Craft J, Simonetti O, et al. Sparsity adaptive reconstruction for highly accelerated cardiac MRI. Magn Reson Med. 2019;81(6):3875-3887.
10 Jin N, Liu Y, Chen C, Giese D, Ahmad R, Simonetti O. Highly accelerated 2D phase contrast imaging on a low-field 0.55T MRI system. ISMRM Workshop on Low Field MRI, March 2022.
11 Speier P, Fenchel M, Rehner R. PT-Nav: a novel respiratory navigation method for continuous acquisitions based on modulation of a pilot tone in the MR-receiver. ESMRMB 2015, 32nd Annual Scientific Meeting, Edinburgh, UK, 1-3 October: Abstracts, Thursday, Magnetic Resonance Materials in Physics, Biology and Medicine. 2015; 28:1–135.

Contact

Orlando P. Simonetti, PhD, MSCMR, FISMRM, FAHA
John W. Wolfe Professor in Cardiovascular Research
Professor of Internal Medicine and Radiology
The Ohio State University
Biomedical Research Tower
460 W. 12th Ave.
Columbus, OH 43210
USA
Tel.: +1 614-293-0739
Orlando.Simonetti@osumc.edu

Clinical Care Should Not Depend on Zip Code: Starting a University Radiology Department in the Countryside

Jan Borggrefe, M.D.

Department for Diagnostic Radiology, Neuroradiology, and Nuclear Medicine, Johannes Wesling University Hospital, Minden, Germany

Introduction

When I started as an advanced radiology resident at University Hospital Cologne in Germany ten years ago, I arrived at a time of major change: The radiology department was in need of modernization, and a new head had just taken over. Within just a few years, and using admirable energy and skill, he transformed the department into a highly attractive, scientifically vibrant, up-and-coming university institute.

The transformation included a comprehensive digital strategy; the in-depth implementation of cutting-edge technologies such as high-focus ultrasound and dual-energy CT; the establishment of various research groups and collaborations; the introduction of highly specialized, clinically excellent consultation hours; and the creation of a strong interventional radiology and neuroradiology department. In this wonderful, dynamic environment, I was able to develop optimally as a radiologist, neuroradiologist, and scientist. It was this experience that eventually enabled me to establish a university radiology department myself.

1 View of Johannes Wesling University Hospital

Diagnostic imaging for everyone – everywhere

In 2020, I was appointed Chair of Radiology at Mühlenkreiskliniken ("Mill County Clinics"), a 2,000-bed group of hospitals in the German countryside, far away from the big cities (Figs. 1, 2). The institution had no animal labs, no preclinical science, and no research structures on site. The comments from my colleagues were varied, but they all went in the same direction: "It looks good on paper, but what are you doing? There are only cows and mills out there and you won't find colleagues to support your project …" Indeed, Minden and the surrounding towns are quite rural. The nearest big city is 50 miles away, and a vast nothingness yawns to the north and south. Coming

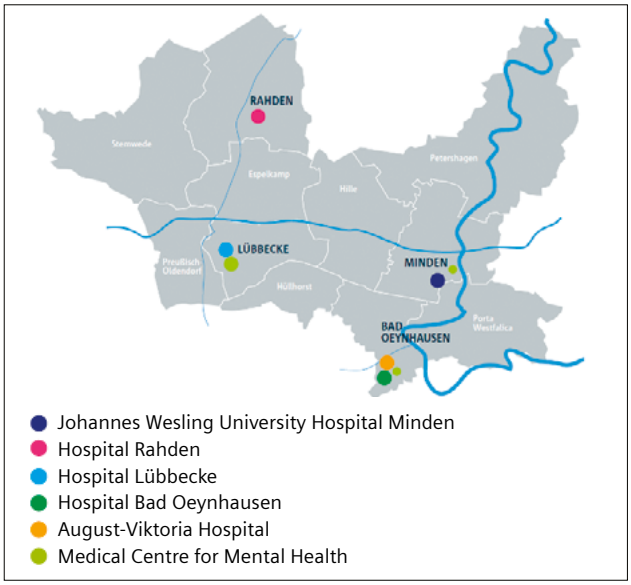

2 **The hospitals in the Mühlenkreiskliniken group**
The map gives an overview of the sites in the Mühlenkreiskliniken group (2,000 beds, 5 hospitals, and a large psychiatric hospital).

from the vibrant Rhine-Ruhr area, I sensed strong social contrasts, but also a refreshing serenity. The radiological fleet and IT status at Johannes Wesling University Hospital in Minden were somewhere between 12 and 20 years old when I started. The group's five peripheral sites that we look after were not well-perfused with doctors and were also in need of modernization. At two of the five sites, it was no longer possible to provide a radiological specialist. However, the main hospital in Minden, which has 920 beds, was rebuilt as a flagship in 2008 and became a university hospital of Ruhr University Bochum in 2016. The goal of the initiative was to train doctors "in the country for the country," in the hope that they would stay. However, a report from the German Science and Humanities Council called the new location into question again one year later, and it was also under considerable pressure to make its contribution academically.

So, after I moved to rural East Westphalia with my family and some anxiety during the COVID-19 pandemic, the site developed with a good momentum. In our network, we were able to attract several bright young radiologists, who found the rural residential location paired with an exciting department rather appealing. However, with an annual research budget of €/US$ 20,000, we didn't have much room for maneuver to make scientific developments beyond the clinical essentials.

Nevertheless, our first grant applications to Ruhr University Bochum were well-supported and they allowed us, together with the hospital, to build up our own artificial intelligence (AI) lab. With the tailwind from our previous research performance and the strategic new acquisition of radiological equipment, we were able to convince start-ups, cooperating university departments, and Siemens Healthineers to support our department. Clearly, I had considerably underestimated the interest in rural care. After all, in times of shortages of skilled workers and increasing economic challenges, it's the rural areas where the current applications of AI and telematics are really needed.

Clinically meaningful digital infrastructure

Therefore, this specific problem of ours became the core issue in the course of the first year. Thanks to our decisive digital strategy, we were given the task of working with IT and hospital management to convert the millions of euros in IT funding into clinically meaningful infrastructures. To this end, we are gradually building a hospital network for interdisciplinary clinical care and science, procuring new RIS/PACS systems and telematics infrastructure for teleradiology work across sites, and leaving room for the partner companies to codevelop solutions for these tasks. Within the first two years, we published about 30 scientific papers with our new infrastructure and thus inspired many local clinical disciplines to participate in research. Once again, it was clear that radiology offers the absolute key position in scientific work for university development when resources are limited.

Cutting-edge technology

In terms of device technology, we are not focusing on ultra-high field or pre-clinical MRI, but rather on applications that both optimize performance in everyday clinical use and offer new scientific inspiration.

We have replaced a MAGNETOM Avanto system with a 1.5T MAGNETOM Sola MR scanner and the Dot engines on the new MAGNETOM Sola have refined our workflow and have nearly halved the scan times we had with our previous 1.5T scanner (Figs. 3, 4).

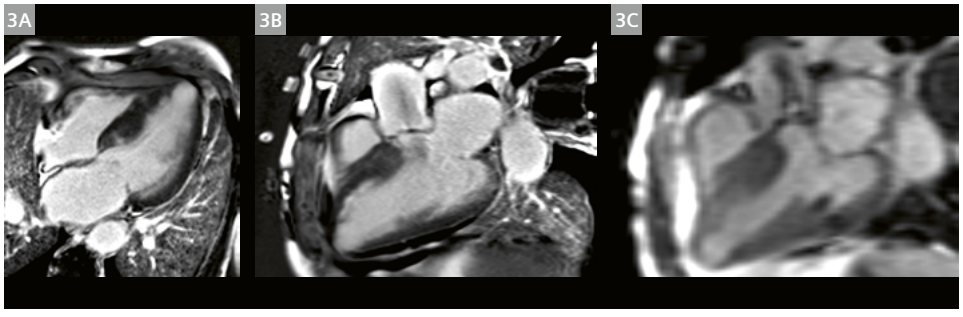

3 **Cardiac amyloidosis**
The Dot engines on the new 1.5T MAGNETOM Sola MR scanner have refined our workflow and have nearly halved the scan times we had with our previous 1.5T MAGNETOM Avanto system. This case shows a 90-year-old male patient with multiple late enhancing lesions, especially of the cardiac septum, due to amyloidosis **(3A)** and high-grade aortic stenosis. About 30% of patients with amyloidosis also present with aortic stenoses.

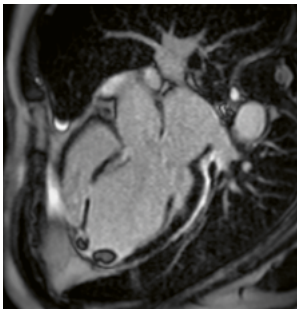

4 **Cardiac scar / thrombus**
A T1 post-contrast MRI scan from our 1.5T MAGNETOM Sola scanner showing a 64-year-old patient with postischemic scarring at the septum and cardiac apex, and intraventricular thrombus at the apex.

With the MAGNETOM Free.Max, a lower-field 0.55T MRI scanner, we are working on a device concept that is helium- and energy-saving[1] and, due to its low cost, has the potential to bring MRI to rural settings and even to developing countries – or maybe, as an "MRI-in-the-Box", to grocery stores in the far future. In the context of sky-rocketing energy costs, however, the scanner is also attracting interest across Germany. Currently w use our MAGNETOM Free.Max for everything except heart and mamma imaging. Here are examples of stroke imaging (Fig. 5); MR angiography (Fig. 6), and MRI for intervention planning (Figs. 7, 8).

With the new ARTIS icono angiography system, we are building a third interventional suite as a hybrid OR. We are pleased about a performance increase of over 40% with more than 1,000 interventions per year. In terms of research and specialist radiological training, we benefit greatly from having radiology, neuroradiology, and nuclear medicine all under one roof. This offers many additional development opportunities for our staff, which we supplement with a variety of collaborations, such as the establishment of an interdisciplinary ultrasound team, and rotations for resident radiologists to an external private praxis for specialization e.g., in muskuloskelettal MRI.

With photon-counting CT, we created a motivated group of residents to specialize in research as a team and, at the same time, managed to work economically with 50 to 60 patients per day. Recently, patients have begun spontaneously traveling to us from various European countries, because they appreciate the low radiation dose and quality, especially of the cardiac photon-counting examinations (Figs. 9, 10).

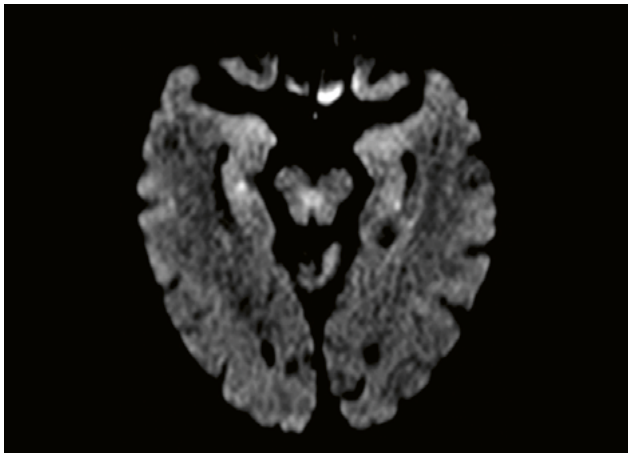

5 Bilateral transient global amnesia (TGA) in the hippocampus
The MAGNETOM Free.Max 0.55T MRI scanner has a lower signal-to-noise ratio than high-field MRI. However, it has distinct advantages in the presence of susceptibility artifacts, e.g., in lung and bone imaging, and with prostheses[2]. We primarily use the scanner for musculoskeletal, spine, thorax, and head imaging, and for patients who are scared of scanners with narrower bores. In stroke imaging, our MAGNETOM Free.Max picks up the smallest DWI lesions, such as in this case of bilateral hippocampal lesions in a patient with TGA.

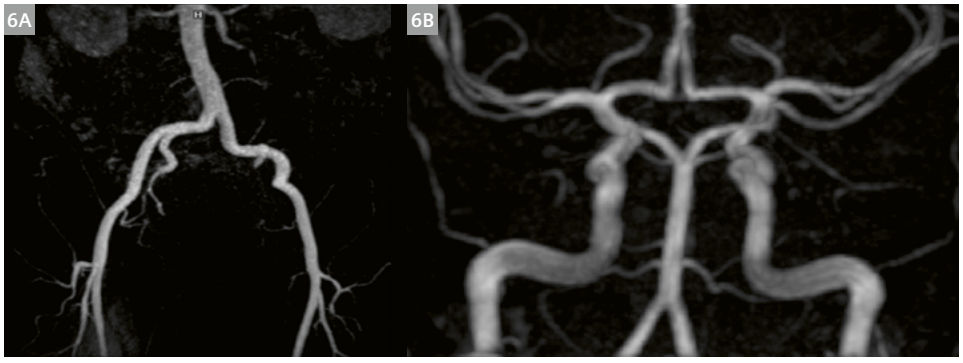

6 MR angiography using MAGNETOM Free.Max and (6A) 3D Flash (6B) TOF
The MAGNETOM Free.Max MRI allows for segmental angiographies with excellent quality. Here we show examples in the pelvic region and a time-of-flight angiography without relevant clinical findings.

[1]The statements by Siemens Healthineers' customers described herein are based on results that were achieved in the customer's unique setting. Since there is no "typical" hospital and many variables exist (e.g., hospital size, case mix, level of IT adoption) there can be no guarantee that other customers will achieve the same results.
[2]The MRI restrictions (if any) of the metal implant must be considered prior to patient undergoing MRI exam. MR imaging of patients with metallic implants brings specific risks. However, certain implants are approved by the governing regulatory bodies to be MR conditionally safe. For such implants, the previously mentioned warning may not be applicable. Please contact the implant manufacturer for the specific conditional information. The conditions for MR safety are the responsibility of the implant manufacturer, not of Siemens Healthineers.

7 **QISS MR angiography (MRA)**
The QISS MRA enables a very decent angiography of the entire pelvis and legs within about 20 minutes and without any contrast enhancement. The sequence changes our procedures: We perform QISS for imaging before interventions in order to plan the treatment indication and pathways. The presented case shows a high-grade stenosis of the superficial femoral artery at the right side, and mid-grade stenoses of smaller vessels such as at the left anterior tibial artery. It also provides a good overview of occlusions in the lower leg vessels.

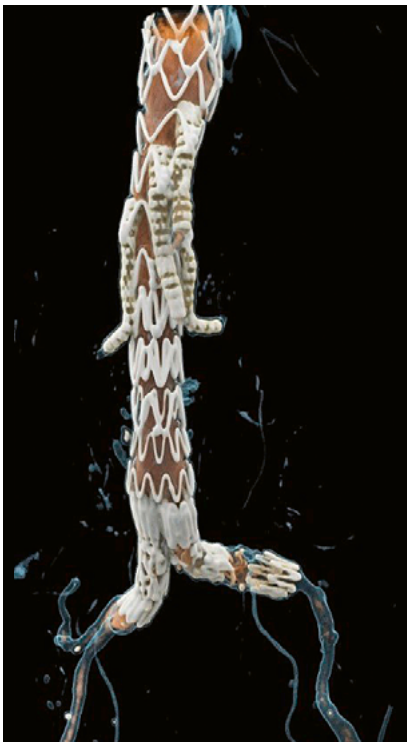

8 **Imaging of a prosthesis**
The excellent image quality produced by photon-counting Computed Tomography provides detailed depictions of prosthesis struts, even in small stents, so that, besides endoleaks, we have strongly improved the evaluation of implants[2].

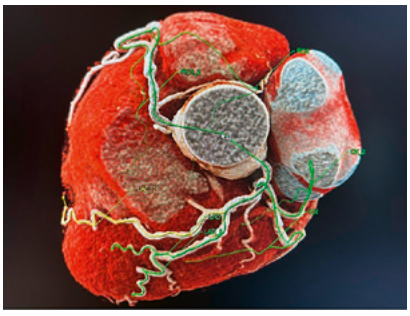

9 **Autosegmentation of the heart**
For me, one of the most striking *syngo*.via features is the cardiac CT platform. It comes with a fully automated and thus fast and easy-to-use heart workflow. When patients travel to us for coronary CT imaging and see their heart in Cinematic Rending and the finely cut MPI reconstruction of their coronary vessels, they usually say something like, "Wow! This is why I came here."

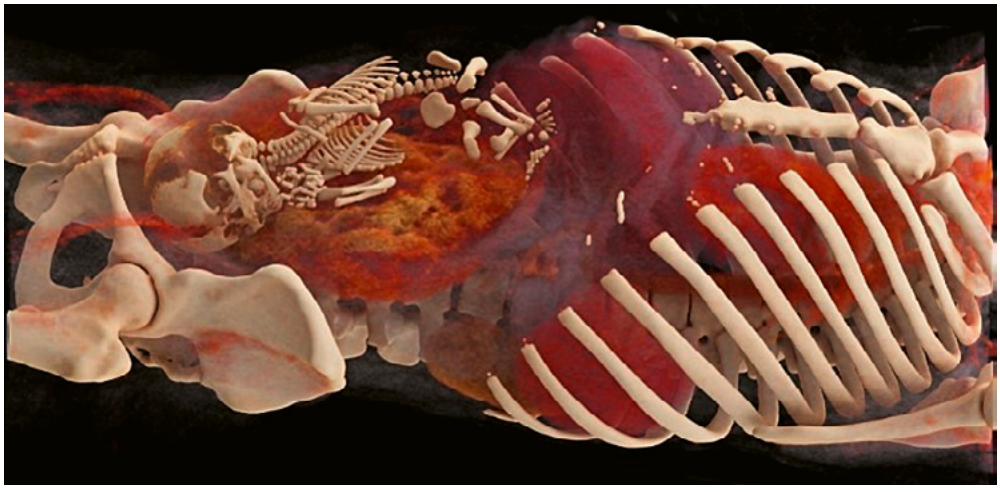

10 **Photon-counting CT allows us to save radiation dose**
Our current photon-counting CT protocols enable massive reductions in radiation dose throughout the body. Particularly in high-contrast investigations, we can halve contrast and radiation dose.

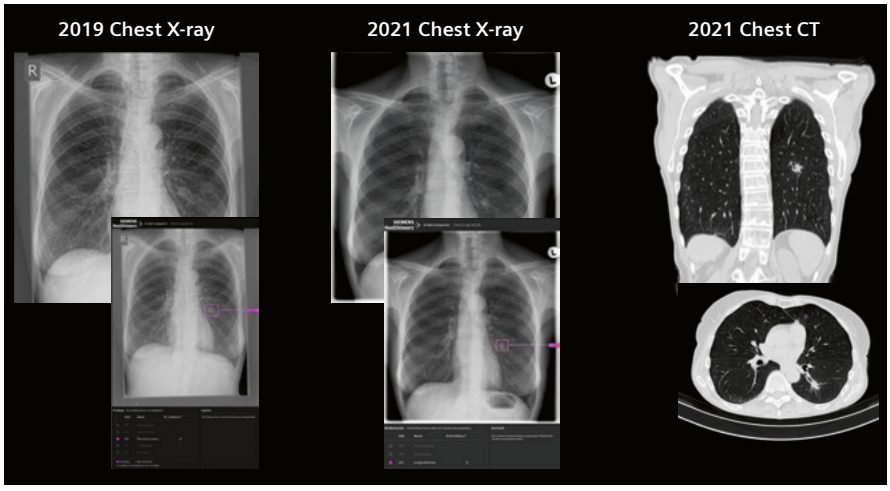

11 **Thorax AI**
AI-Rad Companions support CT and X-ray examinations as a cloud service for our main site in Minden and, via the central server, for the smaller sites in Lübbecke, Bad Oeynhausen, and Rahden. In this case, the AI-Rad Companion found a retrohilar lung tumor that was overlooked in both the current and earlier investigations. The high confidence (10 out of 10) of the deep learning algorithm led to a CT scan. The tumor was fully resected, and as of the 6-month follow-up, we assume the patient is cured.

Motivation by collaboration

Our scientific cooperations and visitors regularly bring fresh ideas to the site and help to set their own accents in the AI field. Working in such a state-of-the art environment and supporting product development and clinical testing is highly motivating for our staff.

Our steadily growing concept is very well received by patients and physicians alike. Instead of one application, we now receive 40 applications in response to a job ad. And while there are shortages elsewhere, we have significant overstaffing in the technologist team. This is allowing us to expand services, which is necessary: With the university outpatient clinic and outpatient specialty care, radiology in Germany is moving from being a cost center to an essential clinical business line. We filter patients for our understaffed rural university hospital, and we are on our way to doubling our services in the near future. The overall structure now also brings seven additional well-trained specialists to the small sites in Rahden, Lübbecke, and Bad Oeynhausen. Further, three high-end servers at the main site provide cloud access to a variety of AI algorithms such as AI-Rad Companions for the peripheral sites, as well as the expertise to read all this information. It is not uncommon for the AI to make essential findings that were overlooked before (Fig. 11).

Conclusion

“Clinical care should not depend on zip code”. Many people agree on that – to meet this challenge, good networks, regional high-performance centers, and attractive training structures are needed to meet the demand for care in rural areas.

Contact

Jan Borggrefe, M.D., EBIR-ES, FCIRSE
Professor of Radiology / Neuroradiology
Director Department for Diagnostic Radiology, Neuroradiology, and Nuclear Medicine
Johannes Wesling University Hospital Minden / Mühlenkreiskliniken
Hans-Nolte-Straße 1
32429 Minden
Germany
Tel.: +49 571 7904601
Jan.Borggrefe@muehlenkreiskliniken.de


Jan Borggrefe, M.D., EBIR-ES, FCIRSE


The MKK team

How To Do Fetal Cardiac MRI at 3T

Rawan Abuzinadah[1]*, David A Broadbent[2]*, Ning Jin[3], Malenka M Bissell[1,4]

[1]Leeds Institute of Cardiovascular and Metabolic Medicine, University of Leeds, United Kingdom
[2]Department of Medical Physics, Leeds Teaching Hospitals Trust, Leeds, United Kingdom
[3]Siemens Medical Solutions USA, Inc., Malvern, PA, USA
[4]Department of Paediatric Cardiology, Leeds Teaching Hospitals Trust, Leeds, United Kingdom
*Both authors contributed equally to the manuscript

Background

Diagnostic uncertainty adds additional burden to an already stressful pregnancy. While fetal echocardiography is the mainstay of antenatal diagnosis, some prognostic uncertainty remains in a number of cases. This can be due to the difficult nature of prenatal diagnosis, such as coarctation of the aorta or due to poor echo windows in oligohydramnios or maternal obesity. In neuro imaging, fetal MRI[1] is already routinely used in a number of centers to enhance diagnosis in the prenatal setting. Fetal cardiac MRI has previously been restricted to a few research centers with access to advanced motion correction and self-gating methods [1]. Over the last 24 months, with the advent of an MRI-compatible ultrasound gating device [2], fetal cardiac MRI has become available to clinical centers, as now standard sequences can be adapted and used for fetal cardiac imaging.

Fetal cardiac MRI can be performed at 1.5 Tesla or 3 Tesla. While 3T creates additional challenges during anatomical data acquisition, it provides better signal-to-noise ratio (SNR) and makes phase contrast imaging for 2D and 4D Flow[2] MRI more achievable.

Despite this, fetal cardiac MRI scans remain challenging due to very small fetal organs in a large maternal field of view, which limits the maximal resolution that can be achieved. Standard sequences are only successful when fetal movement is small. Therefore, fetal cardiac MRI is currently performed in late stages of pregnancy (33–37 weeks of gestational age). SNR will be achieved from the larger fetal body. Moreover, the fetal movement will be restricted due to reduced amniotic fluid and less space for the fetus to move. Additionally, it is important to reduce maternal anxiety as much as possible as calmer mothers often have calmer fetuses. Therefore, for a successful fetal cardiac MRI scan, careful patient preparation and adaptation of standard sequences are important and outlined in detail in this manuscript.

Patient preparation

Pre-appointment preparation

Fetal cardiac MRI can be stressful for expectant mothers, especially for those whose fetuses are suspected to have congenital heart condition or have confirmed congenital anomaly on echocardiography. Parents are frequently concerned about the safety of the MRI scan for the fetus. Therefore, it is important to prepare the patient with all necessary information before the scan. It can be beneficial to send the patient an information leaflet prior to the scan, answering frequently asked questions and providing information about MRI safety for pregnant patients, as well as information about how the scan will be performed. Including pictures makes the information easier to understand.

[1]Siemens Healthineers disclaimer: MR scanning has not been established as safe for imaging fetuses and infants less than two years of age. The responsible physician must evaluate the benefits of the MR examination compared to those of other imaging procedures. Note: This disclaimer does not represent the opinion of the authors.
[2]Work in progress: The application is currently under development and is not for sale in the U.S. and in other countries. Its future availability cannot be ensured.

The day of the scan

It is important to provide a calm environment where the safety screening can be discussed with the patient before the scan. Sufficient time should be allowed prior to each slot so the patient can discuss any concerns, to allow the patient to feel comfortable with the team and less stressed about the outcome of the scan. If possible, offer pregnant mothers to change into hospital scrubs to keep her as comfortable as possible. Hospital gowns rarely fit, and often make women feel more self-conscious and stressed during the MRI scan. Additionally, it is important to ask patients to empty their bladder just before the beginning of the scan.

Scanner room preparation, patient positioning, and gating

The MRI scanner room should be well prepared before the patient arrives (Fig. 1). The setup should be for entering the bore feet first. The spine coil should be in place. At least three pillows should be available as it is more comfortable for some patients to have more than one pillow under their head and an additional pillow between their legs. Also, MRI-compatible wedges should be in place on the right-hand side of the bed to provide support for the patient's back so the pregnant woman is placed in the left-lateral position when lying supine. Moreover, the leg support wedge placed under the patient legs reduces the lower leg pain often experienced in late pregnancy.

1 MRI setup with pillows, wedges, and the crossed straps to keep the ultrasound probe in place.

If the Doppler ultrasound (DUS) gating device is being used, it is important to charge the device before the day of the scan. Also, the ultrasound gel should be to hand and the wireless device should be connected to the MRI scanner. The straps to keep the ultrasound probe in place should be placed in a cross position onto the MRI table at the level of the lumbar spine.

Once the patient arrives in the scanner room, it is vital to make sure the patient is as comfortable as can be. Often, maternal movement degrades imaging more than fetal movement. The patient will be usually positioned left-lateral feet-first into the bore of the magnet. Feet-first reduces anxiety as the patient can look upwards and out when moving into a restricted space. As the scanner bore is a confined place, most patients will have to be placed into the left-lateral position, ideally at least 35 degrees. However, if the patient's hip circumference allows, placing the patient completely onto the left-hand side can improve patient comfort and reduce maternal breathing motion. After making sure the patient is comfortable in her position, the ultrasound gating device will be placed on the maternal abdomen to search for the fetus's heartbeat (Fig. 2). It is useful to palpate the abdomen for the fetal spine and then position the ultrasound head near the left shoulder facing towards the fetus. If the fetus's back is to the mother's back, it can be very difficult to obtain a reliable Doppler gating signal and sometimes only non-gated imaging can be possible.

If struggling with positioning, the device can be placed randomly on the lower abdomen before the localizers are acquired to localize the position of the transducer in regard to the fetal heart. With this information, it is very easy to find the fetal heartbeat. It is very important that the transducer is localized centered above the fetal heart in order to prevent signal loss due to fetal movement. It is

2 Positioning of the ultrasound gating transducer.

also important to have a clear procedure in place to check for fetal well-being if the MRI team is unable to locate a fetal heartbeat. Once the heartbeat is heard clearly through the device headphones and a good signal is observed on the monitor, the ultrasound transducer will be held in place by securing it with the straps. Additional small wedges can be useful to keep a tilted position, if needed. After that, the 18- or 30-channel coil will be placed onto the abdomen. It is helpful to provide music via the headphones to keep the mother calm and distract her during the scan. It is important to stay in contact with the patient during the scan to provide her with updates about the scan's progress and to make sure she is doing well.

In the MRI control room, patient information such as height, weight, feet-first and the fetal heart protocol will be selected to start the scan. The time at the beginning of the scan will be documented to make sure the 30 minutes are not exceeded.

MRI safety considerations

When scanning during pregnancy particularly consideration must be given to both maternal and fetal safety. Radiofrequency (RF) exposure must be limited to avoid undue heating, and excessive acoustic noise must be avoided to mitigate risk of damage to developing hearing organs. When performing fetal CMR it is therefore paramount to remain in normal mode – both specific absorption rate (SAR) and gradients – and use the lowest gradient modes available on each sequence (with Whisper gradients used wherever possible). Low SAR RF pulse types are used where possible. Furthermore, scan duration is limited to approximately 30 minutes to restrict accumulated RF energy deposition (specific energy dose, SED) and to minimize maternal discomfort. To further support maternal comfort, we favor the use of fixed table positions once initial localization has been performed and the fetal heart positioned at isocenter. Scanning should be performed without the use of exogenous contrast agents to avoid the hazards associated with these, as many are known to cross the placenta and enter the fetal bloodstream.

Consequently, there is a need to image rapidly, albeit with restrictions on gradient switching and RF exposure, while exploiting only endogenous contrast mechanisms. Additional challenges arise due to unpredictable fetal movement within the uterus, potential maternal movement due to discomfort, and (when acquiring cardiac synchronized images) significantly higher heart rates than in older children or adults.

Due to the small fetal heart size in the larger maternal field of view, it is challenging to acquire images with sufficient spatial resolution while avoiding wrap from the surrounding maternal body.

In addition to field-of-view and resolution concerns, the extra tissue and fluid around the fetus can cause challenges with signal intensities. SNR can be adversely affected if the fetal heart is deep inside the mother, due to distance to the coil elements. To further maintain acceptable SNR, the use of parallel imaging is avoided for the majority of sequences (except for initial localizers where GRAPPA with acceleration factor 2 is used). However, partial phase Fourier acquisition is used where there is sufficient SNR without averaging and asymmetric echoes and where there is a need to minimize TE. Furthermore, Compressed Sensing allows 4D Flow[2] MR imaging (research sequence) in an acceptable timeframe for fetal imaging.

Signal scaling around the fetal heart can also be adversely affected by dominating signals from material closer to the coil, particularly fat and amniotic fluid, which (depending on the sequence weighting) can have particularly high intensity. Consequently, the Image Scaling Correction is routinely increased (in the System – Tx/Rx window) and high receiver gain selected. This may lead to the signals from maternal fat and fluid appearing saturated, but results in much better contrast resolution over the fetal anatomy of interest. Trial and improvement may be needed to find optimal values, but values between 5 and 15 for different sequences is a good initial guide. Note that the Image Scaling Correcting setting can also be edited in retrospective reconstructions, which can allow fine tuning without the need to repeat image acquisition.

Given the above considerations, image quality comparable with adult CMR should not be expected when performing fetal CMR. Compromises are to be expected and a protocol that carefully prioritizes sequences must be developed, with the flexibility to allow for repeat imaging as and when required due to fetal movement.

Anatomical scanning

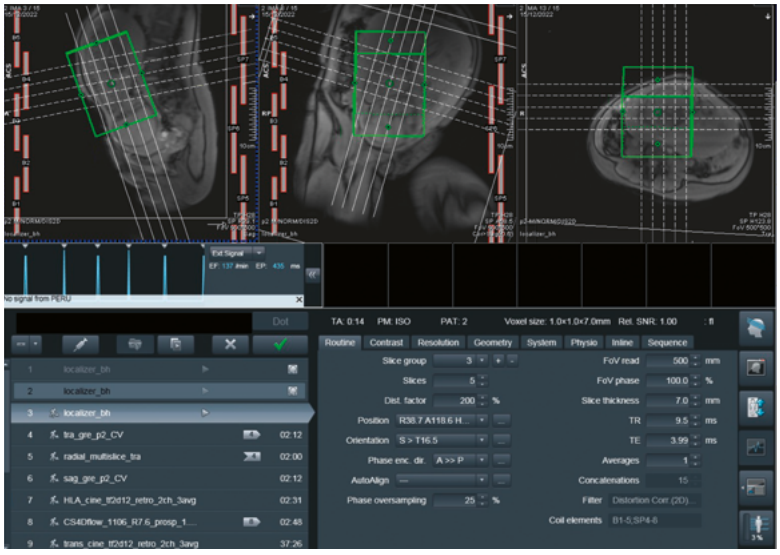

3 It is important to place the final localizer directly over the fetal heart and align it to the fetal thorax orientation. A tight shim box is important to reduce artifacts and improve image quality, especially at 3T.

Vasculature-triggered TurboFLASH (approx. 2 minutes for 30 slices)

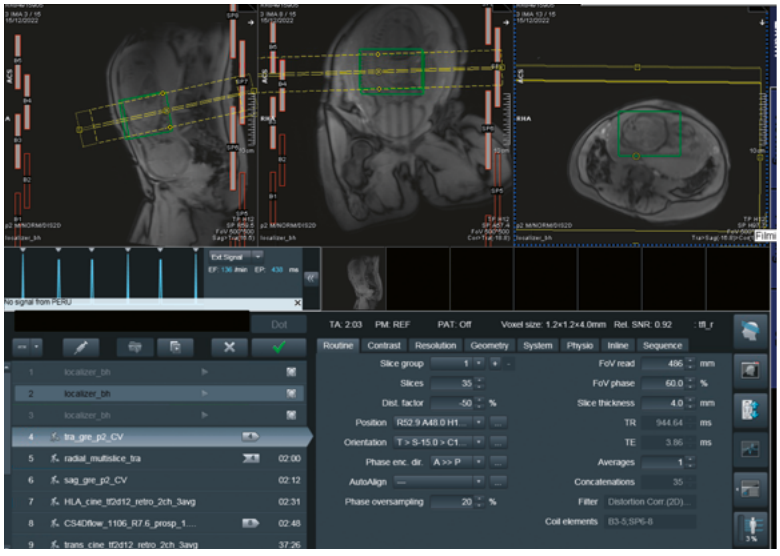

4 Cover the entire thorax with 50% overlap transverse to the fetal thorax.

After standard three-plane localizers aligned to the maternal anatomy, we acquire a stack using 2D TurboFLASH imaging, which generates high signal from the vasculature due to inflow enhancement effects. Single shot (per slice) triggered imaging is performed, providing resilience to motion and allowing stacks of 30 slices to be acquired in approximately 2 minutes. A high flip angle (for a FLASH sequence) of 30° is used to maximize saturation of stationary tissue, yielding high contrast of the flowing blood. We find that a single acquisition (no averaging) and 5/8 phase partial Fourier yields sufficient SNR with this sequence. A base resolution of 400 yields an in-plane resolution of approximately 1.2 × 1.2 mm^2.

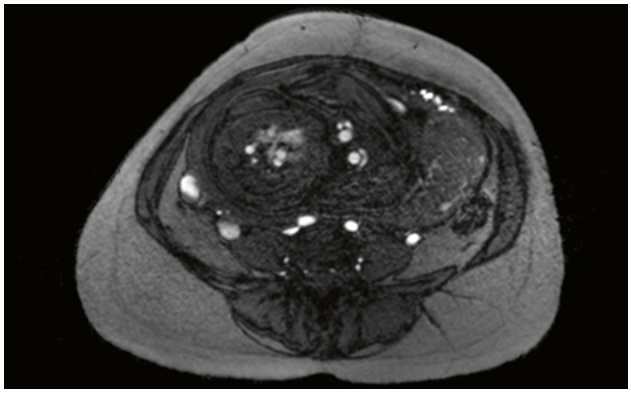

5 Transverse TurboFLASH "white blood" stack depicting the main pulmonary artery and branch pulmonary arteries.

A stack of 4 mm slices overlapping by 2 mm (-50% distance factor) are acquired. Acquisition is triggered (single-phase) using the Doppler US device, to acquire data every other heartbeat with a minimal trigger delay of 1 ms.

This sequence is often repeated with fewer slices to provide targeted views of specific vascular anatomy, for example, aligned to show the aortic arch.

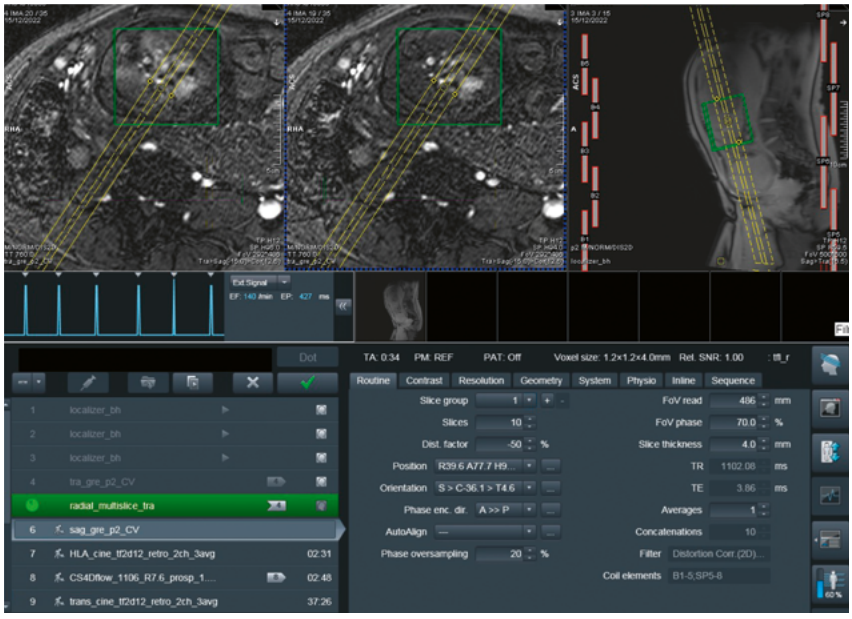

6 Planning of a smaller sagittal stack through the aortic arch perpendicular to the fetus. Watch out for wrap.

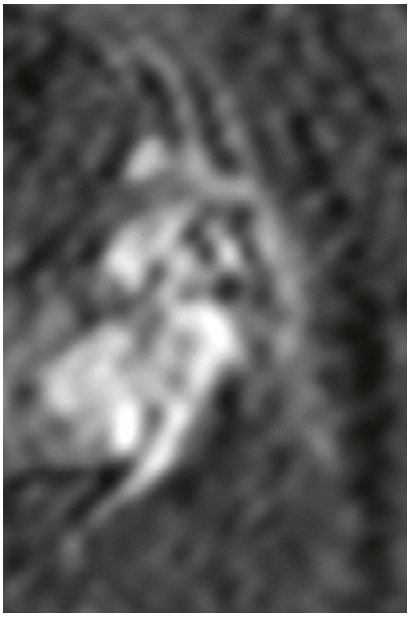

7 TurboFLASH of the aortic arch.

Radial multi-slice TrueFISP (approx. 2 minutes for 30 slices)

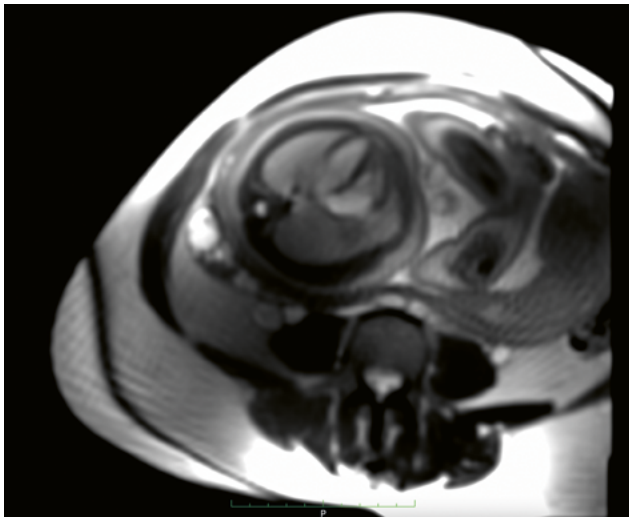

8 Radial transverse stack depicting 4 chambers.

We also acquire a stack of 2D TrueFISP images transverse to the fetus for an overview of fetal anatomy and to aid further planning. These are acquired as 4 mm thick contiguous slices but with 2 mm separation between slice centers (i.e., distance factor of -50%) to provide overlapping slices with the higher SNR associated with the thicker slices than would be achieved with 2 mm slice thickness. As alternate slices are acquired first, followed by the intermediate slices, cross-talk is kept to acceptable levels (despite the negative distance factor). However, fetal movement between the odd and even slices can lead to a jumpy appearance when scrolling through the stack.

Radial *k*-space sampling is used to minimize motion artifacts with a base resolution of 144 (143 radial views), leading to an in-plane resolution of approximately 2.2 × 2.2 mm^2 for a typical field of view. Signal averaging is used (number of acquisitions, NSA = 4) with short-term averaging mode.

Cine imaging (approx. 1 minute per slice)

For Cine imaging, we use a TrueFISP acquisition with 4 mm slice thickness and approximately 1.1 × 1.1 mm² in-plane resolution. To obtain sufficient SNR, we use averaging (NSA = 3) and do not use parallel imaging or partial Fourier acquisition, although weak asymmetric echoes are allowed to minimize TE. Short-term averaging mode is used to minimize motion artifacts.

A Cine transverse stack is useful for initial Cine imaging. Our sequence is retrospectively gated into 25 cardiac phases using the Doppler US device. Where multiple slices are required, they are acquired contiguously in sequential mode. If the DUS ECG is unstable, we choose to change to prospectively gated to allow for improved image quality.

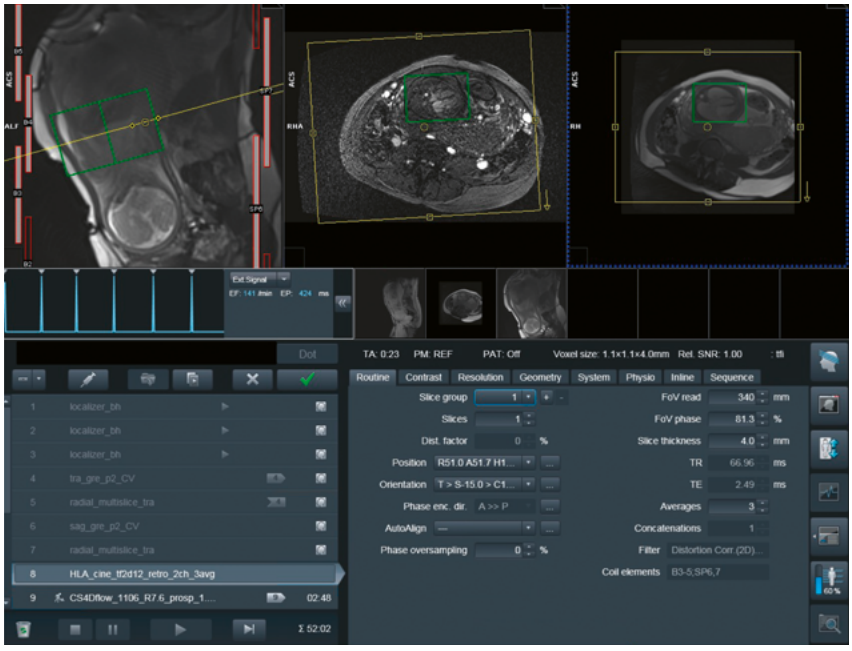

9 Planning of 4-chamber Cine using acquired transverse stacks as planning guide.

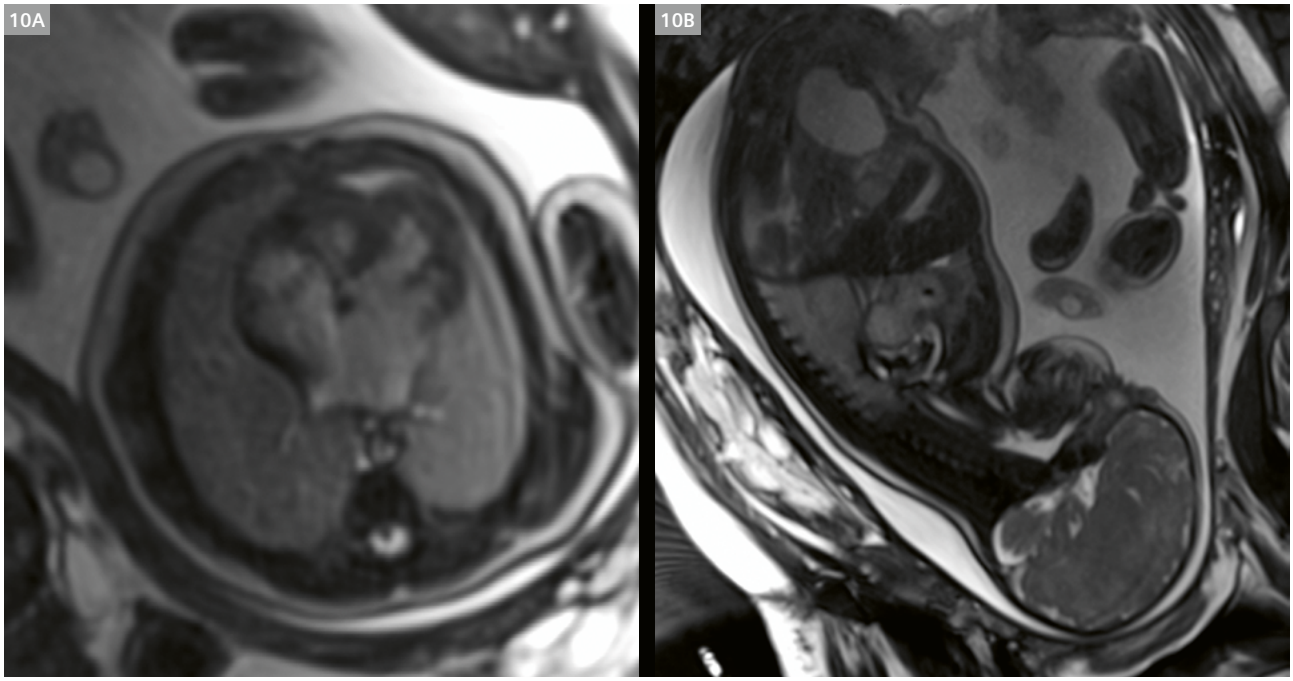

10 **(10A)** 4-chamber-view Cine in a patient with hypoplastic right ventricle and tricuspid regurgitation. **(10B)** Image of the aorta.

CS 4D Flow² MRI (approx. 3 minutes for 40 slices)

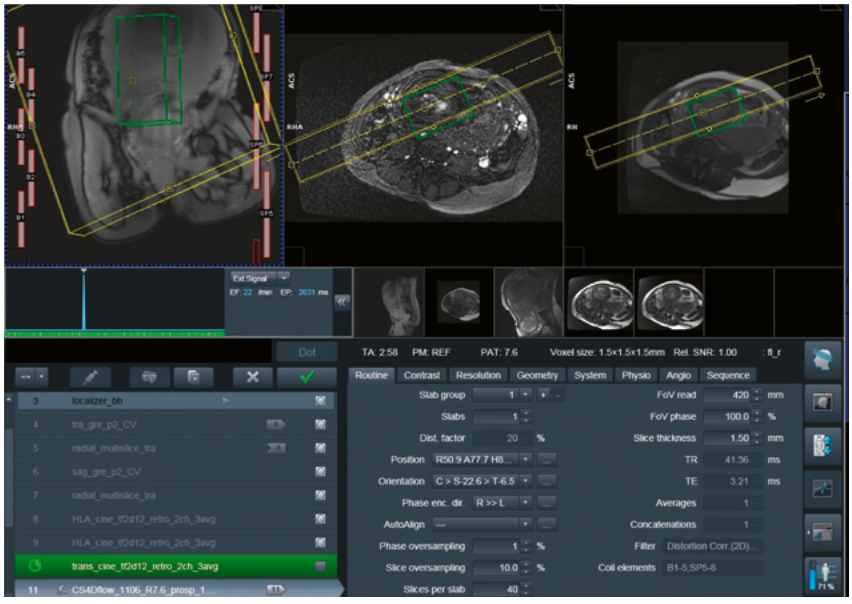

11 Planning of CS 4D Flow MRI using the 4-chamber view as orientation and the transverse stack to check that pulmonary artery and aorta are included. Watch out for wrap and check on localizers.

To assess blood hemodynamics we use Compressed Sensing 4D Flow² MRI, which allows volume coverage of the heart and proximal vasculature in an acceptable time frame for fetal imaging. This approach allows a 3D volume to be acquired with velocity encoding in all three dimensions. It can therefore be significantly simpler and more robust than planning multiple 2D flow acquisitions, particularly in this application, as in a 2D approach, where it is critical for each view to be accurately prescribed, it is common for repeat scanning to be required when the fetus moves during the time required to accurately plan each acquisition.

We acquire data with approximately 1.5 mm³ isotropic resolution, prospectively triggered using the Doppler US device with a minimal (1 ms) trigger delay and 9 cardiac phases. A venc of 70 cm/s is used. Strong asymmetric echoes are allowed to allow TE and TR to be minimized, and a constant 7° is used.

It should be noted that image reconstruction can take significantly longer than acquisition for this sequence (up to around 15 minutes), and other sequences acquired subsequently will not be reconstructed until the 4D Flow MRI reconstruction completes. We therefore generally perform this sequence towards the end and accept that it is not feasible to review the data while the patient is still on the scanner. Instead, we allow the reconstruction to occur while the patient is being removed from the scanner and while the scanner is being prepared for the next patient.

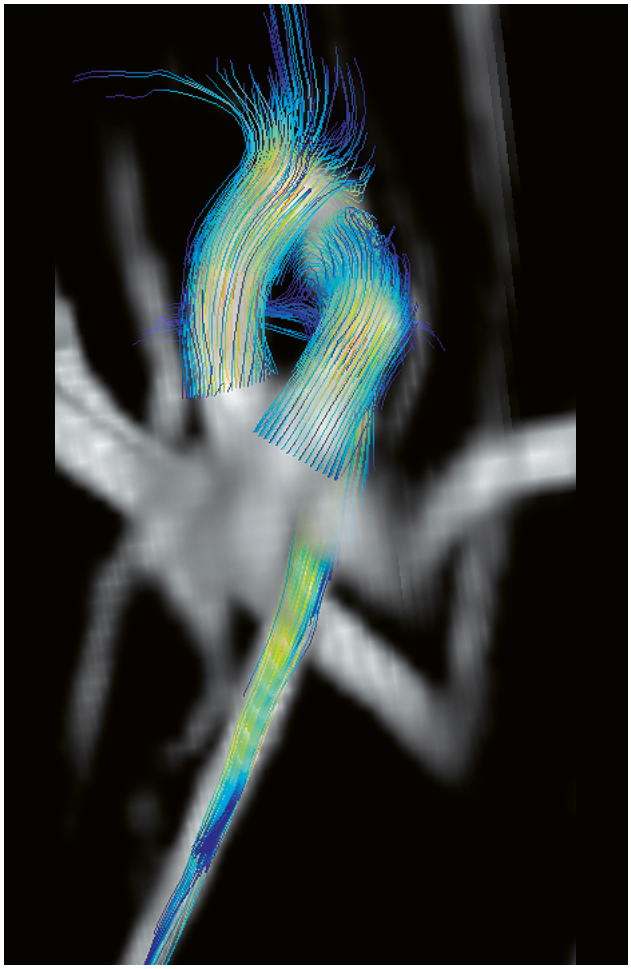

12 Compressed Sensing 4D Flow MRI of the aorta and main pulmonary artery.

Lung HASTE (approx. 3 minutes for 25 slices)

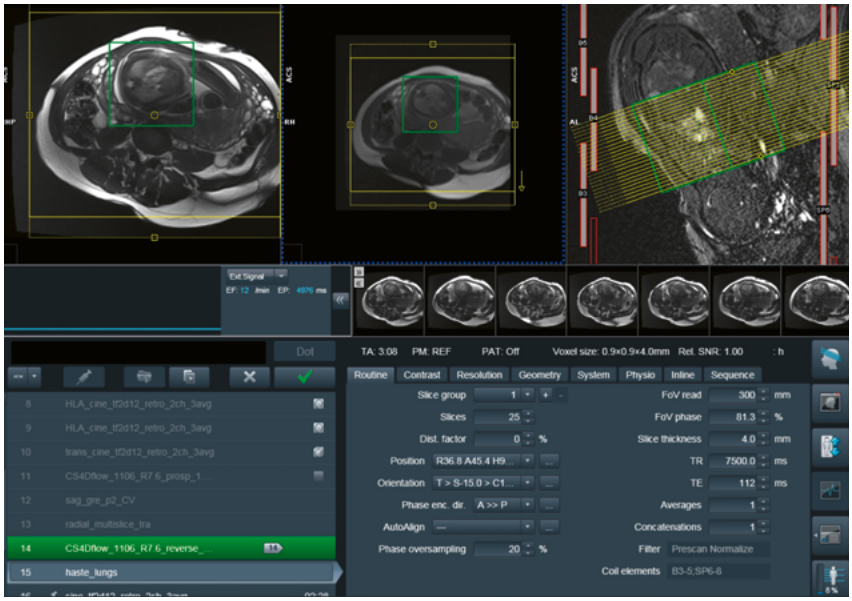

13 Transverse HASTE stack for lung volume using more slices than for the previous stacks to ensure lung volume is acquired completely.

If lung volumetry is required, we acquire a stack of contiguous 4 mm T2-weighted HASTE slices covering the fetal thorax in a transverse orientation (i.e., similar geometry to the above sequences but without overlapping and with larger coverage in the slice direction to encompass the entire fetal thorax). A base resolution of 320 yields approximately 1.1 × 1.1 mm^2 in-plane resolution. This sequence provides sufficient SNR to not require averaging and to allow 4/8 phase partial Fourier sampling. As HASTE is a single-shot sequence, the TR can be minimized without influencing signal contrast, although care must be taken not to increase SAR too much.

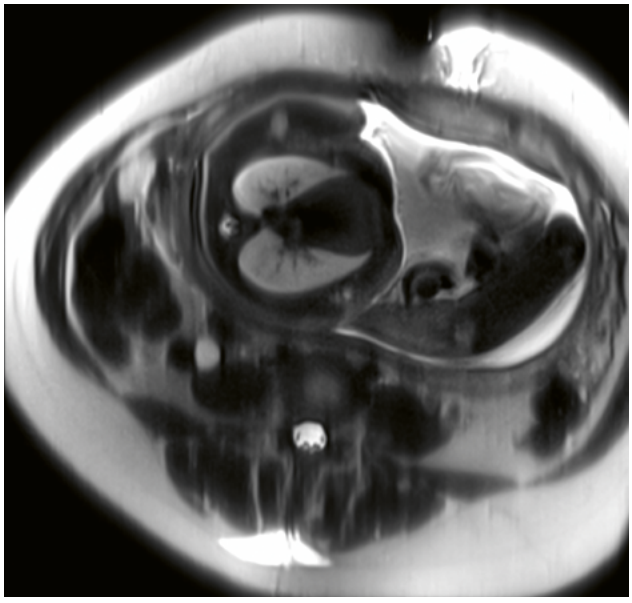

14 HASTE for lung volume quantification.

Frequent challenges in fetal cardiac MRI

Ultrasound gating

The Doppler ultrasound gating device increased the utility of dynamic fetal cardiac MRI scanning, but searching for the fetal heartrate can be challenging due to fetal movement and can require time. Therefore, communication with the patient is important to explain that searching for the heartbeat may take some time and does not mean there is a problem with the fetus.

Positioning the body coil above the ultrasound gating device can cause compression on the device, which results in losing the gating signal and requires repositioning of the device. It is therefore important to ensure that there is no contact between the body coil and the transducer. Applying pads on the side of the ultrasound transducer can avoid the compression caused by the coil.

The trigger signal will be displayed on the scanner computer for signal monitoring under external trigger. Sometimes the fetal heartbeat will be lost during the scan, due to maternal and/or fetal movement, which will increase the scanning time. But it is often useful to wait rather than reposition, as the heartbeat can often be detected again after a pause. Often the signal is lost due to deep inspiration taken by the mother. Therefore, the mother is asked to take shallower breaths, which will reduce the movement and avoid missing the heartbeats. Additionally, the DUS will simulate up to 15 heartbeats if the heartbeat is lost. This often bridges short gaps due to breathing motion. However, retrospective 4D Flow MRI is often not easily achievable at present, as the sequence fails if heart beats are missed.

Maternal breathing artifact is in our experience the largest movement artifact. Breath-holding can be sufficient to eliminate the maternal movement. But the DUS transducer often moves position during breath-holding and the Ultrasound gating is lost all together. It is also very challenging for pregnant patients. Therefore, applying free-breathing techniques is often the more successful option.

Outlook

Fetal cardiac MRI faces a number of challenges, and one has to accept that there will be a percentage of fetuses where image quality might not be of diagnostic quality. We find that running a number of different transverse stacks with some targeted sagittal images will often provide sufficient information to understand the fetal cardiac anatomy. This can be useful to assess, for example, the degree of ventricular disproportion during the third trimester [3, 4]. Lung volume assessment [5] can be useful in significant tricuspid regurgitation and right atrial enlargement to assess the degree of right lung hypoplasia. In hypoplastic left heart syndrome, lung parenchyma can be assessed for damage (nutmeg lung) from a restrictive inter-atrial septum. Flow assessment allows further assessment of whether the inter-atrial septum is restrictive in both hypoplastic left heart syndrome and transposition of the great arteries. Quantification of tricuspid or mitral valve regurgitation can also be useful. Furthermore, comprehensive cine and flow assessment can also add information in borderline left ventricles. As more and more centers start using fetal cardiac MRI, further clinical uses will likely become apparent [6–8].

References

1 Roy CW, van Amerom JFP, Marini D, Seed M, Macgowan CK. Fetal Cardiac MRI: A Review of Technical Advancements. Top Magn Reson Imaging. 2019;28(5):235–244.
2 Kording F, Schoennagel BP, de Sousa MT, Fehrs K, Adam G, Yamamura J, et al. Evaluation of a Portable Doppler Ultrasound Gating Device for Fetal Cardiac MR Imaging: Initial Results at 1.5T and 3T. Magn Reson Med Sci. 2018;17(4):308–317.
3 Al Nafisi B, van Amerom JF, Forsey J, Jaeggi E, Grosse-Wortmann L, Yoo SJ, et al. Fetal circulation in left-sided congenital heart disease measured by cardiovascular magnetic resonance: a case-control study. J Cardiovasc Magn Reson. 2013;15(1):65.
4 Lloyd DFA, van Poppel MPM, Pushparajah K, Vigneswaran TV, Zidere V, Steinweg J, et al. Analysis of 3-Dimensional Arch Anatomy, Vascular Flow, and Postnatal Outcome in Cases of Suspected Coarctation of the Aorta Using Fetal Cardiac Magnetic Resonance Imaging. Circ Cardiovasc Imaging. 2021;14(7):e012411.
5 Mlczoch E, Schmidt L, Schmid M, Kasprian G, Frantal S, Berger-Kulemann V, et al. Fetal cardiac disease and fetal lung volume: an in utero MRI investigation. Prenat Diagn. 2014;34(3):273–278.
6 Dong SZ, Zhu M, Ji H, Ren JY, Liu K. Fetal cardiac MRI: a single center experience over 14-years on the potential utility as an adjunct to fetal technically inadequate echocardiography. Sci Rep. 2020;10(1):12373.
7 Lloyd DF, van Amerom JF, Pushparajah K, Simpson JM, Zidere V, Miller O, et al. An exploration of the potential utility of fetal cardiovascular MRI as an adjunct to fetal echocardiography. Prenat Diagn. 2016;36(10):916–925.
8 Ryd D, Fricke K, Bhat M, Arheden H, Liuba P, Hedstrom E. Utility of Fetal Cardiovascular Magnetic Resonance for Prenatal Diagnosis of Complex Congenital Heart Defects. JAMA Netw Open. 2021;4(3):e213538.

Contact

Dr. Malenka M Bissell, DPhil, MD, BM, MRCPCH
Clinical Lecturer in Paediatric Cardiology
Department of Biomedical Imaging Science
Leeds Institute of Cardiovascular and Metabolic Medicine
Worsley Building, Room 8.49f
Clarendon Way
University of Leeds
Leeds
LS2 9NL
United Kingdom
M.M.Bissell@leeds.ac.uk

3T Cardiac MRI and Acute Myocarditis in the Context of Second-dose mRNA Vaccine. A Case Study

Erin Robins and Claire Harris

Perth Children's Hospital, Nedlands, Western Australia

Abstract

Presentations of acute myocarditis are becoming more common following the second and third dose of mRNA vaccinations. Myocarditis has been recognized as a rare complication of COVID-19 and the mRNA vaccines, especially in young adult and adolescent males. The novelty of this pandemic means we have no standard protocols for imaging this patient cohort. Whether or not to perform MRI remains a little unclear, so we have developed guidelines for which cases to scan. We can, however, be certain that case numbers for these presentations will rise, so robust, quick scanning protocols are important, if we are to manage increasing cases. The representative cohort is favorable for MR imaging in that most patients will be compliant, able to breath hold, and able to withstand the longer exam times of cardiac MRI. Not all patients are equal, however, and keeping scan time short and using some non-breath-hold techniques for those unable to comply, will be discussed. High-quality imaging, especially late gadolinium enhancement (LGE), is crucial for diagnosis. Here we present a case of a fourteen-year-old boy who presented to the ED with severe chest pain and fever two days following his second dose of a COVID-19 mRNA vaccine. He had extremely high troponin levels, an abnormal ECG and echo, and was referred for cardiac MRI (CMRI) for evaluation and as a baseline for monitoring. We have two MAGNETOM Skyra scanners at our site, so all CMRI is performed at 3T.

Introduction

Myocarditis is an inflammatory disease of the heart caused by infiltrates in cardiac muscle resulting in injury without ischemia. In the developed world, the most common cause of myocarditis is viral. In the general population, 20–50 individuals in every 100,000 will present with myocarditis, especially after other vaccines such as smallpox, influenza, and hepatitis B [1, 2]. The rates for mRNA vaccines are thought to be less, and while several studies have been done to report rates of occurrence, the incidence is difficult to establish. However, the U.S. Centers for Disease Control and Prevention claim myocarditis/pericarditis rates are ~12.6 cases per million doses of second-dose mRNA vaccine among individuals 12 to 39 years of age [1], although some publications state this number could be up to 50 per million [2].

Acute myocarditis following COVID-19 vaccination was first reported on February 1, 2021 in Israel, where a 19-year-old male was admitted to ICU with the condition. His second dose of mRNA vaccine was five days prior. At the time it was not confirmed that the inflammation was attributed to the vaccine, but because the symptoms started immediately after the vaccination, suspicions were raised that an immunological reaction may have caused the condition. Concurrently, several COVID-19-related myocarditis cases had been reported, according to the U.S. National Institutes of Health [10]. Now, over one year later, myocarditis is accepted as a known side effect of COVID-19 and of mRNA (Pfizer and Moderna) vaccines [1, 3, 4], occurring largely after the second dose [6]. These cases, however, are almost always mild and self-resolving, and patients make full recoveries [3–5].

Myocarditis can be difficult to diagnose as presentation ranges from mild to acute [5]. The most common symptoms are pleuritic chest pain, palpitations, shortness of breath, fever, ipsilateral (to vaccination site) lymphadenopathy, and headache. Increased troponin levels can be present in patients presenting with myocarditis. Troponin is a type of protein found in heart muscle. When heart muscle is damaged, troponin is released into the bloodstream. Troponin is measured in nanograms per milliliter (ng/mL) and a level of 0.04 ng/mL or less is considered normal. Troponin typically becomes more elevated over a period of days, before peaking. Once the peak has occurred, patient recovery is usually swift.

ECG may also be normal, although sinus tachycardia and nonspecific ST segment and T wave changes can occur, but usually widespread ST elevations are observed [1, 3]. Patients presenting with preserved left ventricular function on echo typically have an excellent prognosis. Those with impaired LV function on echo may benefit from MRI, particularly from a monitoring perspective. CMRI provides a one-stop shop for diagnosis, and longer-term follow-up by providing data on ventricular function, myocardial injury/edema, and longer-term fibrosis, in the setting of myocarditis. Following diagnosis, patients are generally treated conservatively with anti-inflammatory medicines and beta blockers, while troponin levels are monitored.

At our site, we perform CMRI on patients who have impaired left ventricular function. It Is felt that a baseline is important for ongoing clinical monitoring and is considered best practice for the patient. TrueFISP imaging, for ventricular analysis and kinetic wall studies, SPAIR imaging of left ventricle, and late gadolinium enhancement are performed as a minimum. These sequences can be completed within 30 minutes. First-pass perfusion imaging, early gadolinium enhancement, and T1 imaging are considered bonus sequences. For patients unable to tolerate breath-holds, we perform real-time imaging of LV in place of cine imaging for wall motion and late gadolinium enhancement overview for the late gadolinium views. SPAIR imaging in these patients can be performed as inspiratory breath-holds. T1 mapping is not part of our protocol for acute or subacute myocarditis because of rationale (no expectation of fibrosis), although it might be considered in the unusual scenario of chronic myocarditis.

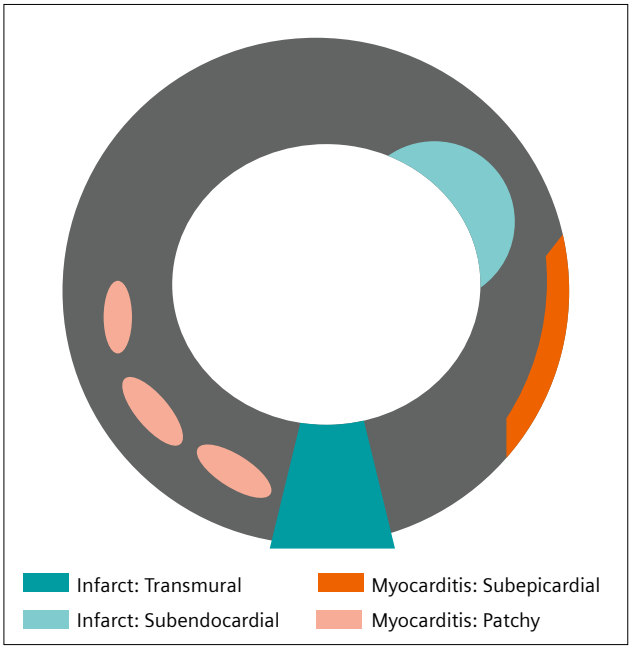

1 Enhancement patterns of myocarditis vs. ischaemia.

Perfusion, early, and late gadolinium enhancement

First-pass perfusion deficits are present in ischemia, but not in myocarditis. Early gadolinium enhancement may demonstrate mural thrombus in ischemia, but this would not be usual in myocarditis. So, while useful in aiding a myocarditis vs. ischemia diagnosis, these techniques are not necessary in an assessment of myocardium in the post-mRNA vaccination setting. Late gadolinium enhancement is important is to demonstrate the extent of myocardial inflammation and long-term follow-up of scar (fibrosis). It is useful to note that the enhancement patterns are different depending on the pathology, myocarditis vs. ischemia (Fig. 1).

Gadolinium does not enter normal myocardial cells, but distributes in the extracellular spaces within a few minutes following injection. Both a normal and diseased myocardium will take up contrast, but will wash out again after about five minutes in normal tissue. Diseased tissue will hold onto the contrast, allowing us to capture shortened T1 values resulting in high signal in the diseased tissue on T1-weighted images. Contrast distribution in ischemic tissue tends to pool in the subendocardium and radiate to the epicardium. The abnormalities are also in the coronary artery distributions. For nonischemic pathologies (myocarditis), the enhancement tends to be subepicardial in the lateral ventricle wall and/or patchy in the mid-ventricular wall.

Case study

Our case involves a 14-year-old boy who presented to a regional emergency department with chest pain, following second-dose of a mRNA vaccine against COVID-19 (Pfizer) three days prior. He described the pain as crushing and constant. The patient had no prior medical history. The pain self-resolved and the patient was discharged. Later the same evening the chest pain recurred and he presented

to the ED where blood tests revealed a blood troponin level of 4,000 ng/mL. The patient was transferred via Royal Flying Doctor Service to the Perth Children's Hospital where he underwent an ECG, which demonstrated changes consistent with pericarditis/myocarditis: ST elevation in lateral leads and PR depression in lead 1. The patient was admitted and an echocardiogram was arranged for the following day. Up to then, he had been treated with oral anti-inflammatory drugs.

The echocardiogram showed impaired left ventricular systolic function. Systolic function is assessed by measuring the global longitudinal strain (GLS) of the longitudinal heart muscle in systole compared to diastole. Reduced GLS may reflect abnormal systolic function and is derived from speckle tracking which is software driven from echocardiogram vendors. Normal GLS ranges from 16–22% [11]. Our patient's GLS was 12%, which was considered abnormal and indicated abnormal LV function. The echo also demonstrated mild hypokinetic basal to mid-inferolateral wall contraction. Troponin levels had increased significantly in the 24 hours since the patient was admitted, peaking at 16,400 ng/mL, so at this juncture, it was deemed that CMRI would be useful to assess baseline myocardial damage with plans to follow up the scan in six months if there were significant findings. The patient commenced oral steroids and bisoprolol, a heart medication called a beta-blocker that lowers heart rate.

Patient preparation

The patient presented in the radiology department and MRI safety and contrast checklists were completed. The patient was changed into appropriate clothing for the scan. Before entering the scan room, we give all our patients thorough, clear instructions for breath-holding. All scans are performed on expiration where possible. Expiration is used as it is easier to reproduce. For patients unable to hold their breath in expiration, we ask that they take a small inspiratory breath in, and that they take the same size breath each time. We find practicing the breath-holds in the waiting room helps. Positioning of ECG placement is explained. We inform patients that the ECG electrodes may get warm and could irritate the skin. We ask that they inform us if this happens.

The patient was positioned supine on the scan table. We ensure the patient is comfortable by placing a pad under the knees and cushions under the elbows. The chest area is cleaned with a skin cleansing agent to lower impedance and improve the ECG signal. We apply four ECG electrodes to the chest (after checking the expiry date and ensuring the electrodes are wet) and attach the ECG device as per scanner graphic user interface. The learning phase is observed. The ECG waveform should always be evaluated to ensure a good waveform is being displayed for adequate gating. If a patient has a *pes excavatum*, leads need to be placed on the same side of the chest. The ECG electrodes should be placed avoiding bony areas and sternal wires.

The Body 18 Coil and Spine Coil are used to obtain images. In order to achieve a good signal-to-noise ratio (SNR), the center of both coils should be aligned with the center of the heart. We always ensure that the coils do not touch the ECG device as this may cause pressure areas and heating. The patient was given headphones for hearing protection and to allow communication for breath-holding. We also provide a mirror so the patient can watch a movie. This is helps the patient to feel relaxed therefore aiding them to maintain the same position throughout the procedure.

Imaging procedure

The Body 18 Coil is placed over the patient's chest with the center of the coil over the heart. The localizing laser is aligned to center of the coil and the patient is moved into the magnet. Orthogonal localizers are performed. The localizers are used to position the heart in the isocenter. Once this is established, the table position will stay at this position for the remainder of the scan. Localizers are performed in transverse, sagittal, and coronal stacks. From these a 2-chamber, 4-chamber, and short axis oblique (SAO) localizers are prescribed. Before commencing the TrueFISP (true fast imaging with steady-state precession) cine imaging, a shim box is applied for homogeneity to optimize image quality. TrueFISP cine imaging is obtained in 2-chamber, 4-chamber, SAO localizers, covering base to apex approximately 8 slices and left ventricular outflow tract (LVOT). If off-resonance artifact occurs, which we experience at 3T, then a frequency scout can help, although in our experience zero frequency adjust is nearly always the best. If the artifact significantly reduces image quality, we use gradient echo (flash). In myocarditis, the TrueFISP cines are obtained to observe ventricular wall motion and for volumetric analysis. In a cooperative patient, such as our case patient, it takes around ten minutes to complete localizers and TrueFISP cines.

A perfusion scan was set up and prepped prior to contrast injection. Contrast was administered through a 22 g cannula inserted into the right cubital fossa, which was placed prior to commencement of the exam. We used a standard MRI-compatible injector pump; contrast (gadovist) was run at a rate of 2.5 mL/sec and a dose of 7.5 mL was administered, with a 15 ml saline flush.

The perfusion scan (dynamic_tfl_sr_ePAT) was run in SAO (4 slice positions) and 4 chamber. Although not pivotal to the diagnosis, these scans were run opportunistically.

Because the late gadolinium enhancement needs to be performed ten minutes after contrast, we performed

the SPAIR (spectral attenuated inversion recovery) images in between contrast and late gadolinium views to minimize the patient's time in the scanner. SPAIR images were also acquired in the same slice positions to show the extent of the myocardial inflammation. 17 minutes of scanning time had elapsed at this point.

A TI scout was performed ten minutes following contrast injection for the late gadolinium enhancement imaging. This provides the optimal inversion time for the late gadolinium images. A phase-sensitive inversion recovery sequence (PSIR) and fast gradient echo sequence (turboflash) is used for late gadolinium enhancement imaging. We want to achieve an intermediate signal blood pool with the signal nulled in myocardium. This is to show maximum enhancement in the ventricular wall. An inversion time of 330 ms was selected. Once again 2-chamber, 4-chamber, SAO, and LVOT views are acquired with breath-holds. For those patients unable to hold their breath, we run the standard Siemens DE overview sequence, which can be run without breath-holds and gives an overview of the entire ventricle, running several planes simultaneously.

Findings

Our case patient tolerated the CMRI extremely well with adequate breath-holding and maintained positioning throughout. It is felt that shorter examination time can really improve patient cooperation, enhancing image quality. CMRI demonstrated moderately ill-defined subepicardial and mid-wall enhancement in the late gadolinium enhanced images in the basal mid and apical thirds of the left ventricular myocardium, typical of acute myocarditis. The patient was discharged from hospital following a three-day stay. After troponin levels peaked at 16,400 ng/mL, the patient recovered quickly and responded extremely well to oral steroids. Upon discharge, the patient was advised to not get a third dose (booster) of the mRNA vaccine, and troponin levels, although trending down, were to be monitored back home in his regional hospital. He was to continue low-dose steroids and bisoprolol for two more days. Follow-up MRI in six months was arranged.

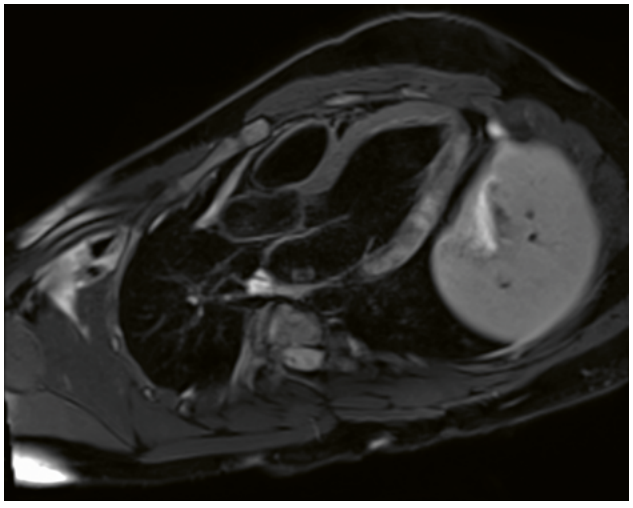

2 LVOT SPAIR image showing patchy increased T2 signal.

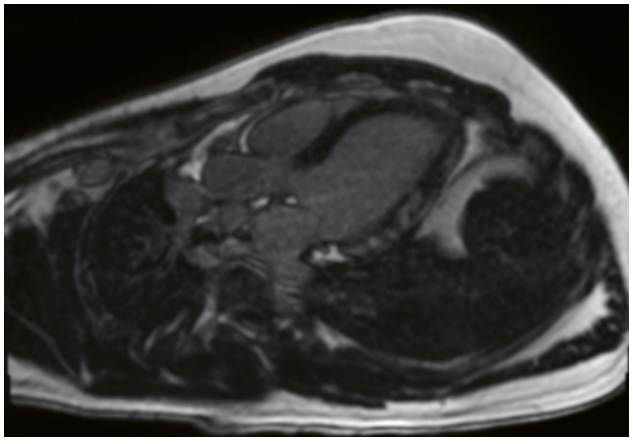

3 LVOT LGE image showing patchy enhancement in corresponding areas on SPAIR image.

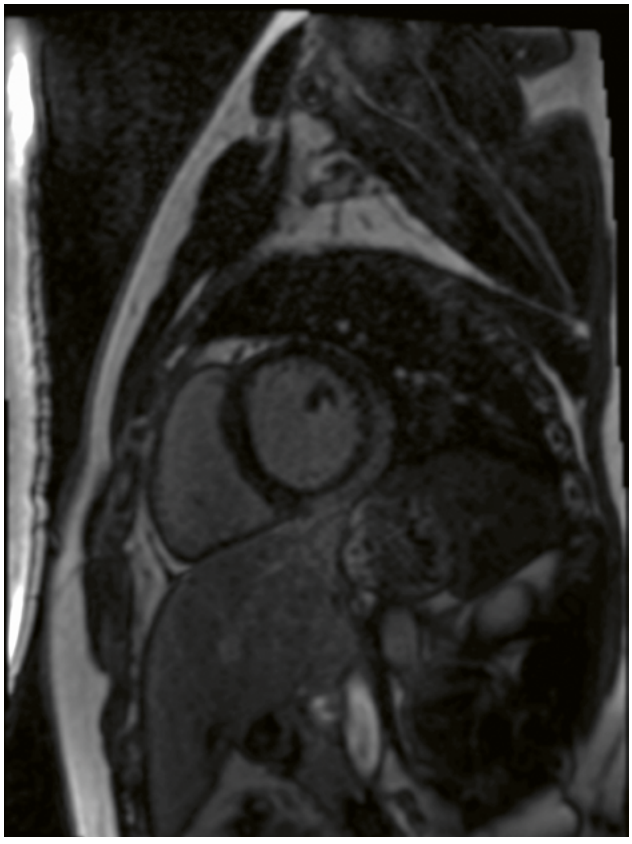

4 SAO LGE image showing subepicardial enhancement.

5 Complete CMRI protocol at Perth Children's Hospital for post-vaccination myocarditis.

Conclusion

In the current situation of mass vaccination, we have seen an increase in patients presenting with vaccine-induced myocarditis. Increased demand for MRI is problematic at most institutions, so a fast, robust protocol is essential and, as shown, possible. Patients at our institution are referred for CMRI if ventricular function is compromised, as determined by reduced GLS in echocardiogram. It is possible to get very high-quality cardiac imaging in under 30 minutes for the assessment of the left ventricle in acute myocarditis, especially if post-vaccination myocarditis diagnosis is likely. The purpose of MRI is to monitor the myocardium over time if left ventricular function is affected. For patients unable to breath hold, real-time cines can be used in place of TrueFISP, and LGE overview scans can be performed instead of conventional breath-hold LGE.

Acknowledgments

We acknowledge Dr Conor Murray and Dr Pankaj Gupta for their assistance with this article.

References

1 Bozkurt B, Kamat I, Hotez P.Circulation: Myocarditis With COVID-19 mRNA Vaccines. Circulation. 2021 Jul;144(6).
2 Stecker E, Mullen B. Vaccine-Associated Myocarditis Risk in Context: Emerging Evidence. ACC. 2022, Feb 09.
3 Wong J, Sharma S, Yao J, Aggarwal A, Grigg L. COVID-19 mRNA vaccine (Comirnaty)-induced myocarditis. Med J Aust. 2022;216(3):122-123. doi: 10.5694/mja2.51394
4 Husby A, Vinsløv Hansen J, Fosbøl E, Myrup Thiesson E, Madsen M, Thomsen R, et al. SARS-CoV-2 Vaccination and Myocarditis or Myopericarditis: Population Based Cohort Study. Br Med J. 2021 Dec;375.
5 Caforio A. Receipt of mRNA Vaccine against Covid-19 and Myocarditis. N Engl J Med. 2021;385:2189-2190.
6 Siripanthong B, Nazarian S, Muser D, Deo R, Santangeli P, Khanji M, et al. Recognizing COVID-19–related myocarditis: The possible pathophysiology and proposed guideline fordiagnosis and management. Heart Rhythm. 2020 Sep;17(9):1463-1471.
7 Singer M, Taub I, Kaelber D. Risk of Myocarditis from COVID-19 Infection in People Under Age 20: A Population-Based Analysis. medRxiv. 2022 Mar.
8 Tijmes F, Thavendiranathan P, Udell J, Seidman M, Hanneman K. Radiology Cardiac MRI Assessment of Nonischemic Myocardial inflammation: State of the Art Review and Update on Myocarditis Associated with COVID-19 Vaccination. Radiol Cardiothorac Imaging. 2021 Nov;3(6).
9 Mather A, Lockie T, Nagel E, Marber M, Perera D, Redwood S, Radjenovic A, et al. Appearance of microvascular obstruction on high resolution first pass perfusion early and late gadolinium enhancement CMR in patients with acute myocardial infarction. J Cardiovasc Magn Reson. 2009 Aug; 11(1):33
10 Kime P. Pentagon Tracking 14 Cases of Heart Inflammation in Troops After COVID-19 Shots. Military.com. April 26, 2021.
11 Yingchoncharoen T, Agarwal S, Popović Z, Marwick T. Normal ranges of left ventricular strain: a meta-analysis. J Am Soc Echocardiogr. 2013; 26(2):185-91.
12 Stirrat J, White J. The Prognostic Role of Late Gadolinium Enhancement Magnetic Resonance Imaging in Patients with Cardiomyopathy. Can J Cardiol. 2013;29(3):329-36.

Contact

Erin Robins, MRI Supervisor
Perth Children's Hospital
Hospital Ave
Nedlands 6009
Western Australia
Erin.Robins@health.wa.gov.au

Claire Harris, Senior MRI MIT
Perth Children's Hospital
Hospital Ave
Nedlands 6009
Western Australia
Claire.Harris@health.wa.gov.au

Ferumoxytol-Enhanced Free-Running 5D Whole-Heart MRI: A Glimpse of a One-Stop-Shop Modality for Cardiac Function and Morphology

Salim Si-Mohamed[1,2,3,4]; Ludovica Romanin[2,9]; Mariana Falcão[1,2]; Jerome Yerly[1,2]; Estelle Tenisch[2]; Tobias Rutz[5]; Juerg Schwitter[5,6,7]; Charles De Bourguignon[8]; Matthias Stuber[1,2]; Christopher Roy[1,2]; Milan Prsa[10]

[1]Center for Biomedical Imaging (CIBM), Lausanne, Switzerland
[2]Department of Diagnostic and Interventional Radiology, Lausanne University Hospital (CHUV) and University of Lausanne (UNIL), Lausanne, Switzerland
[3]University Lyon, INSA-Lyon, University Claude Bernard Lyon 1, UJM-Saint Etienne, CNRS, Inserm, CREATIS UMR 5220, U1206, F-69621, Villeurbanne, France
[4]Department of Radiology, Louis Pradel Hospital, Hospices Civils de Lyon, Bron, France
[5]Service of Cardiology, Lausanne University Hospital (CHUV) and University of Lausanne (UNIL), Lausanne, Switzerland
[6]Director, Cardiac MR Center, University Hospital Lausanne (CHUV), Switzerland
[7]Faculty of Biology & Medicine, University of Lausanne (UNIL), Lausanne, Switzerland
[8]Centre d'Investigation Clinique (CIC), Hospices Civils de Lyon, Bron, France
[9]Advanced Clinical Imaging Technology, Siemens Healthineers International AG, Lausanne, Switzerland
[10]Division of Pediatric Cardiology, Mother-Woman-Child Department, Lausanne University Hospital (CHUV) and University of Lausanne (UNIL), Switzerland

Free-running 5D whole-heart cardiovascular MRI (5D CMR) is an emerging approach in the field of cardiovascular imaging. It captures the entire 3D cardiovascular anatomy during the full cardiac cycle with high temporal and spatial resolution, and without the need for ECG gating or breath-holds [1, 2].

This push-button solution is based on a previously described free-running gradient-echo research sequence[1] [1]. *k*-space data are continuously sampled using a 3D koosh-ball phyllotaxis trajectory [3], interleaved with the acquisition of superior-inferior readouts that are then used for the simultaneous extraction of cardiac and respiratory self-gating (SG) signals [2]. The main sequence parameters are set as follows: radio frequency excitation angle of 15° with an axial slab-selective sync pulse; isotropic spatial resolution of (1.15–1.35 mm)^3; FOV of (220–260 mm)^3; TE/TR of 1.53–1.64/2.69–2.84 ms; and readout bandwidth of 1002 Hz/pixel. The protocol consists of 5,749 radial interleaves and 22 readouts/interleaves, for a total scan time of 5:35–5:59 minutes. To match the current standard 2D cine protocol, each 5D CMR dataset is sorted into a fixed number of 25 cardiac bins based on the SG cardiac triggers. The same datasets are also partitioned into 4 respiratory bins, defined according to the amplitude of the respiratory signal. 5D motion-resolved images (3D + cardiac motion + respiratory motion) are then reconstructed using a compressed sensing algorithm, exploiting sparsity along the cardiac and respiratory dimensions [2, 4].
In terms of sequence planning, only orthogonal plane localizers are required, in order to center the acquisition box on the cardiovascular volume of the thorax. The MR technician needs no prior specific knowledge of the cardiac anatomy. All it takes then is 5 minutes of scanning time.

The potential of this framework rests on the possibility of performing a comprehensive assessment of cardiac morphology and function with a significantly shorter and simpler scanning protocol compared to standard 2D cine bSSFP and 3D contrast-enhanced angiographic imaging, without the need for breath-holds or anesthesia. This also shifts the paradigm from prospective sequence parameter definition and scan planning to a fully flexible and retrospective query of the data both in time and in space.

[1]*Work in progress. The application is currently under development and is not for sale in the U.S. and in other countries. Its future availability cannot be ensured.*

In our center, we have used this ferumoxytol-enhanced 5D CMR framework on a 1.5T scanner to evaluate coronary and great vessel anatomy, and to quantify ventricular volumes and function in patients with congenital heart disease. The high signal-to-noise ratio (SNR), combined with high spatial and temporal resolution, yields images with exceptional quality, and provides the clinician with a high level of diagnostic confidence and accuracy.

As an example, we present the case of an 8-year-old boy who, after repair of common arterial trunk, underwent CMR to evaluate pulmonary arterial anatomy and coronary arterial origins, and to quantify cardiac volumes and function. The high SNR and high-resolution isotropic imaging at $(1.1\ mm)^3$, which allowed dynamic multiplanar reconstructions, showed normal coronary artery origins with excellent visualization of the ostia and vessel course, particularly during systole (Fig. 1). There was severe stenosis of the right pulmonary artery at the bifurcation, and dilatation of the left pulmonary artery (Fig. 2). To measure the systolic function, the ventricles can be segmented semi-automatically on a clinical workstation from a short-axis reconstruction, such as performed on standard 2D cine images (Fig. 3). The analysis showed left and right ventricular end-diastolic volumes of 78 and 108 mL/m^2, and end-systolic volumes of 32 and 61 mL/m^2, for an ejection fraction of 54% and 48%, respectively.

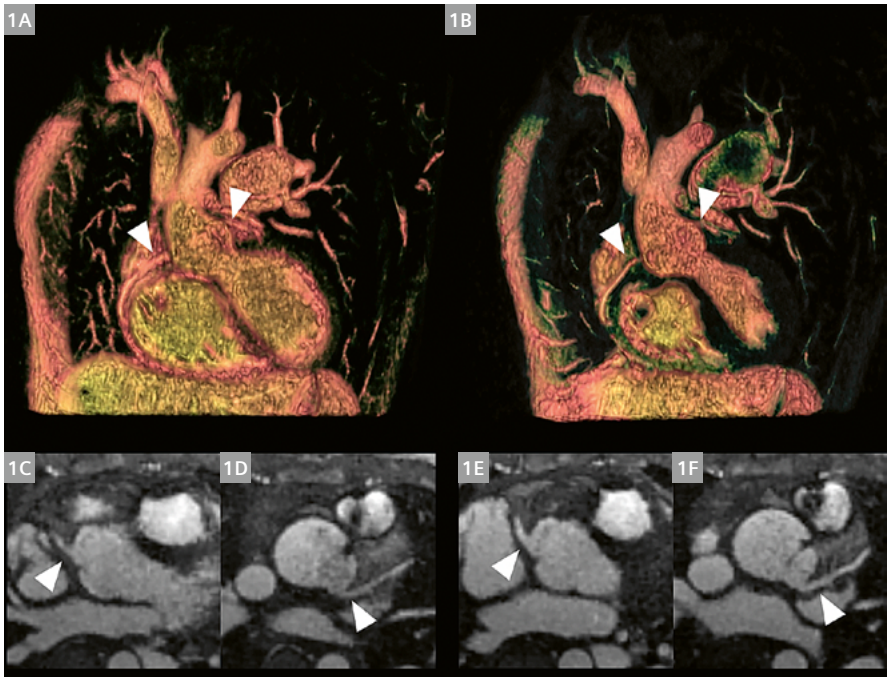

1 Multiphase imaging of the cardiovascular morphology with ferumoxytol-enhanced free-running 5D CMR reconstructed during end-inspiration. **(1A, 1B)** Volume-rendered image of the proximal coronary arteries, **(1C–1F)** high-resolution axial plane images of the coronary arteries. Arrowheads point to the right (1C and 1E) and left (1D and 1F) coronary artery origins, and proximal course. The diastolic volume is depicted on the left side of the figure (1A, 1C, 1D), and the systolic phase is on the right (1B, 1E, 1F).

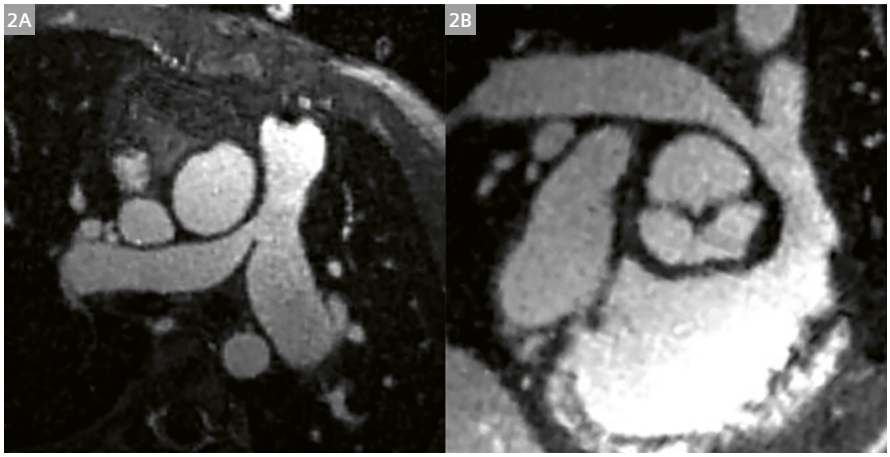

2 Morphological imaging with ferumoxytol-enhanced free-running 5D CMR for multiplanar reconstruction and biometry of the pulmonary tract during end-inspiration **(2A, 2B)**. High SNR and isotropic spatial resolution $(1.1\ mm)^3$ images enable the diagnosis of a right pulmonary stenosis and dilatation of the left pulmonary artery.

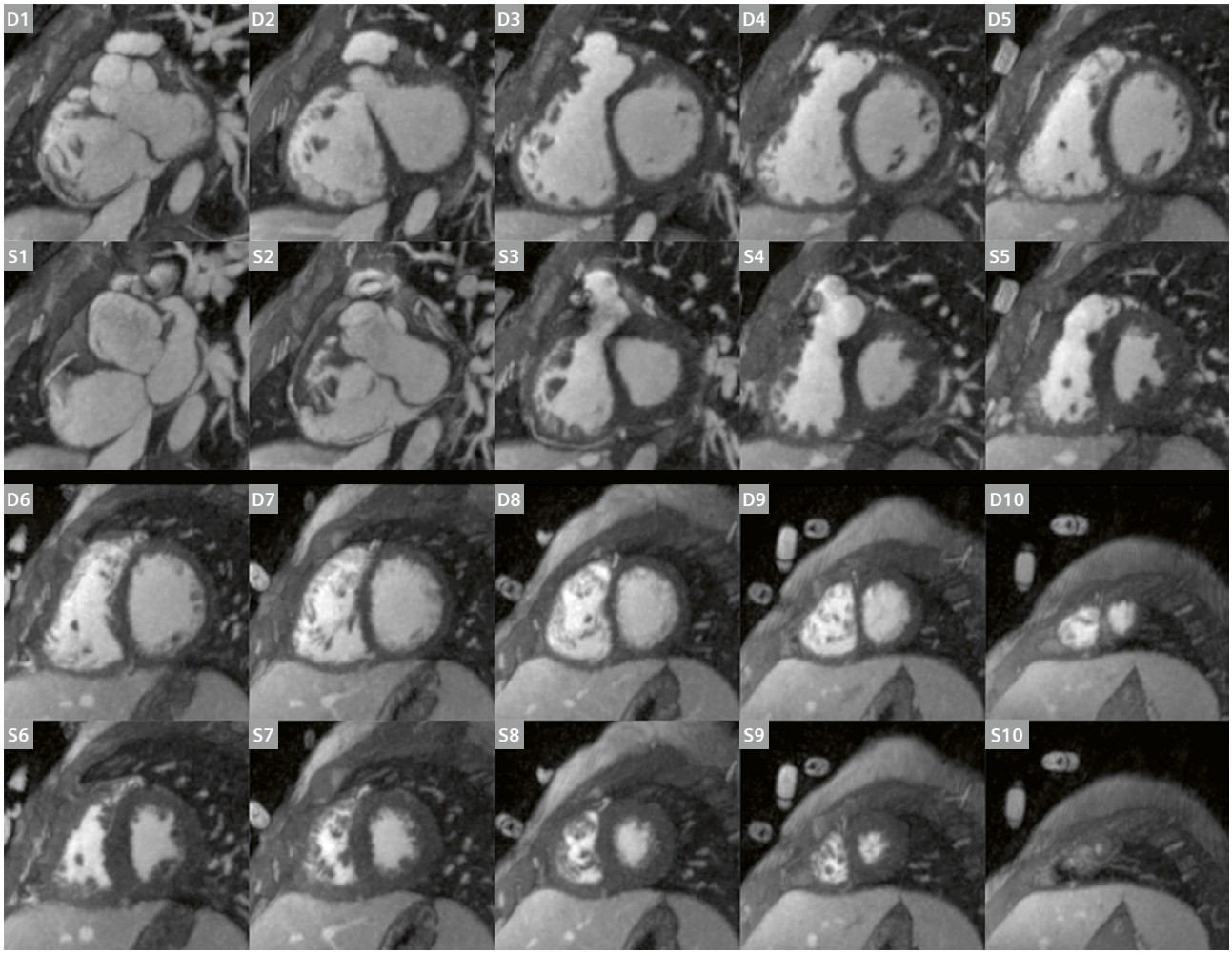

3 Evaluation of ventricular volumes and function with ferumoxytol-enhanced free-running 5D CMR. **(D1–D10)** Reconstructed ventricular short-axis images at end-diastole during end-inspiration, **(S1–S10)** reconstructed ventricular short-axis images at end-systole, both reformatted at a 5 mm slice thickness. High SNR and in-plane spatial resolution $(1.1\ mm)^2$ images show a clear separation between the myocardium and the blood pool, including within the trabeculations.

In conclusion, ferumoxytol-enhanced free-running 5D whole-heart MRI allows high-quality cardiovascular imaging as well as measurement of ventricular volumes and function, derived from a single 5-minute acquisition, which has the potential to trigger a paradigm shift in cardiovascular MRI.

References

1 Roy CW, Di Sopra L, Whitehead KK, Piccini D, Yerly J, Heerfordt J, et al. Free-running cardiac and respiratory motion-resolved 5D whole-heart coronary cardiovascular magnetic resonance angiography in pediatric cardiac patients using ferumoxytol. J Cardiovasc Magn Reson. 2022;24(1):39. https://doi.org/10.1186/s12968-022-00871-3.
2 Di Sopra L, Piccini D, Coppo S, Stuber M, Yerly J. An automated approach to fully self-gated free-running cardiac and respiratory motion-resolved 5D whole-heart MRI. Magn Reson Med. 2019;82(6):2118–2132.
3 Piccini D, Littmann A, Nielles-Vallespin S, Zenge MO. Spiral phyllotaxis: The natural way to construct a 3D radial trajectory in MRI. Magn Reson Med. 2011;66(4):1049–56.
4 Feng L, Coppo S, Piccini D, Yerly J, Lim RP, Masci PG, et al. 5D whole-heart sparse MRI. Magn Reson Med. 2018;79(2):826–838.

Contact

Salim Si-Mohamed, M.D., Ph.D.
Center for Biomedical Imaging (CIBM) and Lausanne University Hospital (CHUV) and University of Lausanne (UNIL)
Rue du Bugnon 46
CH-1011 Lausanne
Switzerland
salim.si-mohamed@chu-lyon.fr

Meet Siemens Healthineers

Siemens Healthineers: Our brand name embodies the pioneering spirit and engineering expertise that is unique in the healthcare industry. The people working for Siemens Healthineers are totally committed to the company they work for, and are passionate about their technology. In this section we introduce you to colleagues from all over the world – people who put their hearts into what they do.

Annemie Steegmans, Ph.D.

Annemie studied at Katholieke Universiteit Leuven in Belgium, where she earned her master's in physics and medical science, and her Ph.D. in MR spectroscopy in superconductors. She started her professional career with a research project on coincidence detection in molecular imaging. In 2008, Annemie became a product specialist for MR at Siemens Healthcare. Since 2012, she has been the business manager for Belgium and a product specialist in MR at Siemens Healthineers, supporting the account managers across various MR projects. Her work involves giving presentations, making configurations, setting prices, and much more.

Groot-Bijgaarden, Belgium

How did you first come into contact with MRI?
When doing my master's in medical science, I needed to write a thesis and one of the subjects was MR spectroscopy on rat liver. This was high-field MRI in small-bore systems. It was fascinating to make and tune the coils. After my master's, I got the opportunity to do a Ph.D. in MR. I seized it with both hands because the technology is wonderful. I started to get curious about MR imaging and how the images are produced. I'm still a big fan of the technology today – I love that it's always evolving.

What do you find motivating and challenging about your job?
I find it motivating that every day is different: different internal contacts at Siemens Healthineers and different external contacts at the customer's site. And of course, there's the never-ending developments in MR. Before convincing our customers, we have to convince our sales force. But that's not actually very difficult when you believe in the products. Also, Siemens Healthineers listens and responds to its customers. This led to the launch of BioMatrix Technology, with its sensors, tuners, and interfaces. I have been with Siemens Healthcare for almost 15 years, and it is not every year that I get to launch breakthrough technology like the BioMatrix Beat Sensor. This is what makes my job so exciting.

What do you think are the most important developments in MRI?
Years ago, everything was about channels in the RF chain, but I believe the most important thing was not the number of channels but the complete redesign of the workflow. Redesigning every step of the workflow – from patient preparation right through to acquisition and postprocessing – was really a revolution. Not focusing on one element in the workflow but on every step in it.

Introducing the Respiratory Sensor, the Beat Sensor, Select&GO, CoilShim, and SliceAdjust was also a breakthrough. And then there's our deep learning solution, Deep Resolve, which is really a game changer. Or, as my customer Dr. Dehem says, "a match made in heaven".

What would you do if you could spend a month doing whatever you wanted?
First of all, I love my job and it is a big part of me, I am passionate about MRI. People who know me know how difficult it is for me to disconnect on vacation. Since we are so busy, I love spending time at home with my family, friends, and our two English Bulldogs, Paulien and Rosie. I love reading, running, working out at the e-gym, and hiking. The last hike we did was the Samaria Gorge in Crete: 16 km through a rugged, beautiful landscape. I also like to travel, and I will never turn down the chance of a meal at a good restaurant.

Peter Speier, Ph.D.

Peter Speier grew up on the edge of a small village in the German state of Hessen. In 1987, he began studying physics at Heidelberg University, where he earned his degree and later his doctorate with a thesis in solid-state NMR. A job offer from an oilfield service company took him to Houston, Texas, where he spent five years developing the first commercial NMR relaxometer for use during drilling. When he and his wife – who he had met while in Heidelberg – became parents, they decided to move back to Germany. In early 2002, a sequence developer position became available in the interventional group led by Arnulf Oppelt at Siemens MR. This allowed Peter to return to Germany without abandoning (N)MR. Since then, he has been working for Siemens on innovations around interventional and cardiac MRI. His contributions have helped shape many of the company's current solutions, such as interactive scanning, radial imaging, cardiac SMS, exam workflow automation, and cardiac motion management. Peter's two eldest children have left home now, but his youngest daughter continues to make sure working from home doesn't become too boring.

Erlangen, Germany

How did you first come into contact with MR?
I studied physics in Heidelberg and was looking for a topic for my degree thesis. A friend suggested a small NMR group at the Max Planck Institute for Medical Research, where he had just started his thesis. In the final-round interview, Professor Haeberlen only asked two questions: "Do you play soccer?" and "Do you smoke?" And even though I gave the "wrong" answer to one of them, I was accepted into his team for my thesis and have been hooked on MR since. I stayed at the institute to write my Ph.D. thesis. Under my professor's supervision, I learned how to work with and extend a lab-built spectrometer to unravel detailed chemical riddles, discovered the power of gaining a detailed and deep understanding of a topic, and learned not to brush over mistakes that will come back to bite you. These lessons have since paid off manyfold.

What is the most fascinating aspect of MR?
The most fascinating aspect of NMR is its versatility. Here are just a few of the things you can use it for: unraveling protein structures, guiding the search for oil and gas, monitoring how concrete dries, measuring flow in plants. Every application has its own challenges, complex apparatus, and methods. Some of these applications have become indispensable in laboratories, and some have become a commercial success, like clinical MRI.

This commercial success has also turned MRI scanners into very complex, multilayered machines in terms of their hardware and software. Being able to learn about, explore, improve, and use the multitude of components that make up an MRI system is for me the most fascinating aspect of MRI.

What do you find motivating about your job?
The creative development at the start of a project is very motivating: When you come up with something that should improve a customer-visible aspect of MRI, and the idea passes the internal peer review and initial tests. After that, it's often a long and grinding process of refining, debugging, and polishing an idea to turn it into a product. But that's when you get your reward: It's a great feeling when the implementation delivers the improvement, and the customers like it and start using it.

What are the biggest challenges in your job?
During my 20 years in MR at Siemens Healthineers, I have worked on many different projects, often in parallel. The challenges vary with each project phase. For an entertaining glimpse into these, I recommend the old but still relevant book The Soul of a New Machine by Tracy Kidder. But the biggest challenge as a developer is managing the build-up of responsibilities over the years: When a development is mature enough, you have to release it into the organization – in other words, you let go of it and hope it will continue to flourish. Then you move on to the next project.

What do you think are the most important developments in MRI and healthcare?
When I started in sequence development, image reconstruction was developed in another department by other developers. These two aspects are now inseparably fused to enable highly accelerated scans, and more and more aspects of the exam process are being connected by software. I was involved in developing the early steps like patient-centric UI parameters, automatic FOV planning, inline postprocessing, and intra-exam information collection and re-use in Dot.

This development work will continue within and across modalities in the future and will include additional auxiliary inputs to simplify and speed up the exam and reading process. Besides improving standardization and quality, this will also reduce access hurdles and free up time for more patient interaction.

If you could do anything you wanted for a month (at work and privately) what would it be?
At work, I would love to be able to spend a whole month on a single fresh project with no interruptions.

Privately, I would probably divide my time between playing guitar (americana and international folk), working on my backlog for repairing mechanical photo cameras, and watching (silent) movies. Or maybe I would continue our Scandinavian camping trip from summer 2021, and visit the Baltic states that we had to skip because of the pandemic.

Get to know us

Find more portraits of our colleagues around the world!

www.magnetomworld.siemens-healthineers.com/meet-siemens-healthineers

The entire editorial staff at CHUV – Centre Hospitalier Universitaire Vaudois, Lausanne, Switzerland and at Siemens Healthineers extends their appreciation to all the radiologists, technologists, physicists, experts, and scholars who donate their time and energy – without payment – in order to share their expertise with the readers of MAGNETOM Flash.

MAGNETOM Flash – Imprint

Publisher:
Siemens Healthcare GmbH
Magnetic Resonance,
Karl-Schall-Str. 6, D-91052 Erlangen, Germany

Editor-in-chief:
Antje Hellwich
(antje.hellwich@siemens-healthineers.com)

Guest Editor:
Professor Matthias Stuber, Ph.D.
Section Head CIBM MRI CHUV-UNIL
CHUV – Centre Hospitalier Universitaire Vaudois
Département de Radiologie Médicale
Lausanne, Switzerland
www.unil.ch/cvmr
www.cibm.ch/research/projects/translational-mr-imaging

Editorial Board:
Christian Geppert, Ph.D.; Jane Kilkenny;
Nadine Leclair, M.D.; Rebecca Ramb, Ph.D.;
Wellesley Were

Review Board:
Gaia Banks, Ph.D.; Daniel Fischer; Carmel Hayes, Ph.D.;
Ning Jin, Ph.D.; Michaela Schmidt

Copy Editing:
Sheila Regan, Jen Metcalf, UNIWORKS,
www.uni-works.org
(with special thanks to Kylie Martin)

Layout:
Agentur Baumgärtner,
Friedrichstr. 4, D-90762 Fürth, Germany

PrePress and Image Editing, Production:
Clemens Ulrich, Paul Linssen,
Siemens Healthcare GmbH

Printer:
Schmidl & Rotaplan Druck GmbH,
Hofer Str. 1, D-93057 Regensburg, Germany

We welcome your questions and comments about the editorial content of MAGNETOM Flash. Please contact us at magnetomworld.team@siemens-healthineers.com

Manuscripts as well as suggestions, proposals and information are always welcome; they are carefully examined and submitted to the editorial board for attention. MAGNETOM Flash is not responsible for loss, damage, or any other injury to unsolicited manuscripts or other materials. We reserve the right to edit for clarity, accuracy, and space. Include your name, address, and phone number and send to the editors, address above.

MAGNETOM Flash is also available online:

www.siemens-healthineers.com/magnetom-world

Not for distribution in the US

On account of certain regional limitations of sales rights and service availability, we cannot guarantee that all products included in this brochure are available through the Siemens sales organization worldwide. Availability and packaging may vary by country and is subject to change without prior notice. Some/All of the features and products described herein may not be available in the United States.

The information in this document contains general technical descriptions of specifications and options as well as standard and optional features which do not always have to be present in individual cases, and which may not be commercially available in all countries.

Due to regulatory reasons their future availability cannot be guaranteed. Please contact your local Siemens organization for further details.

Siemens reserves the right to modify the design, packaging, specifications, and options described herein without prior notice. Please contact your local Siemens sales representative for the most current information.

Note: Any technical data contained in this document may vary within defined tolerances. Original images always lose a certain amount of detail when reproduced.

Siemens Healthineers Headquarters
Siemens Healthcare GmbH
Henkestr. 127
91052 Erlangen, Germany
Phone: +49 9131 84-0
siemens-healthineers.com

Published by Siemens Healthcare GmbH · Order No. A91MR-1000-150M-7600 · Printed in Germany · 13082 0123 ·